Ministry of Higher Education

And Scientific Research

University of Babylon

Using of Unit Cell Method in Micromechanical Stress Analysis of Fiber-Reinforced Composite Beam

A Thesis

Submitted to the College of Engineering

of the University of Babylon in partial

Fulfilment of the degree of Master

of Science in Mechanical

Engineering

By

Luay Muhammad Ali Ismaeel

B.sc. ١٩٨٦

May ٢٠٠٧ Rajab. ٢٩, ٤٤

بِسْمِ اللهِ الرَّحْمنِ الرَّحِيمِ

والضُّحَى{١} وَاللَّيْلِ إِذَا سَجَى{٢} مَا وَدَّعَكَ رَبُّكَ وَمَا قَلَى{٣} وَلَلْآخِرَةُ خَيْرٌ لَّكَ مِنَ الْأُولَى{٤} وَلَسَوْفَ يُعْطِيكَ رَبُّكَ فَتَرْضَى{٥}

صدق الله العلي العظيم

سورة الضحى

الخـــلاصـــــــة:

ان التصميم الجيد لجزءٍ هيكلي[1] مصنوع من مادة مركبة مقواة بالياف يتطلب فهما عميقا وكاملا لتصرف تلك المواد العياني والمجهري. ولتحقيق بعض المتطلبات المعينة والتي من بينها عمر الاستخدام، مقدار الوثوق بالجزء، الاقتصاد والامان فان التصميم المعتمد يجب ان يفي بـِ ، ويستند الى التحليلات العيانية والمجهرية الدقيقـــة.

طريقة وحدة الخلية في التحليل الميكانيكي المجهري للاجهادات باستخدام طريقة العناصر المحددة هي احدى الوسائل الفعالة والمفيدة والمهمة المتبعة لانجاز الغرض اعلاه ولهذا السبب تم تبنيها في هذا البحث. أُفترض هنا النظام السداسي لحشو الالياف – النسيج الاساسي لمادة العتبة موضع الدراسة والتي ارتؤي ان تكون من النوع المقوى بالياف احادية الاتجاه ، ومبررات هذه الاختيارات يمكن اختصارها بان المواد المركبة المقواة بالياف احادية الاتجاه هي من اوسع المواد المركبة استعمالا وانتشارا ومن ناحية اخرى فان العتبات (العوارض) هي الاخرى من اوسع التراكيب او الهياكل انتشارا واستخداما في التطبيقات الصناعية والهندسية.

تم اجراء نوعين من التحليلات على هذه العتبة لايجاد الازاحة العمودية (الشاقولية) عند مقاطع مختلفة منها والاجهادات والانفعالات الناتجة ، بما في ذلك اقصى ازاحة واجهاد وانفعال حاصل. تمت دراسة هذه المتغيرات ذات الطابع المقطعي (ازاحة واجهاد وانفعال) لانواع مختلفة من الالياف والانسجة الاساسية بنسب حجمية مختلفة تحت نوعين من الشروط الحدودية (Boundary Conditions) اسناد شاقولي بسيط وقمط محكم من النهايتين. درس كذلك تاثير تغيير الحمل المسلط

على تصرف العتبة والاجهادات الناشئة عن ذلك. وضعت المعادلات الخاصة بالتحليل وكونت بطريقة العناصر المحددة باستخدام اسلوب الازاحة ومبدأ الطاقة الكامنة الدنيا،كما تم تصميم برنامج حاسوبي بواسطة حقيبة الماتلاب لحل تلك المعادلات وايجاد تلك المتغيرات.

اجري التحليل الثاني بالاتجاه العرضي لتحديد والتعرف على حالة ونمط توزيع الاجهادات المتكونة في المقطع العرضي ويمكن كذلك استخدام احدى نظريات الفشل للتاكد من سلامة العتبة. تم حساب المتغيرات المقطعية المشار اليها اعلاه بطريقة وحدة الخلية ويتم نقل القيم الناتجة الى المقاطع الاخرى للعتبة لايجاد قيمها هناك وفقا لقوانين نظرية انحناء العتبات. ولاثبات صحةهذا الاسلوب المتبع لمعالجة مادة اورثوتروپية، تم تطبيق نفس الاسلوب على مادة آيزوتروپية وقورنت النتائج مع نتائج برنامج الماتلاب ونتائج الحل التحليلي (Exact Solution) وكان تقارب النتائج كبيرا.

تم استعراض نتائج البحث بيانيا من خلال المنحنيات المثبتة في نهاية الفصل الخامس ومن خلال الجداول المثبتة في الملاحق.

CERTIFICATION

We certify that this thesis entitled "***Using of Unit Cell Method in Micromechanical Stress Analysis of Fiber Reinforced Composite Material Beam "*** was prepared by "***Luay Muhammed Ali Ismaeel"*** under our supervision at Babylon University, College of Engineering in partial fulfilment of the requirement for the degree of Master of Science in Mechanical Engineering (Appplied Mechanics).

Signature:

Name: Asst. Prof.

Dr. Hayder A. Hussain

(Supervisor)

Date: / / ٢٠٠٦

Signature:

Name: Asst. Prof.

Dr.Ala'a M. Hussain

(Supervisor)

Date: / / ٢٠٠٦

Abstract

The good design of a structural composite part requires a thorough and deep understanding of the behaviors of that composite on both macro- and microscopic levels. In order to meet some specific requirements among of which, the durability, reliability, economy and safety, the reliable design should meet, base on and satisfy both precise macro- and micromechanical analyses of that composite material.

The unit cell method in micromechanical analysis based on the finite element method is one of the important, beneficial and effective means to achieve the purpose referred to above; this is why this work adopted it. Hexagonal fiber-matrix packing system is idealized for the material from which the structural part of the present work is comprised, and selected to be a unidirectional fiber-reinforced composite. The reasons beyond these selections can be summarized as the unidirectional fiber-reinforced composites are the

most widely used composites; from the other hand the beams are also the most vastly employed engineering structures in various industrial and engineering fields. Two types of analyses are made on the unidirectional fiber-reinforced composite beam under consideration. The first is carried out in the longitudinal direction of the beam to determine the vertical displacements (deflections) at the various sections of the beam, stresses and strains. These field parameters (displacements, stresses & strains) are studied under different types of fibers and matrices with various fiber volume fractions at two different boundary conditions (simply supported and built–in beam cases). The effect of load variations is also studied on the beam behavior and stresses induced. The pertinent equations of the analysis are formulated using the finite element method based on the displacement approach and minimum potential energy principle. A matlab program is implemented to solve these equations. The second analysis made in a transverse direction to define the state and distribution of the stresses induced In the cross-section. A failure criterion can be used to check the stress level with respect to the beam materials strength. In the unit cell method, the field quantities are found at a certain point then; they are mapped to the whole cross-section domain according to the bending theory rules to determine their values wherever required. The package of ANSYS ٥.٤ is used to solve for the stresses, strains and displacements of the beam of interest throughout the current work. The most prominent results obtained can be summarized as follows:

١. The method of unit cell can be efficiently applied to the bending state of stress for the unidirectional fiber-reinforced composite beam.
٢. In case of clamped beam, the stresses induced are more than those of simply supported case.
٣. The deflections are not highly affected by the type of support.

٤. The bending stresses are not considerably influenced by the variation of fiber volume fraction and the applied load due to high elastic moduli of the considered composite.

The method of solution of the transversely isotropic problem in macroscopic analysis is applied to an isotropic counterpart. The results are then compared; good agreement was distinguished between them. As well as the unit cell macro- and micromechanical results are compared with those of isotropic case, the same convergence is also noticed verifying the validity of the analysis method adopted by the current work to such a problem.

Acknowledgements

(By The Name of Allah, The Most Gracious The Most Merciful)

Praise be to Allah, The Lord of All Creations, blessings and peace be upon his prophet Mohammed and his Ahlul-Bait. This work was completed under their benediction, merit and grace.

First of all, I would like to sincerely and wholeheartedly express my deep thankfulness and gratitude to my supervisors, Dr. Hayder A. Hussain and Dr. Ala'a M. Hussain for their great support, guidance, kindness, boundless assistance and invaluable recommendations and comments during the whole period of achieving and completion of this work.

Very special and unlimited gratitude and thankfulness are directed to the dean, deanship, head and staff of higher studies in mechanical engineering department- branch of applied mechanic in college of engineering at Babylon University for their true and unforgotten efforts in opening new worlds of science for me.

My great appreciation is introduced to the dean, staff of computer centre and the head of department of mechanical technologies in Najaf Tech. Inst. for their fraternal and sincere support.

Large and special thankfulness are displayed to my colleagues who greatly assisted and backed me up in the fulfillment of the present work in the college of engineering at Babylon university and out of it.

Immeasurable gratitude and boasting are directed to my forgotten family, which very much sacrificed for me.

Finally, I apologize to all those whom non-intensionally I forgot to mention their names.

Luay M. Ali

٢٠٠٦

NOMENCLATURE

The following symbols are frequently used throughout the text. Others may be defined wherever found.

١. English Symbols:

Symbol	Meaning	Unit
a	Fiber radius.	m
A_x	Area of a unit cell face in the direction of x-axis	$m^٢$
A_y	Area of a unit cell face in the direction of y-axis	$m^٢$
A_z	Area of a unit cell face in the direction of z -axis	$m^٢$
[B]	Strain-displacement matrix	
b	Half of center-to-center distance between two adjacent fibers.	m
C	Contiguity factor or degree of contiguity.	---
C_{ij}	A stiffness matrix or elasticity matrix element in material coordinates.	$N/m^٢$
C'^{n}_{x}	Rotational symmetry through an angle of $\frac{2\pi}{n}$ about x-axis.	
D	Matrix of Material properties.	---
E	Modulus of elasticity of an isotropic material.	$N/m^٢$
E_f	Modulus of elasticity of a fiber.	$N/m^٢$
E_m	Modulus of elasticity of a matrix	$N/m^٢$
$E_١$	Modulus of elasticity of a composite in ١-direction or fiber direction when it is a unidirectional	$N/m^٢$
$E_٢$	Modulus of elasticity of a composite in ٢-direction or a transverse direction.	$N/m^٢$
$E_٣$	Modulus of elasticity of a composite in ٣-direction.	$N/m^٢$
$\{f_e\}$	Elemental force or load vector.	N
[G]	Matrix of partial derivatives of the shape functions	
G_f	Shear modulus of a fiber.	$N/m^٢$
G_m	Shear modulus of a matrix.	$N/m^٢$
$G_{١٢}$, $G_{٢٣}$, $G_{١٣}$	Shear modulus of a composite in ١-٢, ٢-٣,	$N/m^٢$

	١-٣ planes respectively.	
I	Second moment of a cross-sectional area of a beam.	m^4
[J]	Jacobean matrix.	
K	Fiber misalignment factor.	---
[K]	Global stiffness matrix	N/m
$[K^e]$	Elemental stiffness matrix	N/m
K_f	Bulk modulus of a fiber.	---
K_m	Bulk modulus of a matrix	---
l_e	A finite element length.	m
M	Composite modulus $E_٢$, $G_{٢٣}$, ν_{23}	
M_f	Corresponding fiber modulus E_f, G_f, ν_f .	
M_m	Corresponding matrix modulus E_m, G_m, ν_m .	
$M_1^{(e)}$, $M_2^{(e)}$	Elemental internal resisting moments at nodes ١ & ٢ respectively.	N.m
$N_١$-$N_٦$	Shape functions of a six-nodes higher order triangular element	---
$N_١$-$N_٨$	Shape functions of an eight-nodes higher order quadrilateral element	
P	A concentrated load transversely applied.	N
q	Distributed load intensity.	N/m
Q_{ij}	Composite reduced stiffness matrix.	N/m^2
S_{ij}	Compliance matrix defined as the inverse of stiffness matrix.	m^2/N
$\{S^e\}$	Elemental internal force vector.	N
$Sh_١^{(e)}$, $Sh_٢^{(e)}$	Vector of elemental internal shear forces at nodes ١ & ٢ respectively.	N
$T_x^{\Delta x}$	Translational symmetry by a translation distance of Δx along x-axis	---
u	A displacement in x-direction	m
v	A displacement in y-direction	m
$V_{crit.}$	Critical fiber volume fraction.	---
V_f	Fiber volume fraction.	---
V_m	Matrix volume fraction.	---
$V_{min.}$	Minimum fiber volume fraction.	---
w	A displacement in z-direction	m
w_i, w_j	Weight functions in Gauss-Legender	---

	numerical integration method.	
X, Y & Z	Cartesian coordinate axes	---
x_1, x_2 & x_3	Local coordinate axes.	---
١, ٢ &٣	Material principle directions	---

٢.Greek Symbols:

Symbol	Meaning	Unit
γ_{12}	Shear strain in ١-٢ plane	---
γ_{31}	Shear strain in ٣-١ plane	---
γ_{23}	Shear strain in ٢-٣ plane	---
δ	Deflection of a beam due to a bending load	
ε_c	Normal strain in the composite material	---
ε_f	Normal strain in the fiber	---
ε_f^*	Fracture strain of a fiber	
ε_i	Normal strain in i-direction.	---
ε_j	Normal strain in j-direction.	---
ε_m	Normal strain in the matrix.	---
ε_x , ε_y	Normal strain in x- and y-directions respectively	
ε_1	Normal strain in ١-direction.	---
ε_2	Normal strain in ٢-direction.	---
ε_3	Normal strain in ٣-direction.	---
η_j , ξ_i	Positions of Gaussian points over which the numerical integration is performed.	---
η	Reduced factor	---
ξ	Reinforcement or fiber geometry	---

$\xi-\eta$	Intrinsic coordinate axes	---
ν_f	Poisson's ratio of a fiber	---
ν_m	Poisson's ratio of a matrix	---
ν_{12}	Poisson's ratio of a composite for transverse strain in ٢-direction and longitudinal strain in ١-direction.	---
ν_{23}	Poisson's ratio of a composite for transverse strain in ٣-direction and longitudinal strain in ٢-direction.	---
ν_{13}	Poisson's ratio of a composite for transverse strain in ٣-direction and longitudinal strain in ١-direction.	---
ρ_c	Density of a composite material	kg/m^{٣}
ρ_f	Density of a fiber.	kg/m^{٣}
ρ_m	Density of a matrix**.**	kg/m^{٣}
Σ	Denotes the reflectional symmetry or summation	
Σ_x	Reflectional symmetry in a plane normal to x-axis	
σ_c	Normal stress in the composite material	N/m^{٢}
σ_f	Normal stress in the fiber	N/m^{٢}
σ_i	Normal stress in i-direction.	N/m^{٢}
σ_m	Normal stress in the matrix.	N/m^{٢}
σ_{cu}	Ultimate strength of a composite material	N/m^{٢}
σ_{fu}	Ultimate strength of the fibers	N/m^{٢}
$(\sigma_m)_{\varepsilon_f^*}$	The matrix stress at the fiber fracture strain $\left(\varepsilon_f^*\right)$	N/m^{٢}
σ_{mu}	Ultimate strength of the matrix material	N/m^{٢}
τ_{12}	Shear stress in ١-٢ plane	N/m^{٢}

τ_{23}	Shear stress in ٢-٣ plane	N/m^{٢}
τ_{13}	Shear stress in ١-٣ plane	N/m^{٢}

Superscripts:

Superscript	Description
e	Element.
n	Number of Gaussian points over which the numerical integration is performed.
'n	Magnitude of rotation angle in a rotational symmetry transformation through which the figure moves.
Δx	Magnitude of translation inx-direction
T	Transpose of a matrix.
-T	Inverse transpose.

Subscripts:

Subscript	Description
c	Composite
cu	Ultimate parameter of the composite.
crit.	Critical.
f	Fiber.
fu	Ultimate parameter of the fiber.
m	Matrix.
min.	Minimum.
mu	Ultimate parameter of the matrix.
i, j	Local or nodal values or directions.
x	Direction of translation.
x, y, z	Local coordinate axes.

١,٢,٣	Principal material directions representing longitudinal, transverse and out of plane directions.
١→٨	Number of a shape function
ε_f^*	Fiber fracture strain.

Abbreviations:

B.C.	Boundary conditions.
CSM	Chopped strand material
det.	Determinant.
Eq.	Equation.
Eqs.	Equations.
FEMF	Finite element method formulation.
Fig.	Figure.
GMC	Generalized method of cells.
ILSS	Inter-laminar shear strength.
LCM	Laminated composite material.
MAC	Micromechanics analysis code.
MATLAB	Matrix laboratory
PMCM	Polymeric matrix composite material.
S.C.M.	Self-consistent method.
Symm.	Symmetric.
UDFRCM	Unidirectional fiber-reinforced composite material.

EXAMINING COMMITTEE CERTIFICATE

We certify that this thesis entitled ***"Using of Unit Cell Method in Micromechanical Stress Analysis of Fiber Reinforced Composite Material Beam"*** *and as examining committee, examined the student '***Luay Muhammed Ali Ismaeel "*** *in its contents and that in our opinion it meets the standard of thesis for the degree of Master of Science in Mechanical Engineering.*

Signature:

Name: ***Asst. Prof.***

Dr. Hayder A. Hussain

(Supervisor)

Date: / /٢٠٠٧

Signature

Name: ***Asst. Prof.***

Dr. *Ala'a M. Hussain*

(Supervisor)

Date: / /٢٠٠٧

Signature:

Name: ***Assit. Prof.***

Dr. Baha'a Ibrahim Kadhum

(Member)

Date: / /٢٠٠٧

Signature:

Name: ***Asst. Prof.***

Dr. Najim Abdul-Amir Sae'ed

(Member)

Date: / /٢٠٠٧

Signature:

Name: ***Asst. Prof.***

Dr. Ahmed A. Al – Rajihy

(Chairman)

Date: / /٢٠٠٧

Approval of the Mechanical Engineering Department

Head of the Mechanical Engineering Dept.

Signature:

Name: ***Asst. Prof. Dr. Adil A. Alwan Al- Moosawy***

Date: / /٢٠٠٧

Approval of the College Engineering

Dean of the College of Engineering

Signature:

Name: ***Prof. Dr. Abdul alwahid K. Rajih Al- Bakri***

Date: / /٢٠٠٧

List of Contents

Appendix- A

A.١ Shear Correction Factor of a Circular Cross-Section:

For parabolic distribution of shear stress in a circular cross-section, the shear stress τ is given by [٤٥]:

$$\tau = Q\frac{r^2 - y^2}{3I} \qquad \text{----- (A.١.١)}$$

Where:

Q: shear force at the section (N)

r: radius of the circular cross-section (m)

y: distance from the section neutral axis to the layer at which the shear stress required to be found (m)

I: second moment of area or area moment of inertia of a circular cross-section (m^4).

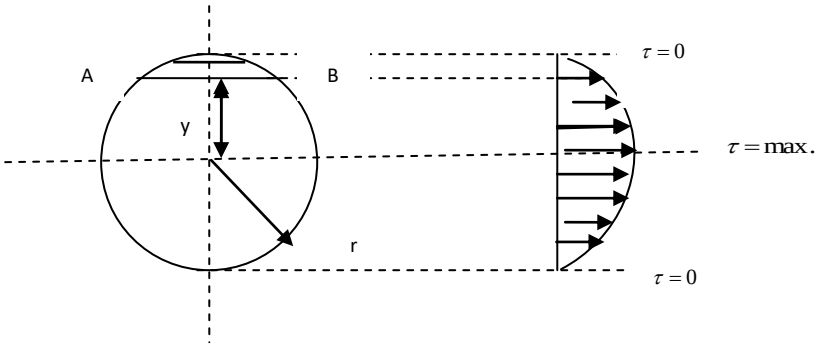

The parabolic distribution of the shear stress through a circular cross-section [٤٥]

The strain energy under shearing strain is given by:

$$\Omega = \int_{vol.} \frac{1}{2} \tau \ \gamma d\left(vol\right) = \int_{vol} \frac{\tau^2}{2G} d\left(vol\right) \qquad \text{----- (A.١.٢)}$$

For constant shear stress distribution:

$$\Omega_1 = \int_{vol} \frac{\tau^2}{2KG} d\left(vol\right) \qquad \text{----- (A.١.٣)}$$

Where K: shear correction factor. **A.١**

Assuming a segment of a beam of a circular cross-section of a unit length, Eq. ٣ becomes:

$$\Omega_1 = \frac{Q^2}{2KGA^2}\left(A*1\right) = \frac{Q^2}{2KG\left(\pi r^2\right)} \qquad \text{----- (A.١.٤)}$$

For parabolic shear stress distribution the strain energy Ω_2 can be given as:

$$\Omega_2 = \int_{vol} \frac{\tau^2}{2G}\, d\,(vol.) = \frac{1}{2G} \int_{vol} \frac{Q^2}{9\left(\frac{\pi}{4} r^4\right)^2} \left(r^2 - y^2\right)^2 * 2\sqrt{r^2 - y^2}\, dy$$

-----(A.١.٥)

Where d (vol.) = dA.l =dA at l = ١ unit

For a circular segment [٤٦]:

$$dA = ٢\sqrt{r^2 - y^2} * dy \qquad \text{----- (A.١.٦)}$$

Eq. A.١.٥ can be simplified as:

$$\Omega_2 = \frac{32Q^2}{18G\left(\pi r^2\right)^2 r^4} [2 * \int_0^r \left(r^2 - y^2\right)^{\frac{5}{2}} dy\,] \qquad \text{----- (A.١.٧)}$$

From integration tables [٤٦]:

$$\int \left(r^2 - y^2\right)^{\frac{5}{2}} dy = \frac{y}{6}\left(r^2 - y^2\right)^{\frac{5}{2}} + \frac{5r^2}{6}[\frac{1}{8}\{2y\sqrt{\left(r^2 - y^2\right)^3} \qquad \text{----- (A.١.٨)}$$

$$+3r^2 y\sqrt{\left(r^2 - y^2\right)} + 3r^4 \sin^{-1}\frac{y}{r}\}]$$

Insertion the integration limits and performing the above integration yields:

$$\int_0^r \left(r^2 - y^2\right)^{\frac{5}{2}} dy = \frac{5\pi r^6}{32} \qquad \text{----- (A.١.٩)}$$

Substituting Eq. ٩ into Eq. ٧ results in·

$$\Omega_2 = \frac{5\pi Q^2 r^2}{9G\left(\pi r^2\right)^2}$$ ----- (A.١.١٠)

Equating Ω_1 & Ω_2 gives:

$$\frac{Q^2}{2KG\left(\pi r^2\right)} = \frac{5\pi Q^2 r^2}{9G\left(\pi r^2\right)^2}$$ ----- (A.١.١١)

From which:

$$K = 0.9$$ ----- (A.١.١٢)

While for a rectangular cross-section [٤٧]:

$$K = 0.834$$ ----- (A.١.١٣)

A.٢ Proof of dA=det J $d\xi\, d\eta$:

Consider a mapping of variables from x, y to u_1, u_2, given as :

$x = x(u_1, u_2)$ & $y = y(u_1, u_2)$ -----(A.٢.١)

We assume that the above equations can be reversed to express u_1& u_2 in terms of x & y as that the correspondence is unique.

If a particle moves from a point P in such a way that u_2 is held constant and only u_1 varies, then a curve in the plane is generated. We call this the u_1 curve (Fig. A.٢.١). Similarly, the u_2 curve is generated by keeping u_1 constant and letting u_2 vary. Let r represent the vector of a point P:

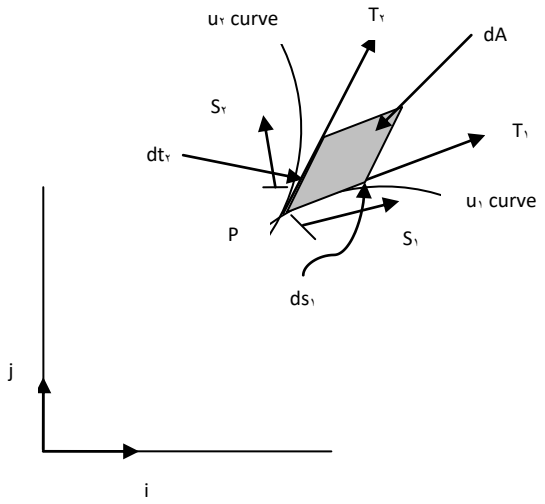

Fig. A.۲.۱

$$r = xi + yj \qquad \text{-----(A.۲.۲)}$$

Where i, j are unit vectors along x, y respectively. Consider the vectors

$$T_1 = \frac{\partial r}{\partial u_1} \qquad T_2 = \frac{\partial r}{\partial u_2} \qquad \text{-----(A.۲.۳)}$$

Or in view of Eq.(A.۲.۲):

$$T_1 = \frac{\partial x}{\partial u_1} i + \frac{\partial y}{\partial u_1} j \qquad \& \qquad T_2 = \frac{\partial x}{\partial u_2} i + \frac{\partial y}{\partial u_2} j \qquad \text{-----(A.۲.٤)}$$

We can show that T_1 is a vector tangent to the u_1 curve and T_2 is a vector tangent to the u_2 curve (Fig. A.۲.۱). To see this, we use the definition:

$$\frac{\partial r}{\partial u_1} = \lim_{\Delta u_1 \to 0} \frac{\Delta r}{\Delta u_1} \qquad \text{----- (A.۲.٥)}$$

Where $\Delta r = r(u_1+\Delta u_1) - r(u_1)$. In the limit, the chord Δr becomes tangent to the u_1 curve (Fig.A.٢.٢). However, $\partial r/\partial u_1$ or $(\partial r/\partial u_2)$ is not a unit vector. To determine its magnitude (length), we write:

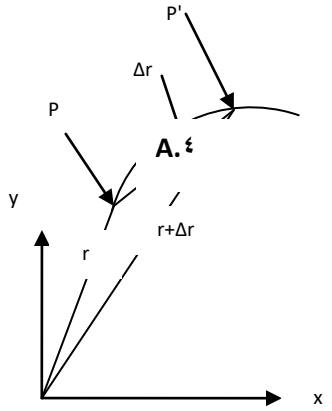

Fig. A.٢.٢

$$\frac{\partial r}{\partial u_1} = \frac{\partial r}{\partial s_1}\frac{ds_1}{du_1} \qquad \text{----- (A.٢.٦)}$$

Where s_1 is the arc length along the u_1 curve and ds_1 is the differential arc length. The magnitude of the vector:

$$\frac{\partial r}{\partial s_1} = \lim_{\Delta s_1 \to 0} \frac{\Delta r}{\Delta s_1}$$

Is the limiting ratio of the chord length to the arc length, which equals unity. Thus, we conclude that the magnitude of the vector $\partial r/\partial u_1$ is ds_1/du_1. We have

$$T_1 = \left(\frac{ds_1}{du_1}\right)t_1 \qquad \& \qquad T_2 = \left(\frac{ds_2}{du_2}\right)t_2 \qquad \text{----- (A.٢.٧)}$$

Where t_1 and t_2 are unit vectors tangents to the u_1 and u_2 curves respectively. Using Eq. A.٢.٧, we have the representation of the vectors $\mathbf{ds}_1$ & $\mathbf{ds}_2$ whose lengths are ds_1 & ds_2 (Fig. A.٢.١):

$\mathbf{ds_1} = t_1\, ds_1 = T_1\, du_1$

$\mathbf{ds_2} = t_2\, ds_2 = T_2\, du_2$ ----- (A.٢.٨)

The differential area **dA** is a vector with magnitude of *dA* and direction normal to the element area, which in this case is **K**. The vector **dA** in view of equations (A.٢.٤ & A.٢.٨) is given by the determinant rule:

$\mathbf{dA} = \mathbf{dS_1} * \mathbf{ds_2}$

$= \mathbf{T_1} \times \mathbf{T_2}\, du_1\, du_2$ A.٥

$$= \begin{vmatrix} \mathbf{i} & \mathbf{j} & \mathbf{k} \\ \dfrac{\partial x}{\partial u_1} & \dfrac{\partial y}{\partial u_1} & 0 \\ \dfrac{\partial x}{\partial u_2} & \dfrac{\partial y}{\partial u_2} & 0 \end{vmatrix} du_1\, du_2$$

$$= \left(\frac{\partial x}{\partial u_1}\frac{\partial y}{\partial u_2} - \frac{\partial x}{\partial u_2}\frac{\partial y}{\partial u_2} \right) du_1\, du_2 \mathbf{k}$$ ----- (A.٢.٨)

We denote the Jacobian matrix as:

$$\mathbf{J} = \begin{bmatrix} \dfrac{\partial x}{\partial u_1} & \dfrac{\partial y}{\partial u_1} \\ \dfrac{\partial x}{\partial u_2} & \dfrac{\partial y}{\partial u_2} \end{bmatrix}$$ ----- (A.٢.٩)

The magnitude *dA* can now be written as:

$$dA = \det \mathrm{J}\, du_1\, du_2$$ ----- (A.٢.١٠)

Which is the desired result. Note that if we work with ξ, η coordinates instead of u_1, u_2 coordinates, as in the text, then:

$$dA = detJ\, d\xi\, d\eta \qquad \text{----- (A.٢.١١)}$$

The relation derived above can be generalized to the three dimensions case as:

$$dv = \det \mathbf{J}\, d\xi\, d\eta\, d\zeta \qquad \text{----- (A.٢.١١)}$$

Where the Jacobian determinant det **J** expresses the ratio of the volume element dx dy dz in terms of dξ dη dζ.

Appendix – B

B.١ Shape Functions of an ٨-Nodes Quadrilateral Element:

This element belongs to the "serendipity" family of elements. The element consists ٨ nodes (Fig. B.١a) all of which are located on the boundary. Our task is to define shape functions N_i such that N_i=١ at node I and ٠ at all other nodes. In defining N_i, we refere to the master element shown in Fig. B.١b. First we define N_1-$N_٤$. For N_1, we note that N_1=١ at node ١ and zero at other nodes. Thus, N_1 has to vanish along the lines ξ = +١, η = +١ and ξ + η = -١ (Fig. B.١a). Therefore, N_1 is of the form:

$$N_1 = c\,(١-\xi)\,(١-\eta)\,(١+\xi+\eta) \qquad \text{-----(B.١.١)}$$

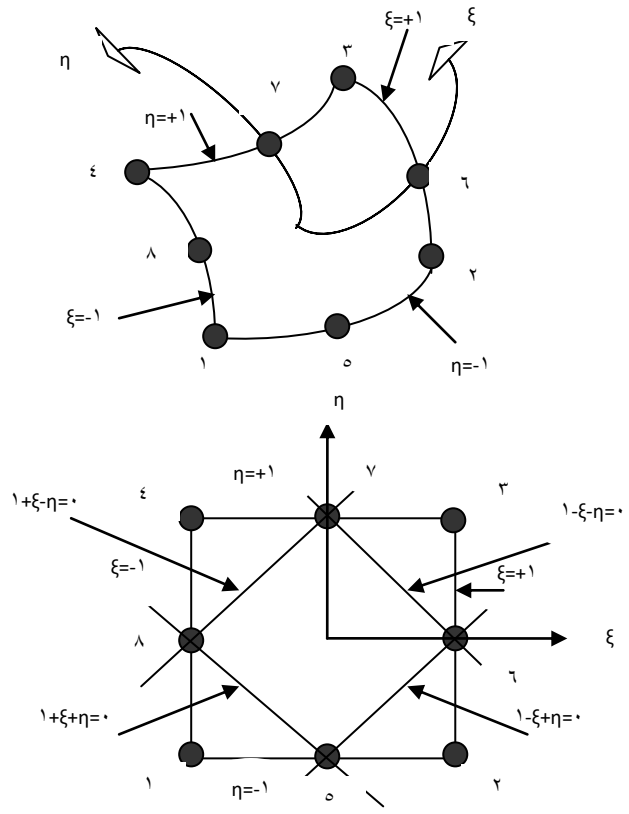

Fig. B.١.١

At node ١, N_1 = ١, ξ = η = -١. Thus, c = $-\frac{1}{4}$. Thereby and similarly, the shape functions $N_1 \rightarrow N_4$ will be in the form of:

$$N_1 = -\frac{(1-\xi)(1-\eta)(1+\xi+\eta)}{4}$$

B.١

$$N_2 = -\frac{(1+\xi)(1-\eta)(1-\xi \ldots,}{4}$$

$$N_3 = -\frac{(1+\xi)(1+\eta)(1-\xi-\eta)}{4}$$

$$N_4 = -\frac{(1-\xi)(1+\eta)(1+\xi-\eta)}{4}$$

----- (B.١.٢)

Now N_5, N_6, N_7 & N_8 are defined at the midpoints. For N_5, it vanishes along edges ξ = +١, η = +١ and ξ = -١. Consequently, it has to be of the form :

$$N_5 = c(1-\xi)(1-\eta)(1+\xi)$$
$$= c\left(1-\xi^2\right)(1-\eta) \qquad \text{-----(B.١.٣)}$$

The constant c in the above equation is found from the condition N٥ = ١ at node (٥) or N٥ =١ at ξ = ٠, η = -١. Therefore, c=(١/٢) and:

$$N_5 = \frac{\left(1-\xi^2\right)(1-\eta)}{2} \qquad \text{-----(B.١.٤)}$$

Similarly:

$$N_6 = \frac{(1+\xi)\left(1-\eta^2\right)}{2}$$
$$N_7 = \frac{\left(1-\xi^2\right)(1+\eta)}{2} \qquad \text{-----(B.١.٥)}$$
$$N_8 = \frac{(1-\xi)\left(1-\eta^2\right)}{2}$$

B.٢ Stress Transformation Matrix of B.٢ thotropic composite:

Sometimes the principal directions of orthotropy often don't coincide with the coordinate direction as shown in Fig. B.٢.١.a&b, where xy are the composite geometric coordinates x'y' are the principal material coordinates

such that the wrap angle is defined by cos (y',y) =cos θ. thus, a transformation matrix is required to transform the stresses from one set of a coordinate axes at a certain orientation to an other set at different orientation called "stress transformation matrix" which is (٦×٦) matrix for a three-dimensional state of stress and (٣×٣) for an orthotropic material under plain strain state of stress.

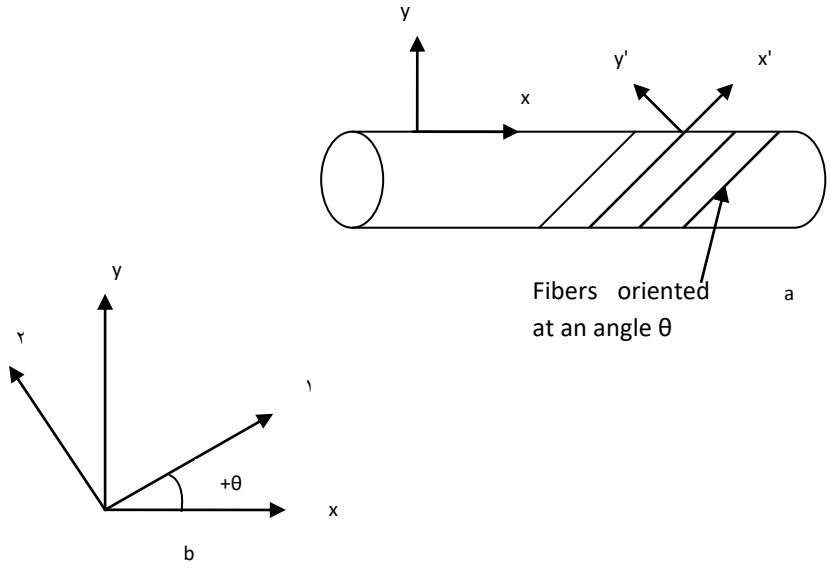

Fig. B.٢.١

From elementary mechanics of materials the transformation equations for expressing stresses in an x-y coordinate system in terms of those in ١-٢ coordinate system can be given as[٥٢]:

$$\begin{Bmatrix}\sigma_x\\ \sigma_y\\ \sigma_z\end{Bmatrix}=\begin{bmatrix}\cos^2\theta & \sin^2\theta & -2\sin\theta\cos\theta\\ \sin^2\theta & \cos^2\theta & 2\sin\theta\cos\theta\\ \sin\theta\cos\theta & -\sin\theta\cos\theta & \cos^2\theta-\sin^2\theta\end{bmatrix}\begin{Bmatrix}\sigma_1\\ \sigma_2\\ \tau_{12}\end{Bmatrix} \quad \text{-----(B.٢.١)}$$

Similarly, the strain transformation matrix is:

(If the tensor definition of shear strain is used which is equivalent to dividing the engineering shear strain by ٢) [١]:

$$\begin{Bmatrix} \varepsilon_x \\ \varepsilon_y \\ \dfrac{\gamma_{xy}}{2} \end{Bmatrix} = \begin{bmatrix} \cos^2\theta & \sin^2\theta & -2\sin\theta\cos\theta \\ \sin^2\theta & \cos^2\theta & 2\sin\theta\cos\theta \\ \sin\theta\cos\theta & -\sin\theta\cos\theta & \cos^2\theta - \sin^2\theta \end{bmatrix} \begin{Bmatrix} \varepsilon_1 \\ \varepsilon_2 \\ \dfrac{\gamma_{12}}{2} \end{Bmatrix} \qquad \text{-----(B.٢.٢)}$$

The transformations are commonly written as:

$$\begin{Bmatrix} \sigma_x \\ \sigma_y \\ \tau_{xy} \end{Bmatrix} = [T]^{-1} \begin{Bmatrix} \sigma_1 \\ \sigma_2 \\ \tau_{12} \end{Bmatrix}$$

$$\begin{Bmatrix} \varepsilon_x \\ \varepsilon_y \\ \dfrac{\gamma_{xy}}{2} \end{Bmatrix} = [T]^{-1} \begin{Bmatrix} \varepsilon_1 \\ \varepsilon_2 \\ \dfrac{\gamma_{12}}{2} \end{Bmatrix} \qquad \text{-----(B.٢.٣)}$$

Where the superscript -١ refers to the inverse of the matrix and:

$$T = \begin{bmatrix} \cos^2\theta & \sin^2\theta & 2\sin\theta\cos\theta \\ \sin^2\theta & \cos^2\theta & -2\sin\theta\cos\theta \\ -\sin\theta\cos\theta & \sin\theta\cos\theta & \cos^2\theta - \sin^2\theta \end{bmatrix} \qquad \text{-----(B.٢.٤)}$$

If a matrix [R] due to Reuter [٥٠] is introduced such that:

$$[R] = \begin{bmatrix} 1 & 0 & 0 \\ 0 & 1 & 0 \\ 0 & 0 & 2 \end{bmatrix} \qquad \text{-----(B.٢.٥)}$$

Then, the more natural strain vectors may be put in the form of:

$$\begin{Bmatrix} \varepsilon_1 \\ \varepsilon_2 \\ \gamma_{12} \end{Bmatrix} = [R] \begin{Bmatrix} \varepsilon_1 \\ \varepsilon_2 \\ \frac{\gamma_{12}}{2} \end{Bmatrix} \qquad \text{-----(B.٢.٦)}$$

$$\begin{Bmatrix} \varepsilon_x \\ \varepsilon_y \\ \gamma_{xy} \end{Bmatrix} = [R] \begin{Bmatrix} \varepsilon_x \\ \varepsilon_y \\ \frac{\gamma_{xy}}{2} \end{Bmatrix} \qquad \text{-----(B.٢.٧)}$$

Appendix – C:

C.١ Effective properties of E-glass/polyester:

The elastic properties of the constituent materials considered are:

For E-glass as a fiber and polyester as a matrix [٤٥]:

E_f GPa	ν_f	G_f GPa	E_m GPa	G_m GPa	ν_m
٧٢	٠.٢٢	٣٠	٣.٢	١.١٧٥	٠.٣٦

Table C.١.١: Elastic properties of E-Glass/Polyester at different fiber volume fractions

V_f %	E_1 *Gpa*	E_2 *Gpa*	ν_{12}	G_{12} *Gpa*	ν_{23}	G_{23} *Gpa*
٩٠	٦٥.١٢	٢٢.٨٦	٠.٢٣٤	٨.٦٨٧	٠.٣٤٥	٨.٥
٦٠	٤٤.٤٨	٧.٥	٠.٣٥	٢.٧٧	٠.٣٦	٣
٥٠	٣٧.٦	٦.١٣	٠.٢٩	٢.٢٩	٠.٢٨	٢.٤
٤٠	٣٠.٧٢	٥.٢	٠.٣٠٤	١.٩٠٨	٠.٢٩	٢.٠١٦

٣٠	٢٣.٨٤	٤.٤٨	٠.٣١٨	١.٦٥	٠.٣١١	١.٧
١٠	١٠.١	٣.٥٤	٠.٣٤٦	١.٢٩	٠.٣٦١	١.٣١

Table C.١.٢: Elastic properties of Kevlar-٤٩/polyester at different fiber volume fraction

V_f %	E_1 *Gpa*	E_2 *Gpa*	ν_{12}	G_{12} *Gpa*	ν_{23}	G_{23} *Gpa*
٦٠	٧٦.٢٨	٧.٧٠٤	٠.٣٥٤	٢.٨٣	٠.٣٦	٣
٥٠	٦٤.١	٦.٢٤	٠.٣٥	٢.٣	٠.٣٥٦	٢.٤
٤٠	٥١.٩٢	٥.٢٤	٠.٣٥٦	١.٩٢٦	٠.٣٦	١.٩٣
٣٠	٣٩.٧٤	٤.٥٢	٠.٣٥٧	١.٦٦	٠.٣٣٥	١.٧

Table C.١.٣: Elastic properties of the composite with various fibers of Kevlar-٤٩/Polyester **c.١** ٠٪ at E_m = ٣.٢GPa

E_f Gpa	G_f Gpa	ν_f	$E_{١}$ Gpa	$E_{٢}$ Gpa	$G_{١٢}$ Gpa	$G_{٢٣}$ Gpa	ν_{12}	ν_{23}
٧٢	٣٠	٠.٢٢	٣٧.٦	٦.١٣	٢.٢٩	٢.٤	٠.٢٩	٠.٢٨
١٢٥	٤٦.٣	٠.٣٥	٦٤.١	٦.٢٤	٢.٣٢	٢.٤	٠.٣٥٥	٠.٣
٣٠٠	١٠٧.١٤	٠.٤	١٥١.١	٦.٣٣	٢.٣٢	٢.٣٨٦	٠.٣٨	٠.٣٢٦
٤٠٠	١٤٨.١٥	٠.٣٥	٢٠١.٦	٦.٣٥	٢.٣٣	٢.٣٨٦	٠.٣٥٥	٠.٣٢٦

Table C.١.٤: Elastic properties of Kevlar-٤٩ with different matrices at a given fiber volume fraction V_f of ٤٠٪ at E_f =١٢٥ GPa

E_m Gpa	G_m Gpa	ν_m	$E_{١}$ Gpa	$E_{٢}$ Gpa	$G_{١٢}$ Gpa	$G_{٢٣}$ Gpa	ν_{12}	ν_{23}
٢	٠.٨	٠.٢٨	٥١.٢	٣.٣	١.٣٢	١.٣٤	.٣١	٠.٢٣
٢.٥	١	٠.٣	٥١.٥	٤.١١	١.٧	١.٦٣	٠.٣٢	٠.٢٦

٣.٢	١.١٧٥	٠.٣٦	٥١.٩٢	٥.٢٤	١.٩٢	١.٩٣	٠.٣٥٦	٠.٣٦
٤.٢٥	١.٦	٠.٣٥	٥٢.٥٥	٧	٢.٦	٢.٧	٠.٣٥	٠.٣
٥	١.٨٥	٠.٣٥	٥٣	١١.٨	٣	٤.٣٢	٠.٣٥	٠.٣٦

Table C.١.٥: Beam deflections and stresses induced at different fiber volume fractions for E-Glass/Polyester under a force of ١٥٠٠N

V_f %	$\sigma_{x,\max.}$ *Mpa*	$\sigma_{y,\max.}$ *Mpa*	$\sigma_{z,\max.}$ *Mpa*	$\tau_{yz,\max.}$ *Mpa*	$U_{y,\max.}$ mm
٩٠	٥.٩	٧	٤٥.٥	٣.٩	١.٨١٥
٦٠	٣.٩٢	٣.٩٢	٤٥.٤	٢.٢٩	٢.٩٩
٥٠	٢.٨٢	٢.٨	٤٥.٤	١.٨٩	٣.٥
٤٠	٣.٠٢	٢.٨٩	٤٥.٤	١.٩٢	٤.٣
٣٠	٣.٦٣	٣.٥٣	٤٥.٣	٢.١٤	٥.٦
١٠	٨.١٥	٨.٢	٤٥.٣	٤.١	١٢.٥٢

Table C.١.٦: Beam deflections and stresses induced at different fiber volume fractions for E-Glass/Polyester under a **C.٢** of ٣٠٠٠N- clamped case

V_f %	$\sigma_{x,\max.}$ *Mpa*	$\sigma_{y,\max.}$ *Mpa*	$\sigma_{z,\max.}$ *Mpa*	$\tau_{yz,\max.}$ *Mpa*	$U_{y,\max.}$ mm
٩٠	١١.٨	١٤	٩٠.٩	٧.٨	٣.٩٣
٦٠	٧.٨٤	١٢.٤	٩٠.٨	٤.٥٦	٥.٩٩
٥٠	٥.٤٨	١٢.٣	٩٠.٧	٣.٨٥	٧.١٢
٤٠	٦.٠٣	١٢.٣	٩٠.٧	٣.٨	٨.٧
٣٠	٧.٢٧	١٢.٥	٩٠.٧	٦.١١	١١.١٤٤
١٠	١٦.٣	١٦.٣	٩٠.٧	٨.١٩	٢٥.٣١

Table C.١.٧: Beam deflections and stresses induced at different fiber volume fractions for E-Glass/Polyester under a force of ٦٠٠٠N- clamped case

V_f %	$\sigma_{x,\max.}$ *Mpa*	$\sigma_{y,\max.}$ *Mpa*	$\sigma_{z,\max.}$ *Mpa*	$\tau_{yz,\max.}$ *Mpa*	$U_{y,\max.}$ mm
٩٠	٢٣.٦	٢٨.٤	١٨١	٨.٦	٧.٨٦
٦٠	١٥.٧	٢٤.٩	١٨٢	١٢.٥	١١.٩٨
٥٠	١١	٢٤.٥	١٨١	٧.٥٩	١٤.٢٤
٤٠	١٢.١	٢٤.٦	١٨١	٧.٦٩	١٧.٤
٣٠	١٤.٥	٢٤.٩	١٨١	١٢.٢	٢٢.٢٥
١٠	٣٢.٥	٣٢.٨	١٨١	١٦.٤	٥٠.٦٣

Table C.١.٨: Beam deflections and stresses induced at different fiber volume fractions for E-Glass/Polyester under a force of ١٢٠٠٠N- clamped case

V_f %	$\sigma_{x,\max.}$ *Mpa*	$\sigma_{y,\max.}$ *Mpa*	$\sigma_{z,\max.}$ *Mpa*	$\tau_{yz,\max.}$ *Mpa*	$U_{y,\max.}$ mm
٩٠	٤٧.٢	٥٦.٨	٣٦٣	٢٥.٢	١٤.٧٢
٦٠	٣١.٤	٤٩	٣٦٣	٢٤.٩	٢٣.٩٧
٥٠	٢١.٩	٤٩	٣٦٣	٢٤.٦	٢٨.٥
٤٠	٢٤.١	٤٩.٣	٣٦٣	٢٤.٥	٣٤.٨
٣٠	٢٩	٤٩.٧	٣٦٣	٢٤.٤	٤٤.٥
١٠	٦٥	٦٥.٦	٣٦٣	٣٢.٨	١٠١.٢٦

Table C.١.٩: Beam deflections and stresses with various matrix materials

C.٣

E_m GPa	G_m GPa	υ_m	$\sigma_{x\ max.}$ MPa	$\sigma_{y\ max.}$ MPa	$\sigma_{z\ max.}$ MPa	$\tau_{yz\ max.}$ MPa	$U_{max.}$ mm
٢	٠.٨	٠.٢٨	٢.٢٢	١١.٩	٩١.٨	٦.٢٤	٥.٨٥
٢.٥	١	٠.٣	٢.٨٣	١٢	٩١.٣	٦.٢	٥.٦٣
٣.٢	١.١٧٥	٠.٣٦	٤.٧٩	١٢.٣	٩١.٢	٦.١٤	٥.٤٣
٤.٢٥	١.٦	٠.٣٥	٥.٤	١٢.٣	٩٠.٨	٦.١٤	٥.٢
٥	١.٨٥	٠.٣٥	١٠.٤	١٢.٨	٩٠.٩	٦.٣١	٤.٩

Table C.١.١٠:Beam deflections and stresses with various Fiber materials

E_f GPa	G_f GPa	υ_f	$\sigma_{x\ max.}$ MPa	$\sigma_{y\ max.}$ MPa	$\sigma_{z\ max.}$ MPa	$\tau_{yz\ max.}$ MPa	$U_{max.}$ mm
٧٢	٣٠	٠.٢٢	٥.٤٨	١٢.٣	٩٠.٧	٣.٨	٧.١٢٣
١٢٥	٤٦.٣	٠.٣٥	٤.٠٥	١٢.٢	٩١.٢	٦.١٥	٤.٤٢٣
٣٠٠	١٠٧.١٤	٠.٤	٢.٥٤	١٢.١	٩٣.٢	٣.٩٣	٢.٢١٣
٤٠٠	١٤٨.١٥	٠.٣٥	٢.٥	١٢	٩٤.٢	٣.٩٦	١.٨١

Table C.١.١١: Beam deflections and stresses with composite elastic properties

For E-Glass/Polyester under ٣٠٠٠N

ν_{12}	G_{12} GPa	$\sigma_{x\ max.}$ MPa	$\sigma_{y\ max.}$ MPa	$\tau_{12\ max.}$ MPa	$U_{max.}$ mm
٠.٣٤٦	١.٢٩	١٦.٣	١٦.٤	٨.١٩	٢٥.٣١
٠.٣١٨	١.٥	٧.٢٧	١٢.٥	٦.١١	١١.١٤
٠.٣٠٤	٢	٦.٠٣	١٢.٣	٣.٨	٨.٧
٠.٢٩	٢.٢٦	٥.٤٨	١٢.٣	٣.٨	٧.١٢
٠.٢٧٦	٢.٧٥٥	٧.٨٤	١٢.٤	٤.٥٦	٥.٩٩
٠.٢٣٤	٨.٦٨٧	١١.٨	١٤	٧.٨	٣.٩٣

Appendix – D:

Macro- and microstresses and displacements of the unit cell, fibers and matrix as obtained by ANSYS v-٥.٤ at constant fiber diameter under a bending load of ٣٠٠٠N.

D.١ For the unit cell, the macroscopic values at various fiber volume fractions are as following:

V_f %		σ_x max. GPa	σ_y max. GPa	σ_z max. GP	U_x max. mm	U_y max. mm	U_z max. mm
				C.٤			
٩٠	cl.	٧٦.٢	١٤٦	٥٩.٢	٠.٠٤	٠.٠٧	٠.٠٠٤
	s.s.	٣٦.٨	١٣.٨	١٥.٤	٠.٠٢	٠.٠١٤	٠.٠٠٤
٦٠	cl.	٣٧	٣٨	١٨	٠.٠٩	.٠٧٧	.٠١
	s.s.	٣٦.٣	١٣.٥	١٧.٥	٠.٠٧٤	٠.٠٧٧	٠.٠١
٥٠	cl.	٢٦.٤	٣٦	٢١	٠.٠٧٥	٠.١	٠.٠١٦
	s.s.	٢٩.٤	٣٢.٤	١٧	٠.٠٨٤	٠.٠٩٣	٠.٠١٣
٤٠	cl.	٣١	٤٤.٦	٢٢.٧	٠.١٠٨	٠.٠٠٥٨	٠.٠٢
	s.s.	١٨	١٦.٦	١٦.٧	٠.٠٦٧	٠.٠٦٣	٠.٠١٧
٣٠	cl.	٢٧.٥	٩.٤١	٢١	٠.١٣٥	٠.٠٠٥٥	٠.٠٣١
	s.s.	١٩.٢	٩	١٦.٦	١	٠.٠٤٥	٠.٠٢٤
١٠	cl.	٣٤	٤٧.٥	٢١.٢	٠.٣٥٨	٠.٠٠٤٦	٠.٠٨٣٧
	s.s.	٢١	٨.١	١٥.٨	٠.٢١٦	٧ ٠.٠٨٣	٠.٠٧

D.٢. The nodal microscopic elastic strains at the corner nodes of the unit cell are as following for the clamped case at various fiber volume fractions:

D.٢.١ At V_f = ٩٠٪:

Node no.	ε_x	ε_y	ε_z
١٢٢	-٠.٤٣e-٤	-٠.٤٦e-٣	٠.٠٠١
١٢٣	-٠.٣٤e-٢	-٠.٢٢٦e-٢	٠.٠٠١
١٣٣	-٠.٠١٠٣	-٠.٢٨١e-٣	٠.١٦e-٢
١٤٣	-٠.٦٢e-٢	-٠.١٣٦e-١	٠.١٤٣e-٢

D.٢.٢ At V_f = ٦٠٪:

D.١

Node no.	ε_x	ε_y	ε_z
١٢٢	٠.١٦e-٢	-٠.٢٦e-٢	٠.٦٢٤e-
١٢٣	٣٠.٣٨٢e-٢	٠.٣٧٤e-٢	-٠.١٨e-٢
١٣٣	-٠.٥٥٥e-٢	-٠.١٣٦e-٢	٠.٥٦e-٣
١٤٣	-٠.٥٦e-٢	-٠.١٠٥e-١	٠.١٢٤e-٢

D.٢.٣ At V_f = ٥٠٪:

Node no.	ε_x	ε_y	ε_z
١٢٢	٠.٦٥e-٣	-٠.١١٤e-٢	٠.٧٦e-٣
١٢٣	-٠.٤١٦e-٢	-٠.٢٥e-٢	٠.٤٤e-٣
١٣٣	-٠.٠١٣٦	٠.٠٠١٠٢	٠.٠٠١١
١٤٣	-٠.٠١	-٠.٠١٥	٠.٠٠٠٨

D.٢.٤ At V_f = ٤٠٪:

Node no.	ε_x	ε_y	ε_z

١٢٢	٠.٠٠٣	-٠.٠٠٢٠٥	٠.٠٠١١٢
١٢٣	-٠.٠٠٥٣	-٠.٠٠٣٠١	٠.٠٠٠٦١
١٣٣	-٠.٠٢١	-٠.٠٠٢	٠.٠٠١٢٥
١٤٣	-٠.٠١٢٦	-٠.٠٢٤٥	٠.٠٠٠٥٥

D.٢.٥ At V_f = ٣٠٪:

Node no.	ε_x	ε_y	ε_z
١٢٢	٠.٠٠٠٢٣	٠.٠٠٠٢١	٠.٠٠٠٥٤
١٢٣	-٠.٠٠٦٣	-٠.٠٠٤١	٠.٠٠٠٧٧
١٣٣	-٠.٠٢٠٢	٠.٠٠٢٦	٠.٠٠٢٥
١٤٣	-٠.٠٢	-٠.٠٢	٠.٠٠٥٧٣

D.٢.٦ At V_f = ١٠٪:

D.٢

Node no.	ε_x	ε_y	ε_z
١٢٢	-٠.٠٠١٦	-٠.٠٠٠٣٧	٠.٠٠٢
١٢٣	-٠.٠٠٨٨	-٠.٠٠٣٦٦	٠.٠٠٢٢
١٣٣	-٠.٠٢٥٣	٠.٠٠٣٥٢	٠.٠٠٧٨
١٤٣	-٠.٠١٦	-٠.٠٣	٠.٠٠٨١٥

D.٣ The nodal microscopic elastic strains at the corner nodes of the unit cell are as following for the simply supported case at various fiber volume fractions with constant fiber diameter:

D.٣.١ At V_f = ٩٠٪:

Node no.	ε_x	ε_y	ε_z
١٢٢	٠.٢٧e-٤	-٠.٤٢٥e-٣	٠.٣٣٥e-٣
١٢٣	٠.٧٣٢e-٣	٠.٨٦e-٣	-٠.١٦e-٣
١٣٣	-٠.٢٠٦e-٢	-٠.٦e-٣	٠.٤٣e-٣

١٤٣	-٠.١٦e-٢	-٠.٠٠٤	٠.٧٧e-٣

D.٣.٢ At V_f = ٦٠٪

Node no.	ε_x	ε_y	ε_z
١٢٢	٠.١٦e-٢	-٠.٢٦e-٢	٠.٦٢e-٣
١٢٣	٠.٣٨e-٢	٠.٣٧e-٢	-٠.٢e-٣
١٣٣	-٠.٥٧e-٢	-٠.١٤e-٢	٠.٥٣٣e-٣
١٤٣	-٠.٥٥e-٢	-٠.١٠٧e-١	٠.١٢٧e-٢

D.٣.٣ At V_f = ٥٠٪:

Node no.	ε_x	ε_y	ε_z
١٢٢	٠.١٣e-٤	-٠.٢٦e-٢	٠.٦e-٣
١٢٣	٠.٤٥e-٢	٠.٤٥e-٢	-٠.٢e-٣
١٣٣	-٠.٥٢٢e-٢	-٠.١e-٢	٠.٧٣e-٣
١٤٣	-٠.٦e-٢	-٠.١٠٧	٠.٠٠١٤

D.٣.٤ At V_f = ٤٠٪:

D.٣

Node no.	ε_x	ε_y	ε_z
١٢٢	٠.٨٤٣e-٣	-٠.٠٠١٧	٠.٤٦e-٣
١٢٣	٠.٢٨e-٢	٠.٢٨e-٢	-٠.١١e-٣
١٣٣	-٠.٤٦e-٣	-٠.٤e-٣	٠.٦٤e-٣
١٤٣	-٠.٥e-٢	-٠.٧٤٤e-٢	٠.١٠١

D.٣.٥ At V_f = ٣٠٪:

Node no.	ε_x	ε_y	ε_z
١٢٢	٠.٨٦e-٣	-٠.٢e-٢	٠.٦e-٣
١٢٣	٠.٢e-٢	٠.٢٣٥e-٢	-٠.٣e-٤
١٣٣	-٠.٧٤e-٢	٠.٤٢e-٣	٠١٢٤e-٢
١٤٣	-٠.٦٥e-٢	-٠.٠١	٠.١٦٥e-٢

D.٣.٦ At V_f = ١٠٪:

Node no.	ε_x	ε_y	ε_z
١٢٢	٠.٢٢٧e-٣	-٠.١٦e-٢	٠.١٤e-
١٢٣	٠.٠٠١٤	٠.٠٠٢٤	-٠.٤١٣e-٣
١٣٣	-٠.٠١	-٠.١٢e-٢	٠.٢١e-٢
١٤٣	-٠.٦٧٣e-٢	-٠.٠١٤٣	٠.٣٤٢

D.٤ Unit Cell Results Based on Fiber Diameter Variation:

Macro- and microscopic results of the unit cell obtained when fiber diameter is changed at constant fiber volume fraction are as tabulated in the following tables:

D.٤.١ the macroscopic values of D.٤ the unit cell at various fiber diameters:

Fiber diam. mm	σ_x max. GPa	σ_y max. GPa	σ_z max. GPa	U_x max. mm	U_y max. mm	U_z max. mm

٠.٩	cl.	١.٩٦	٢.٨٧	١.٥٥	٠.٠٢٦	-٠.٠٠١	٠.٠٠٥٧
	s.s.	٧.٦٧	٢٤.٨	١٥.٩	٠.٠٧٢	٠.٣٣	٠.٠٥٧
٠.٦	cl.	٥.٥	٤.٢٧	٧.٦٢	٠.١	٠.٠٠٨	٠.٠٥٣
	s.s.	١١.٥	٣٧.٢	١٧.٩	٠.٠٧٢	٠.٣٣	٠.٠٤
٠.٤	cl.	١٠.٦	١٥.٥	٨.٠٧	٠.٠٦٢	٠.٠٠٢٧	٠.٠١٣
	s.s.	١٧.٣	٥٥.٩	٢٣.٨	٠.٠٧	٠.٣٣	٠.٠٢٦

D.٤.٢ The nodal microscopic elastic strains at the corner nodes of the unit cell are as listed below for the clamped case at various fiber diameters:

D.٤.٢.١ At D_f = ٠.٩mm:

Node no.	ε_x	ε_y	ε_z
١٢٢	٠.١٦e-٤	-٠.٧٦e-٤	٠.٦٧e-٤
١٢٣	-٠.٤٢e-٣	-٠.٢٤e-٣	٠.٤١e-٤
١٣٣	-٠.٠٠١٢	٠.١٦e-٣	٠.١٣٢e-٣
١٤٣	-٠.٨٥e-٣	-٠.٠٠١٣	٠.١٠٢e-٣

D.٤.٢.٢ At D_f = ٠.٦mm:

Node no.	ε_x	ε_y	ε_z
١٢٢	-٠.٠٠٢٢	٠.٠٠٣٨	-٠.٠٠٠٢١٧
١٢٣	-٠.٢e-٢	٠.١٤e-٤	-٠.٥٦e-٤
١٣٣	-٠.٣٧٣e-٢	-٠.١e-٢	-٠.٥٦e-٤
١٤٣	-٠.٥٣e-٣	-٠.٠٠٥١٥	٠.٠٠١٠٧

D.٤.٢.٣ At D_f = ٠.٤mm:

D.٥

Node no.	ε_x	ε_y	ε_z
١٢٢	٠.٤e-٣	-٠.٥٢e-٣	٠.٣٨٧e-٣
١٢٣	-٠.٢١e-٢	-٠.١٢e-٢	٠.٢٢e-٣
١٣٣	-٠.٠٠٧	٠.٤١٤e-٣	٠.٥٧e-٣
١٤٣	-٠.٤٧e-٢	-٠.٧٥e-٢	٠.٤٥e-٣

D.٤.٣ The nodal microscopic elastic strains at the corner nodes of the unit cell are as listed below at constant fiber volume fraction for the simply supported case at various fiber diameters:

D.٤.٣.١ At D_f = ٠.٩mm:

Node no.	ε_x	ε_y	ε_z
١٢٢	-٠.١٤٥e-٣	-٠.٣e-٤	-٠.٣e-٣
١٢٣	٠.٣٥٦e-٢	٠.٢٥٥e-٢	-٠.٣٠٣e-٣
١٣٣	٠.٦٥e-٢	-٠.٥٨e-٣	-٠.٤e-٣
١٤٣	٠.٤٠٤e-٢	٠.٦٠٨e-٢	-١e-٤

D.٤.٣.٢ At D_f = ٠.٦mm:

Node no.	ε_x	ε_y	ε_z
١٢٢	-٠.٢٢١e-٣	-٠.٤٣e-٤	-٠.٤٢١e-٣

١٢٣	٠.٥٣١e-٢	٠.٣٧٨e-٢	-٠.٤٤e-٣
١٣٣	٠.٠١	-٠.٨٨e-٣	-٠.٥e-٣
١٤٣	٠.٥٤e-٢	٠.٨٢e-٢	-٠.٢٨e-٣

D.٤.٣.٣ At D_f = ٠.٤mm:

D.٦

Node no.	ε_x	ε_y	ε_z
١٢٢	-٠.٣١٣	-٠.٨e-٤	-٠.٦٣e-٣
١٢٣	٠.٨e-٢	٠.٠٠٥٦٧	-٠.٧e-٣
١٣٣	٠.٠١٤٦	-٠.٠٠١٣٧	-٠.٠٠٠٨٨
١٤٣	٠.٠٠٨٤	٠.٠١٣٣	-٠.٠٠٠١١٤

Appendix – E:

The dimensions of the unit cells according to fibers volume fractions and the forces applied with the associated areas considered in the present study can be listed in the following tables:

E.١ For simply supported case:

V_f %	σ_x MPa	σ_y MPa	σ_z MPa	A_x $mm^٢$	A_y $mm^٢$	A_z $mm^٢$	F_x N	F_y N	F_z N
٩٠	٢.٩	١.٤	٧٠.٢	٠.٨٧	١.٥٠٦	٠.٠١٤	٢.٥	٢.١١	١
٦٠	٣.٤٢	٢.٥٧	٧٣.٩	١.٠٦٧	١.٨٥٥	٠.٠٢٠٥	٣.٦٥	٤.٧٥	١.٥
٥٠	٣.٢	٢.٥٦	٧٣	١.١٨	٢.٠٤	٠.٠٢٥	٣.٧٨	٥.٢٢	١.٨٢٥

٤٠	٢.١٧	١.٤٤	٧١	١.٣٢	٢.٢٨	٠.٠٣١٣	٢.٨٦٦	٣.٣	٢.٢٢
٣٠	٢.٦٥	٠.٩١٦	٧١.٠٧	١.٥٢٤	٢.٦٤	٠.٠٤٢	٤.٠٤	٢.٤٢	٣
١٠	٤.٨	١.٢٨	٧١.٤	٢.٦٠٥	٤.٥١٢	٠.١٢٥	١٢.٥	٥.٧٧	٩

E.٢ For clamped case:

E.١

V_f %	b mm	σ_x MPa	σ_y MPa	σ_z MPa	A_x mm^2	A_y mm^2	A_z mm^2	F_x N	F_y N	F_z N
٩٠	٠.١٢٥٥	٦.٣٣	٧.٩	٩٠.٩	٠.٨٧	١.٥٠٦	٠.٠١٤	٥.٥١	١١.٩	١.٢٤
٦٠	٠.١٥٤	٤.١	٤.٣٦	٩٠.٧٧	١.٠٦٧	١.٨٥٥	٠.٠٢٠٥	٤.٤	٨.٠٦	١.٨٦٥
٥٠	٠.١٧	٣	٣.٣٤	٩٠.٧	١.١٨	٢.٠٤	٠.٠٢٥	٣.٥٣٤	٦.٨١٤	٢.٣
٤٠	٠.١٩	٣.٢	٣.٣٦	٩٠.٧	١.٣٢	٢.٢٨	٠.٠٣١٣	٤.٢١٢	٧.٧	٢.٨٣
٣٠	٠.٢٢	٣.٨٥	٤.٠٢٥	٩٠.٦٦	١.٥٢٤	٢.٦٤	٠.٠٤٢	٥.٨٧	١٠.٦٢	٣.٨
١٠	٠.٣٧٦	٨.٨٦	٨.٨٨	٩٠.٧	٢.٦٠٥	٤.٥١٢	٠.١٢٥	٢٣.١	٤٠.٠٧	١١.١٠٥

E.٣ Unit cell data based on fiber diameter variation:

E.٣.١ For clamped case:

Fiber diam. mm	b mm	A_x mm^2	A_y mm^2	A_z mm^2	F_x N	F_y N	F_z N
٠.٩	٠.٦٧٧	٤.٦٩	٨.١٢٤	٠.٣٩٦	١٥	٢٧.١٣	٣٦

٠.٦	٠.٣	٢.٠٧٨	٣.٦	٠.٠٧٧	٦.٦٥	١٢	٧.١
٠.٤	٠.٤٥٢	٣.١٣	٥.٤٢٤	٠.١٧٧	١٠.٠٢	١٨.١١	١٦
٠.٢٥	٠.١٩	١.٣٢	٢.٢٨	٠.٠٣١٣	٤.٢٢٤	٧.٦٦	٢.٨٣٨

E.٣.٢ For simply supported case:

Fiber diam. mm	F_x N	F_y N	F_z N
٠.٩	١١.٤	٦٢.٧	٢٨.٣٣
٠.٦	٧.٦١	٤١.٨٧	١٢.٦٣
٠.٤	٥	٢٧.٨	٥.٥٦٣
٠.٢٥	٣.٢	١٧.٦	٢.٢٣

CHAPTER ONE

Introduction :

١.١ General:

A composite material can be defined as a result of a combination of two or more of distinct constituents or phases on a macroscopic scale, yielding a material meeting some required mechanical, physical, chemical and / or thermal properties [١ & ٢]. The composites consist of one or more of discontinuous phases embedded in a continuous. The discontinuous phase is usually harder & stronger than the continuous phase and is called "Reinforcement or Reinforcing material" where as the continuous phase is

known as the matrix. The most notable exception to this rule is the class of materials known as the "Rubber-Modified Polymers" consisting of a rigid polymer matrix, filled with rubber particles.

The properties of composites are strongly affected by the properties of the constituent materials, their distribution & the interaction among them. To describe a composite material, in addition to specifications of constituent materials & their properties, it is necessary to specify the geometry of the reinforcing phase in terms of shape, size & size distribution. The properties that can be enhanced by the process of forming a composite material are:

١. Strength ٢. Stiffness ٣. Corrosion & Wear resistance ٤.Attractiveness ٥. Fatigue Life ٦. Weight ٧.Thermal and/or Sound insulation ٨. Temperature - dependant behavior ٩. Chemical resistance. One or more of the above properties can be simultaneously enhanced.

١.٢ Classification of Composite Materials :

Generally composite materials can be classified according to the geometry & type of reinforcing phase to the following main categories [٣], namely:

١. Fiber reinforced composite materials (FRCM) which consist of fibers and matrix, where the fiber is distinguished by its length being much greater than its cross-sectional dimensions.

٢. Particle-Reinforced composite materials (PRCM) which consist of particles in matrix, where the particle is nonfibrous in nature & of spherical, cubic, tetragonal, a platelet or of other regular or irregular shapes, but it is approximately equiaxed.

٣. Laminated composite materials (LCM) which consist of layers in a matrix.

٤. Foams composite materials which consist of solid & gas.

There are subclassified types which are in fact a preferred combination of two or more of the main types, such as fiber- reinforced laminated composite materials which is a combination of the first and the third types or fiber-reinforced particulated composite materials which consist of layers containing particles & reinforced by a certain type of fibers [٣].

Fibers can be geometrically characterized by their high length-to-diameter ratio and their crystallized diameter. Properties of some types of fibers are listed in table ١.١ whose data are assembled and gathered with other conventional engineering structural materials in order to show the effectiveness of fibers especially in weight-sensitive applications as in aerospace industries.

Table ١.١ Properties of fibers & conventional bulk materials [٢ & ٣]

Material of Fiber	Tensile Modulus (GN/m^2) (E)	Tensile Strength (GN/m^2) (σu)	Density (ρ) (g/cm^3)	Specific Modulus (E/ρ)	Specific Strength ($\sigma u/\rho$)
E-glass	٧.٢٤	٣.٥٩	٢.٥٤	٢٨.٥	١.٣٨
S-glass	٨٥.٥	٤.٦[a]	٢.٤٨	٣٤.٥	١.٨٥
Graphite(high modulus)	٣٩٠	٢.١	١.٩	٢٠٥	١.١
Graphite(high tensile)	٢٤٠	٢.٥	١.٩	١٢٦	١.٣
Boron	٣٨٥	٢.٨	٢.٦٣	١٤٦	١.١
Silica	٧٢.٤	٥.٨	٢.١٩	٣٣	٢.٦٥
Tungsten	٤١٤	٤.٢	١٩.٣	٢١	٠.٢٢

Beryllium	٢٤٠	١.٣	١.٨٣	١٣١	٠.٧١
Kevelar-٤٩ Aramid Polymer	١٣٠	٢.٨	١.٥	٨٧	١.٨٧
Steel	٢١٠	٠.٣٢-٢.١	٧.٨	٢٦.٩	٠.٠٣٤-٠.٢٧
Al-alloys	٧٠	٠.١٤-٠.٦٢	٢.٧	٢٥.٩	٠.٠٥٢-٠.٢٣

One of the important steps in specifying a composite material for a certain application is the assessment of its constituent materials, i.e. the reinforcing and matrix phases, an equal attention should be payed to compatibility and processability. Clearly these are interrelated as the processes of forming the material and fabricating the structure occur concurrently. In almost all cases of structural applications, the fibers act as the primary load bearing constituent.

The matrix is a multi-function constituent, such that it combines the fibers and other inter-phases (if any) together to form the overall and final configuration of the composite material. It mainly serves as the medium of load transferring onto the fibers. A further function of the matrix is to protect the interface and the fibers from the action of any environmental effects.

For many components, the role of the matrix may not be entirely non-structural, however, as it can not always be assumed that all loads will act along the fibers direction. When this is the case, the properties become strongly influenced by the matrix characteristics. In general terms, a matrix can take the form of any material (metallic, ceramic or polymeric). However, those that have attracted most interest are those based on polymeric systems, the others are still in their formative stages of development.

Polymers used as matrices can be one of two types. The first and the most common are those known as "Thermosetting Plastics" where the solidification from the liquid phase takes place by the action of an irreversible chemical cross linking reaction. The second type are thermoplastics in nature, their forming can be carried out as a result of the physical processes of melting and freezing. Generally speaking these reactions are reversible. Table ١.٢ shows the properties of some well-known polymeric-base-matrix fiber reinforced composite materials.

Table ١.٢ Typical mechanical properties of composites [٣]

Composite type	Modulus ٠° (GPa)	Modulus ٩٠° (GPa)	Shear Modulus (GPa)	ILSS (MPa)	Poisson's Ratio(ν)	Density g/cm^3
UD E-Glass/epoxy	٣٩	١٥	٤	٩٠	-	١.٩٢
UD carbon/epoxy	١٣٤	١١	٥	٩٤	٠.٢٦	١.٥٧
± ٤٥woven E-glass/epoxy	١٠	١٠	٨	٤٨	٠.٧	١.٩٢
CSM E-glass/polyester	٨	٨	٢.٧٥	-	٠.٣٢	١.٤٥
UD aramid/epoxy	٧٦	٥	٢	٨٣	٠.٣٤	١.٣٨

٠/٩٠ woven carbon/epoxy	٧٠	٧٠	٥	٥٧	-	١.٥٣
± ٤٥ woven carbon/epoxy	١٨	١٨	٢٧	٥٧	-	١.٥٣
٠/٩٠ woven aramid/epoxy	٣١	٣١	٢	٧٠	-	١.٣٣

Note: UD unidirectional , CSM chopped strand mat , ILSS interlaminar shear strength .

١.٣ Present and Future Applications of PMCM:

Currently the composite materials are the most commonly used engineering materials in various industries and fields of economy starting from the simplest toys passing by the medium and heavy civil and military machineries & finishing at the largest aerospace applications .

Nearly every aerospace company is developing products made with fiber reinforced composite materials. The usages of composites have progressed through several stages in the past ٧٠ years [١]. First, was the stage of demonstration pieces were built under the philosophy "let us see If we can build one". They may have never been any intention to put the part in the actual service. The second stage was the "replacement parts" which can be characterized by replacing the malfunctioned metallic parts by a corresponding composite one. Boron/epoxy fuselage sections and horizontal tail on the "General Dynamics F-١١١" are examples of both stages mentioned above. The third and serious stage is the "Actual production pieces" where the plane designed and fabricated from the beginning to have various parts produced from fiber-reinforced composites. The final striking stage is the whole-

composite airplane. The following table whose data are assembled and gathered gives a synopsis for some main applications of composite materials .

Table ١.٣ some main applications of composites [١ & ٤]

Applications or Industries	Parts
Marines	Boats, Fairing, Deck houses, Tanks, Deep submergence.
Airplanes	Rudders,Radomes,Fuselags,Stabilizers
Aerospace	Rocket motor cases,Radoms,Air launched missile.
Automobiles	Windshields,Tyres,Interior parts of persons cabinet.
Sports	Ping-pong & Tennis rackets,Gymnastic Equipments.
Machineries	Engine joints & pads, Electric & electronic parts.
Medical Applications	Medical bedstead mats, medical and some surgery appliances.

١.٤ The Objective of the Present Work:

The objective of the present work is to study & analyze the stresses induced in a unidirectional fiber-reinforced composite beam subjected to transverse bending loads. There are various methods for carrying this function out, the exact method for example is sometimes adopted to solve a number of structural designing problems especially when the governing equations

describing the structure behavior are available [٣]. Otherwise the finite element method [FEM] is assorted to, to perform this purpose or any other numerical solution method such as finite difference. The unit cell method in micromechanical analysis is adopted in this study to capture the state of stresses and strains in the beam referred to above due to its multiple and ramified advantages mentioned later by using the finite element formulation as a numerical approach for the solution. In this analysis the effects of the following parameters are investigated:-

١. Fiber size at a given fiber volume fraction.
٢. Type of fiber & matrix.
٣. Fibers distribution method.
٤. Boundary conditions of the model of interest such as type of loading and supporting method.

Chapter Two

Literature Review

٢.١ General:

The analysis of mechanics of composite material response can take place on a number of levels. On micromechanical basis assumptions can be made regarding the nature of the interaction between the constituents and expressions derived to relate the behavior of fiber and matrix directly to that of composite.

Modern technology has found vast applications for unidirectionally fiber-reinforced composite materials. To make an effective use of these materials, knowledge of their properties and performance is of a major importance [٥]. Many aspects of their behavior are directly related to the microstructure. The need and wish to understand and interpret these materials drive the researches in this field into the micro-mechanics of this type of materials [٦ & ٧].

However, when the micromechanical behavior of such a composite material is of interest, one has to take account of the heterogeneity between fibers and matrix. All the foregoing concepts make the need of a more realistic prediction of the structural behavior of composite materials too much

necessary. Generally, there are two basic approaches to the micromechanics of the composite materials, namely:-

١. Mechanics of materials approach.
٢. Elasticity approach.

The objective of all of the micromechanics approaches is to determine the elastic moduli, stiffnesses or compliances of a composite material in terms of its constituents moduli, for example the elastic moduli of a fiber reinforced composite must be determined in terms of those of fibers and matrix and fiber volume fractions of them, the same is said about the other composite properties determination [١].

٢.٢ Review of Micromechanical Approaches of Composites:

With rapidly growing computational modeling capacity, the micromechanical analysis of FRCM has become an important means of understanding the behavior of these materials. The works that have been done on the micromechanical study of the composite structures can be divided into four groups.

Some of the important works of these groups assumed a perfect bonding between the fibers and matrix. The first group includes:

Barry, p.w. [٨] presented a model used to guess the ranges of composite strengths both of static and dynamic stress concentration effects on intact fibers resulting from a fiber failure are considered in this model. The obtained results are used to predict the ranges of strengths for composite materials prepared from three types of carbon fibers, and then compared with their corresponding experimental ones.

Malcolm , D.J. [٩] completed the analogy of the linear elastic behavior of a unidirectional composite and an isotropic material with an oriented microstructure . The physical interpretation of the additional stresses and the constitutive constants presented in the theory of the micro-elasticity is given and the shear stress between the fiber and the matrix is presented in terms of these stresses. A constant strain finite element model analysis is achieved and the stiffness matrix is presented in full. Finite element results are presented for the case of a circular hole in a uniform (plane stress) tension field when load is applied normal to fibers direction where the maximum tensile strength is shown to be decreased with fiber size increasing .

Hashin, Z. [١٠] found expressions and bounds for the five elastic moduli, thermal expansion coefficient and conductivities of unidirectional fiber composites consisting of transversely isotropic phases (i.e. fibers and matrix). The expressions have been obtained on the basis of analogies between isotropic and transversely isotropic elasticity equations. Application results for determination of the five elastic moduli of graphite fiber were discussed. Thus, these results were of a high importance for carbon and graphite fiber composites since such fibers are considerably anisotropic.

Zhang , W. C. & Evans , K. E. [١١] put a numerical method to predict the mechanical properties of composite materials with anisotropic constituents and used this method to predict the properties of fiber-reinforced composites (FRC) . The FRC were treated as anisotropic but homogeneous continua and

the elastic constants were determined by using an energy equivalence method. Finite element method (FEM) was used to calculate strain energies or complementary energies of constituents. A comparison was made with previous techniques to determine the longitudinal and transverse moduli with Poisson's ratios for isotropic and transversely isotropic fibers in isotropic matrices.

Shuguang Li [٥] presented the unit cell method for micro-mechanical analysis of unidirectional fiber reinforced composites. A systymatic consideration has been made of the symmetries existed prese-nting an idealized fiber-matrix packing systems. Suitable and adequate boundary conditions of the unit cell have been derived from these symmetry considerations for micromechanical analysis. The loads on the unit cell and their responses in terms of macroscopic stresses and strains have been addressed in such a way that the effective properties of the composite can be obtained from micromechanical analysis of the unit cell in a standard manner.

Shuguang Li [١٢] employed two idealized packing systems for unidirectional fiber reinforced composites namely, square and hexagonal packing systems. Only the translational symmetry transformation has been considered. The unit cells so derived are capable of accommodating fibers of irregular cross-sections and imperfections symmetrically distributed around the fibers such as the micro-cracks and local debonding in the system provided that the regularity of the packing and imperfections is assumed to be present (i.e. regular irregularities). All the unit cells are subjected to arbitrary combinations of macroscopic stresses or strains.

The unit cell boundary conditions have been derived from appropriate considerations of the conditions of symmetry transformations. The expressions of the effective properties of the composite represented by the unit cell are then determined in terms of the applied load to the extra degrees freedom which are available from the output of an appropriate analysis of such a unit cell . The results of this work, validating the unit cells, draw interesting comparisons between the two unit cells established representing the square and hexagonal packing systems.

Shuguang Li & Zhenmin Zou [١٣] , reviewed the use of the unit cells in finite element analyses of unidirectional fiber reinforced composite . Both square and hexagonal fiber-matrix packing systems have been included. The appropriate boundary conditions for each unit cell have been provided under all possible loading conditions corresponding to uniaxial macroscopic longitudinal transverse tension/ compression and shear stress states. The results obtained from the unit cells have been discussed in such a way that they can introduce a typical series of simple but necessary benchmark cases for correct use of such unit cell in finite element analysis of unidirectional fiber reinforced composites.

The second group includes the works done on the short fibers by micromechanical analysis and the effect of the broken fibers on the strength of the unidirectional composite materials , such as :-

Law, N. & Maclaughlin, R. [١٤], showed an application of the self-consistent method (S.C.M.) to the problem of determining overall moduli for

short fiber-reinforced composites , assuming that the fibers can be considered as spheroids. For fully aligned fibers, the numerical results are graphically displayed and show the dependence of the compliances on aspects ratio and volume fraction. By making use of some ideas on how to handle the misalignment of the fibers, the S.C.M.results are shown to compare favorably with experiment.

Schultrich, B. et al [١٥], attempted to calculate the (σ-ε) curve of short fiber composites by considering regular arrays of plates in a ductile matrix, several quantities of interest, such as variation along the fiber, Young's modulus and yield stress are calculated as functions of parameters and structure of the composite. Among the latter, the overlap of the fibers may affect the properties strongly. The change of the composite behavior from mainly elastic to yield may occur in several ways depending on the parameters involved.

Akberzadeh, A. [١٦], studied the effect of the broken fibers on the strength of the unidirectional composite materials. The breaking of a fiber has a negligible effect on the axial strength, but the void arouse at the breaking point has a considerable effect on the transverse strength of the composite body. The stress intensity at the vicinity of the broken fiber has been compared with a similar case but without a broken fiber, and it has been found that breaking of the fibers can substantially increase stress intensity. Curves for predicting the maximum stresses at the vicinity of the broken fibers are presented for unidirectional composite materials transversely loaded.

GÖran Tolf [١٧], achieved a theoretical investigation of the stress field in a short-fiber composite. The concept of a typical region is introduced and the boundary conditions for such region are derived by using these boundary conditions, these stresses are calculated defining this stress field, the macroscopic properties are then calculated. Conclusions are made about the mechanical behavior of the composite, like critical fiber length and fracture toughness.

Luake, B. et. al. [١٨] introduced a theoretical model for calculating the work of fracture in such composites of short, sub critical fibers in a ductile matrix with relatively weak interface. Starting from a micromechanical analysis of the debonding and sliding length, the fracture energies are calculated in general terms. Depending on the relative contributions to the total energy which is itself depending on the loading rate, the composite fracture energy varies with volume fraction in a qualitatively different manner.

The third group includes the works involving the considerations of the interface between the fibers and matrix by a different way such as:

Agarwal, B. D. and Bansal, R. K. [١٩], performed a study by a single fiber model and by using an axisymmetric finite element analysis which has been carried out to study the effect of the interfacial conditions on the properties on discontinuous fiber composites. This study has been possible to take into

account the interaction between the fibers by appropriately selected boundary conditions. The influence of interfacial conditions on load transfer length, elastic moduli of the composite, critical attraction length and composite strengths were established by presenting results.

Laws. V. [٢٠] extended Lawrence's theory to calculate load/di-splacement curve during pullout, the crack spacing and strength of the aligned short fiber composite. The effect of the bonds, interfacial & frictional on fiber pullout, crack spacing and strength is outlined, and the calculation of the strength of the bonds are discussed.

Shirazi-Adl, A. [٢١], using a penalty function, proposed a disp-lacement-based modified potential energy, which enforced the continuity of stresses at a two-material interface. The finite element formulation has been developed and applied for stress analysis of a number of structures made of highly dissimilar materials. His results were compared with those obtained from the conventional finite element analysis and the exact solution. On the contrary, the usual finite element formulations have been resulted in significantly discontinuous stresses at the two-material interface.

Lepetitcorps, Y. et. al. [٢٢], studied the mechanical adhesion between filaments (B & Sic) and titanium matrices. Because a single fiber composite was chosen for this purpose, the critical length measurement and the shear strength were calculated. Using a statistical analysis, the study indicated the role played by the surface treatments of the fibers on the

reinforcement/matrix adhesion. The conclusions obtained on model materials are in an agreement with the result obtained on real composites.

Finally, the fourth group included the works that have studied the stress concentration factor and stresses due to a circular hole in uniform plate composed from unidirectional fiber-reinforced composite. This group involves the following works:

Shastry, B. P. and Rao, G. V. [٢٣], studied the effect of fibers orientation on stress concentration in a finite width composite laminate using finite element techniques. The stress concentration factor was found to be maximum when the fibers direction are parallel to the loading and minimum when they make an angle of ٤٥^{0}. In all cases the maximum stress concentration occurs on the hole boundary at the minimum cross-section.

Paul, T. K. and Rao, K. M. [٢٤], evaluated stresses and stress concentration factor due to a circular hole in fiber reinforced composite laminates subjected to transverse loads and presented the variation of stress concentration factor with plate thickness, hole size and nature of load distribution.

Other than what is mentioned above, there are some miscellaneous works adopts micromechanics approaches to either predict the elastic properties of various types of fiber- or particulated-reinforced composite

materials, [FRCM or PRCM] or analyze some structural behaviors of laminated structures. The following works are some examples of which:

Bendarcyk, A. [٢٥] adopted NASA's Micromechanics Analysis Code with Generalized Method of Cells (MAC/GMC) to predict the elastic properties of plain weave polymer matrix composites (PMCs). He stated that the traditional one step three-dimensional homogenization procedure that has been used in conjunction with MAC/GMC for modeling woven composites in the past is inaccurate due to the lack of shear coupling inherent to the model. However, by performing a two step homogenization procedure in which the woven composite repeating unit cell is homogenized independently in the through-thickness direction prior to homogenization in the plane of the weave, MAC/GMC can now accurately model woven PMCs. The two step procedure is outlined and implemented with comparisons of predictions are made with the results of traditional one step approach and other models and experiments from the literature.

Babu, E. J. et. al. [٢٦] presented a three-dimensional model based on the generalized method of cells (GMC) principle to predict the effective properties of particulate-reinforced metal matrix composites (PMMCs). The effect of the constituent phases on the elastic properties of PMMCs are predicted using GMC. The predictions are compared with an assortment of finite element predictions and experimental results available in literature. The computational efficiency accuracy of the GMC model is also discussed in his study. Moreover, the effect of particle shape and orientation on the elastic properties of PMMCs has been predicted and analyzed. Cubic and parallelepiped shaped particles having different orientations are also considered. Significant variations are

noted on the elastic properties of the PMMC systems by altering the shape and orientation of the particles.

Soykasap, Ö. [٢٧] presented some micromechanical models for the analysis of bending behavior of woven composites and stated that although

in plane properties of these materials can be calculated accurately using the classical lamination theory (CLT), the corresponding bending properties lack any accuracy for one or two-ply woven laminates. Experiments on thin laminates made from woven composites disagree with the estimates of the bending stiffness and strains using CLT. Such estimates can result in errors up to ٢٠٠٪ in the maximum bending strains or stresses, and up to ٤٠٠٪ in the bending stiffnesses. This is because CLT assumes that the fibers and matrix are uniformly distributed in each lamina, and relies on this uniformity in the integration of the transformed laminate stiffness over the laminate thickness.

However, a thin laminate made from fabrics, in fact consists of bundles of fibers which are typically much thinner than the overall thickness of the laminate; these bundles are not homogeneous through the thickness. The researcher introduced micromechanical models for bending behavior of woven composites considering the fibers and matrix and their interactions. Finite elements are developed to estimate the bending properties of plain weave composites. The results are compared to experimental data, showing very good agreement particularly for a lamina.

٢.٣ Review of Macromechanical works of Fiber-Reinforced Composites:

The perfect and complete understanding of the composites materials behavior should meet the requirements of both micro- and macromechanical analyses. The micromechanical works and studies have already been reviewed with petty expansion, while now the macromechanical counterparts are mentioned with lesser extension:

Yeh & Richards [٣١] investigated the Yeh-Stratton Failure Criterion with the stress concentrations on fiber reinforced composites materials under tensile stresses. The Yeh-Stratton Failure Criterion was developed from the initial yielding of materials based on macromechanics. To investigate this criterion, the influence of the materials anisotropic properties and far field loading on the composite materials with central hole and normal crack were studied. Special emphasis was placed on defining the crack tip stress fields and their applications. The study of Yeh-Stratton criterion for damage zone stress fields on fiber-reinforced composites under tensile loading was compared with several fracture criteria; Tsai-Wu Theory, Hoffman Theory, Fischer Theory, and Cowin Theory. Theoretical predictions from these criteria are examined using experimental results.

Yeh & Richards [٣٢] presented the newly developed Yeh-Stratton (Y-S) Strength Criterion to study the failure of composite materials with central holes and normal cracks. To evaluate the interaction parameters for the Y-S failure theory, it is necessary to perform several biaxial loading tests. However, it is indisputable that the inhomogeneous and anisotropic natures of composite materials have made their own contribution to the complication of the biaxial testing problem. To avoid the difficulties of performing many biaxial

tests and still consider the effects of the interaction term in the Y-S Criterion, a simple modification of the Y-S Criterion was developed. The preliminary predictions by the modified Y-S Criterion were relatively conservative compared to the testing data. Thus, the modified Y-S Criterion could be used as a design tool. To further understand the composite failure problem, an investigation of the damage zone in front of the crack tip coupled with the Y-S Criterion is imperative.

Sarkissov, et al [٣٣] described mechanical properties of polymer-clay nanocomposites with platelet and fibrous like nanoparticles evaluated on a of nano, meso and micro length scale. Platelet reinforced materials were found to display a mixed morphology consisting of intercalated and exfoliated regions. A better dispersion was obtained for fibrous clay nanocomposites where homogeneous distribution of single particles was achieved. The deformation behavior was investigated by in-situ XRD and ESEM experiments during drawing; the macro-mechanical characteristics were extracted from tensile tests. The stiffness was found to increase in both platelet and fibrous clay nanocomposites. The presence of intercalated stacks in the latter resulted in a significant reduction in drawability.

Chakraborty and Pradhan [٣٤] dealt with the delamination growth behaviour of FRP composite laminates having two embedded delaminations at the interface under uniaxial and transverse loadings. A full ٣D FE analysis has been performed to calculate the interlaminar stresses at the interface responsible for delamination. The concept of fracture mechanics has been used to calculate the strain energy release rate components at the interface.

Elliptical delaminations have been simulated to be present at the interface of two sublaminates each consisting of several plies and the effect of the neighboring delaminations on the other delamination has been studied under concentrated transverse loading as well as uniaxial tensile loading. Effects of delamination size, shape and the center distance between the two delaminations on individual strain energy release rate components have been evaluated to assess the delamination behavior. It has been observed that the shape, size and the relative spacing of the two delaminations have a strong effect on the overlapping stress field, and the two delaminations grow in size to form a single delamination depending upon these parameters.

Karakuzu, et al [٣٥] carried out an elasto-plastic finite element analysis in woven steel fiber reinforced laminated thermoplastic composite plates subjected to transverse uniform loads. The laminated composite plate is clamped at all its edges. Numerical simulation is performed using the well-established commercial software ANSYS. To investigate the effects of ply number, orientation angle and bonding type for optimum design of fully clamped laminated composite plates, yielding loads and residual stresses are obtained. Three-load step is carried out for each analysis consecutively. The yielding transverse load is applied at first. Then, a series of load increments added until the load reaches ‘‘Yielding Load٠.٠٠٥ MPa’’. At the last step the external load is released to obtain the residual stress components.

He, et al [٣٦] produced a work in which, the interlaminar fracture behavior of internally-tapered composite laminates that have cracks in the drop-off region is investigated using J-integral and direct calculation methods. The

influences of cracks at the resin layer–interleaf interface and at the interface between adjacent plies are studied. The composite laminate is modeled and analyzed using partial hybrid stress finite elements that are formulated based on the Hellinger–Reissner variational principle and the generalized plane deformation theory. In the formulation, only three interlaminar stress components that cause delamination at the interface are independently assumed in addition to displacement interpolation. Both the six-node triangular and eight-node quadrilateral hybrid finite elements (formulated and presented in a companion paper [He, K., Hoa, S.V. and Ganesan, R. ‘‘Stress Analysis of Tapered Composite Laminate Using Partial Hybrid Finite Elements’’, J. Reinforced Plastics and Composities, ٢٣:٦, ٢٠٠٤.]) are used in the fracture analysis. A parametric study is conducted to determine the influences of geometric and material properties on the fracture behavior of the tapered laminate. Experimental work was carried out for the observation of fracture. The analysis results and the experimental observation are compared.

Mümin Küçük [٣٧] investigated the effects of the lateral strip delamination width on the buckling loads of the simply supported woven steel reinforced thermoplastic laminated composite plates. The mechanical properties of the manufactured composite layers have been measured. Three dimensional finite element models of the square laminated plates have been established. Each of these models possesses four layers and a different delamination width between the second and third layers. The orientation angle of the fibers is chosen as ٠, ١٥, ٣٠ and ٤٥_. The buckling loads have been determined for each model having different lateral delamination width. The results show that important decreases in the buckling loads occur after a

certain value of the delamination width. The variation ratios of the results of the symmetric or antisymmetric cases are approximately the same for each angle.

Zor, et al [٣٨] studied the effects of the square delamination, around a square hole, on the buckling loads of the simply supported and clamped woven steel-reinforced thermoplastic (LDPE) laminated composite plates have been investigated. Three-dimensional finite element models of laminated plates with four layers have been established. The square delaminations exist between second/third layers. The stacking sequences are chosen as $[٠_]_{٤}$, $[١٥_/_١٥_]_{s}$, $[١٥_/_١٥_]_{٢}$, $[٣٠_/_٣٠_]_{s}$, $[٣٠_/_٣٠_]_{٢}$, $[٤٥_]_{٤}$. Firstly the harmony between theoretical and finite element solution results of the plate without hole and delamination has been shown. Then, the buckling loads have been determined for each of the models having different square delamination dimensions. Significant decreases in the buckling loads occur after a certain value of delamination dimension. It is seen, for clamped plates that the changing ratios of the results of the symmetric or antisymmetric cases are approximately the same and there is a linear relationship between the values of the fiber angles and buckling loads.

Talooklaei and Ahmmadian [٣٩] introduced a free vibration analysis of a cross-ply laminated composite beam (LCB) on Pasternak foundation. Natural frequencies of beam on Pasternak foundation are computed using finite element method (FEM) on the basis of Timoshenko beam theory. Effect of both shear deformation and rotary inertia are implemented in the modeling of stiffness and mass matrices. The model was designed in such a way that it can be used for

single-stepped cross-section, stepped foundation and multi-span beams. Results of few examples are compared with finding in literature and good agreements were achieved. Natural frequencies of LCBs with different layers arrangements (symmetric and non-symmetric) are compared. For multi-span beam, variation of frequency with respect to number of spans was also studied.

٢.٤ Summary:

The behavior of the composites depends on variety of the parameters such as the properties of the components, bonding of the components, alignment, volume fraction & dimensions of fibers and so on. Thus, the micromechanical finite element, which has been employed increasingly for fiber-reinforced composites in the past decade, has become an important means of understanding this behavior of composites. The theoretical and experimental methods usually applied in micromechanical analysis in order to tackle the problems that caused by the above parameters. The theoretical methods can be divided into two complementary categories:

First, the numerical method which provides more or less exact solutions of the stress fields for special sets of parameters. Thus, there are numerous detailed results for elastic or elastic-plastic fibrous composites. The information that one can get from them is limited, of course due to special geometry, etc.

Second, the analytical approach which makes use of comparatively crude models which enable the problem to be treated in a more general manner and to attain finally some mathematical expression which contain all the parameters under consideration. It can be easily seen, from the literature

review that the works dealt with mechanical behavior of unidirectional fiber-reinforced materials by experimental micromechanical approach are limited due to many reasons.

The present work refers to a stress analysis of a fiber-reinforced composite beam. By two dimensional plane elasticity theory and using two - dimensional finite element displacement method for the problem formulation the unit cell method in micromechanical analysis based on MATLAB compu-

ter programs in ٢-dimension analysis can be adopted. In the case of three-dimensional applications, it is resorted to some well known relevant engineering and mathematical packages or programs such as the package of ANSYS V-٥.٤ to process and manipulate the large and numerous data concerned to it, that's what is done in this work due to the high reliability, accuracy, conservativeness and versatility this package characterized with.

Chapter Three

Theoretical Analysis Of Fiber-Reinforced Composite Materials

٣.١ Introduction:

The composite material may be in the form of a lamina arranged of unidirectional or woven fibers in a matrix or may be in the form of a beam or rod. All of these configurations are regarded as the building or basic units of majority of engineering structures [١ & ٣].

Beams are perhaps the most common type that can be found in engineering applications, so the knowledge and ability to analyze their mechanical behavior and prediction of the stress and strain fields induced in them are necessary and essential from many viewpoints when dealing with fiber reinforced composite structures. The values of stiffness and strength in the direction of fiber represent the maximum values in all directions [٢٩ & ٣٠] and completely depend on the constituent materials properties, volume fractions, stacking sequence and geometry.

An accurate determination and precise specifying of mechanical behavior of a fiber reinforced composite are very difficult, because of the high differences between the constituting phases what results in a complex stress and strain distribution on the microscopic level. Reasonably an accurate prediction can be made for the unidirectional FRC using some simplifying assumptions about stress and strain distribution.

In this work, static analysis of unidirectional fiber-reinforced composite beam has been done assuming that [٣ & ٥]:

١- The longitudinal stress in the fibers varies linearly across its width while the transverse stress is uniform across the fiber.

٢- Perfect bonding between fibers and matrix is assumed to be existed.

٣- Fibers are straight and aligned parallel to each other.

٤- Fibers and matrix are assumed isotropic and homogeneous.

٥- No voids, inclusions, impurities or manufacturing defects and deficiencies are assumed to be involved in beam material.

٦- The composite material is considered homogeneous on macroscopic level.

٧- The loads are assumed to be applied at the infinity [٣٦].

In this chapter, stress equations of equilibrium in Cartesian coordinates, stress-strain relationships for anisotropic, orthotropic and other types of materials under plane stress state are mentioned. Also micromechanics approach of composite materials is briefly reviewed. The unit cell method in micromechanical analysis, which is adopted in this work for unidirectional fiber-reinforced composite beam, is discussed.

٣.٢ Stress- Strain Relationships For Orthotropic Materials:

Hook's law relating stresses to strain can be put in a generalized form as:

$\sigma_i = C_{ij} \times \varepsilon_j$ or ---------- (٣-١)

$\varepsilon_i = S_{ij} \times \sigma_j$ ---------- (٣-٢)

where σ_i are the stress components, C_{ij} are the stiffness matrix terms and

ε_j are the strain components & S_{ij} are the compliance matrix obtained by matrix inversion from Eq.-(٣-١) [٤٠].

The contracted notation is defined in comparison to the usual tensor notation for three-dimensional stresses & strains in table (٣-١) for situations in which the stress & strain tensors are symmetric (the usual case when body force is

absent). By virtue of table (٣-١), the strains in contracted notation are therefore defined as:

$$\varepsilon_1 = \frac{\partial u}{\partial x} \quad , \quad \varepsilon_2 = \frac{\partial v}{\partial y} \quad , \quad \varepsilon_3 = \frac{\partial w}{\partial z}$$

$$\gamma_{23} = \frac{\partial v}{\partial z} + \frac{\partial w}{\partial y} \quad , \quad \gamma_{31} = \frac{\partial w}{\partial x} + \frac{\partial u}{\partial z} \quad , \quad \gamma_{12} = \frac{\partial u}{\partial y} + \frac{\partial v}{\partial x} \qquad \text{--------- (٣-٣)}$$

The stiffness matrix, C_{ij}, has ٣٦ constants in Eq.-(٣-١). But:

$$C_{ij} = C_{ji} \qquad \text{---- (٣-٤)}$$

And

$$S_{ij} = S_{ji} \qquad \text{---- (٣-٥)}$$

This means that the stiffness matrix (and also the compliance matrix) is symmetric and hence has only ٢١ independent constants [١]. Therefore, the stress-strain relationships for an anisotropic (triclinic) elastic material can take the following form:

$$\sigma_i = \begin{bmatrix} \sigma_1 \\ \sigma_2 \\ \sigma_3 \\ \tau_{23} \\ \tau_{31} \\ \tau_{12} \end{bmatrix} = \begin{bmatrix} c_{11} & c_{12} & c_{13} & c_{14} & c_{15} & c_{16} \\ & c_{22} & c_{23} & c_{24} & c_{25} & c_{26} \\ & & c_{33} & c_{34} & c_{35} & c_{36} \\ & & & c_{44} & c_{45} & c_{46} \\ & symmetric & & & c_{55} & c_{56} \\ & & & & & c_{66} \end{bmatrix} \begin{bmatrix} \varepsilon_1 \\ \varepsilon_2 \\ \varepsilon_3 \\ \gamma_{23} \\ \gamma_{31} \\ \gamma_{12} \end{bmatrix} \qquad \text{-------- (٣-٦)}$$

Table ٣-١ Comparison between Tensor & Contracted Notation for Stresses & Strains[١]

Stresses		Strains	
Tensor Notation	Contracted Notation	Tensor Notation	Contracted

			Notation
σ_{11}	σ_1	ε_{11}	ε_1
σ_{22}	σ_2	ε_{22}	ε_2
σ_{33}	σ_3	ε_{33}	ε_3
$\tau_{23}=\sigma_{23}$	σ_4	$\gamma_{23}=2\varepsilon_{23}$ *	ε_4
$\tau_{31}=\sigma_{31}$	σ_5	$\gamma_{31}=2\varepsilon_{31}$	ε_5
$\tau_{12}=\sigma_{12}$	σ_6	$\gamma_{12}=2\varepsilon_{12}$	ε_6

The term “triclinic" means that the material has no planes of symmetry for the material properties. If there are two perpendicular planes of material properties symmetry, then the symmetry will exist with respect to a third mutually orthogonal plane. The stress-strain relations in coordinates aligned with principal material directions (i.e. directions parallel to the intersections of the three orthogonal planes of material symmetry), are [٤١]:

$$\sigma_i = \begin{bmatrix} c_{11} & c_{12} & c_{13} & 0 & 0 & 0 \\ & c_{22} & c_{23} & 0 & 0 & 0 \\ & & c_{33} & 0 & 0 & 0 \\ & & & c_{44} & 0 & 0 \\ & \textit{symmetric} & & & c_{55} & 0 \\ & & & & & c_{66} \end{bmatrix} \times \varepsilon_j \qquad \text{---------- (٣-٧)}$$

Such a material is characterized as an "Orthotropic Material". It is worth to mention now that there is no interaction between normal stresses $\sigma_1, \sigma_2, \sigma_3$ and shearing strains γ_{23}, γ_{31} and γ_{12} which as occurs in anisotropic materials

since there are no values (for example) of c_{14}, c_{15} and c_{16}. Similarly, there is no interaction between shearing stresses and normal strains, as well as none between shearing stresses and shearing strains in different planes. There are only nine independent constants in the stiffness matrix. The above stress-strain relationships in Eqs.(٣-٨) can be inverted by matrix algebra to determine strain components in terms of stresses as following:

$$\varepsilon_j = \begin{bmatrix} S_{11} & S_{12} & S_{13} & 0 & 0 & 0 \\ & S_{22} & S_{23} & 0 & 0 & 0 \\ & & S_{33} & 0 & 0 & 0 \\ & symmetric & & S_{44} & 0 & 0 \\ & & & & S_{55} & 0 \\ & & & & & S_{66} \end{bmatrix} \times \sigma_i \qquad \text{---------- (٣-٨)}$$

The compliance matrix terms S_{ij} are inter-related with those of stiffness matrix C_{ij}, and elastic constants of the material by the following set of expressions for orthotropic material [١ &٣١]:

$$C_{11} = \frac{S_{11}S_{22} - S_{23}^2}{S} \quad , \quad C_{12} = \frac{S_{13}S_{23} - S_{12}S_{33}}{S}$$

$$C_{22} = \frac{S_{33}S_{11} - S_{13}^2}{S} \quad , \quad C_{13} = \frac{S_{12}S_{23} - S_{13}S_{22}}{S}$$

$$C_{33} = \frac{S_{11}S_{22} - S_{12}^2}{S} \quad , \quad C_{23} = \frac{S_{12}S_{13} - S_{23}S_{11}}{S}$$

$$C_{44} = \frac{1}{S_{44}} \quad , \quad C_{55} = \frac{1}{S_{55}} \quad , \quad C_{66} = \frac{1}{S_{66}} \qquad \text{---------- (٣-٩)}$$

Where :

$$S = S_{11}S_{22}S_{33} - S_{11}S_{23}^2 - S_{22}S_{13}^2 - S_{33}S_{12}^2 + 2S_{12}S_{23}S_{13} \qquad \text{--------- (٣-١٠)}$$

In Eqs. (٣-٩) above, the symbols (C & S) can be interchanged to get the converse relationships. The stiffnesses, C_{ij} can be given in terms of elastic constants for orthotropic materials as [١ & ٣١] :

$$C_{11} = \frac{1-\nu_{23}\nu_{32}}{E_2E_3.\Delta} \quad , \quad C_{12} = \frac{\nu_{21}+\nu_{31}\nu_{23}}{E_2E_3.\Delta}$$

$$C_{13} = \frac{\nu_{31}+\nu_{21}\nu_{32}}{E_2E_3.\Delta} = \frac{\nu_{13}+\nu_{12}\nu_{23}}{E_1E_2.\Delta} \quad , \quad C_{22} = \frac{1-\nu_{13}\nu_{31}}{E_1E_3.\Delta}$$

$$C_{23} = \frac{\nu_{32}+\nu_{12}\nu_{31}}{E_1E_3.\Delta} = \frac{\nu_{23}+\nu_{21}\nu_{13}}{E_2E_1.\Delta} \quad , \quad C_{33} = \frac{1-\nu_{12}\nu_{21}}{E_1E_2.\Delta}$$

$$C_{44} = G_{23} \quad , \quad C_{55} = G_{13} \quad , \quad C_{66} = G_{12}$$

Where :

$$\Delta = \frac{1-\nu_{12}\nu_{21}-\nu_{23}\nu_{32}-\nu_{31}\nu_{13}-2\nu_{21}\nu_{32}\nu_{13}}{E_1E_2E_3} \qquad \text{---------- (٣-١١)}$$

Plane stress state in an orthotropic material as a lamina in the ١-٢ plane, shown in Fig.-(٣-١) can be defined when:

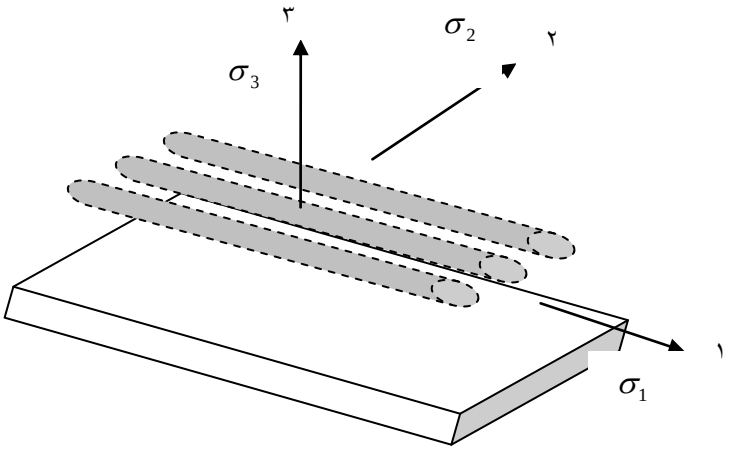

Fig. ۳-۱: unidirectional fiber-reinforced lamina
in ۱-۲ plane under plane stress condition

$$\sigma_3 = 0 \quad , \quad \tau_{23} = 0 \quad \& \quad \tau_{31} = 0 \qquad \text{---------- (۳-۱۲)}$$

Which results in strains of:

$$\varepsilon_3 = S_{13}\sigma_1 + S_{23}\sigma_2$$

$$\gamma_{23} = \gamma_{31} = 0 \qquad \text{---------- (۳-۱۲)}$$

Furthermore, the strain-stress relationships in Eqs.-(٣-٩) are reduced to be:

$$\begin{Bmatrix} \varepsilon_1 \\ \varepsilon_2 \\ \gamma_{12} \end{Bmatrix} = \begin{bmatrix} S_{11} & S_{12} & 0 \\ S_{12} & S_{22} & 0 \\ 0 & 0 & S_{66} \end{bmatrix} \begin{Bmatrix} \sigma_1 \\ \sigma_2 \\ \tau_{12} \end{Bmatrix} \qquad \text{---------- (٣-١٣)}$$

Where:

$$S_{11} = \frac{1}{E_{11}} \quad , \quad S_{12} = \frac{-\nu_{12}}{E_1} = \frac{-\nu_{21}}{E_2} \quad , \quad S_{22} = \frac{1}{E_2}$$

And $$S_{66} = \frac{1}{G_{12}} \qquad \text{---------- (٣-١٤)}$$

Eqs. (٣-١٣) can be solved by inversion to obtain stress components in terms of strains:

$$\begin{Bmatrix} \sigma_1 \\ \sigma_2 \\ \tau_{12} \end{Bmatrix} = \begin{bmatrix} Q_{11} & Q_{12} & 0 \\ Q_{12} & Q_{22} & 0 \\ 0 & 0 & Q_{66} \end{bmatrix} \begin{Bmatrix} \varepsilon_1 \\ \varepsilon_2 \\ \gamma_{12} \end{Bmatrix} \qquad \text{---------- (٣-١٥)}$$

Where Q_{ij} terms, the reduced stiffnesses, [٤٢] and can be put in terms of compliances, S_{ij} as following :

$$Q_{11} = \frac{S_{22}}{S_{11}S_{22} - S_{12}^2} \quad , \qquad Q_{12} = \frac{-S_{12}}{S_{11}S_{22} - S_{12}^2}$$

$$Q_{22} = \frac{S_{11}}{S_{11}S_{22} - S_{12}^2} \quad , \qquad Q_{66} = \frac{1}{S_{66}} \qquad \text{----------(٣-١٦)}$$

and in terms of the engineering constants :

$$Q_{11} = \frac{E_1}{1 - \nu_{12}\nu_{21}} \quad , \qquad Q_{12}\,\frac{\nu_{21}E_1}{1 - \nu_{12}\nu_{21}} = \frac{\nu_{12}E_2}{1 - \nu_{12}\nu_{21}}$$

$$Q_{22} = \frac{E_2}{1 - \nu_{12}\nu_{21}} \quad \& \quad Q_{66} = G_{12} \qquad \text{----------(٣-١٧)}$$

٣.٣ Micromechanical Approaches of Composite Materials:

As formerly cited, the micromechanics is briefly defined as the study of composite material behavior wherein the interaction of the constituent materials are examined in detail as a part of the definition of the behavior of the heterogeneous composite material, while the macro- mechanics is the study of the composite material behavior, wherein the material is presumed homogeneous and the effects of the constituent materials are detected only as averaged apparent properties of the composite [١].

Thus, the properties of a composite material can be mathematically derived on the basis of the properties of the constituents using micromechanics criteria.

There are two basic approaches to the micromechanics of composite materials:

١. Mechanics of materials approach.

٢. Elasticity approach.

The mechanics of materials approach embodies the usual concepts of vastly simplifying assumptions regarding the hypothesized behavior of the mechanical system. The elasticity approach actually is at least three approaches:

١. Bounding principles.

٢. Exact solutions.

٣. Approximate solutions.

The objective of all of the micromechanics approaches is to determine the elastic moduli, stiffnesses or compliances of a composite material in terms of

those of constituent materials as the relative volumes of fibers and matrix and their properties. An additional objective is to determine the strengths of the composite in terms of the strength of the constituent materials as the strength of the fibers and matrix and their relative volumes. The foregoing definitions could be modified to account for different strengths under tensile and compressive loading [١].

Irrespective of the micromechanical stiffness approach used, the basic restrictions on the composite material that can be treated are:

The material is:

١. Macroscopically homogeneous.
٢. Linearly elastic.
٣. Macroscopically orthotropic.
٤. Initially stress-free (or not pre-stressed)

٣.٣.١ Mechanics of Materials Approach :

This approach may be divided into the following subdivisions:

— Mechanics Of Material Approach To Stiffness :

In this approach, the elastic moduli and strengths of a composite are used to be predicted in terms of those of the constituent materials. The most prominent assumption is that the strains in the fiber direction in a unidirectional fibrous composite are the same in both fibers and matrix as shown in Fig.(٣-٢) below:

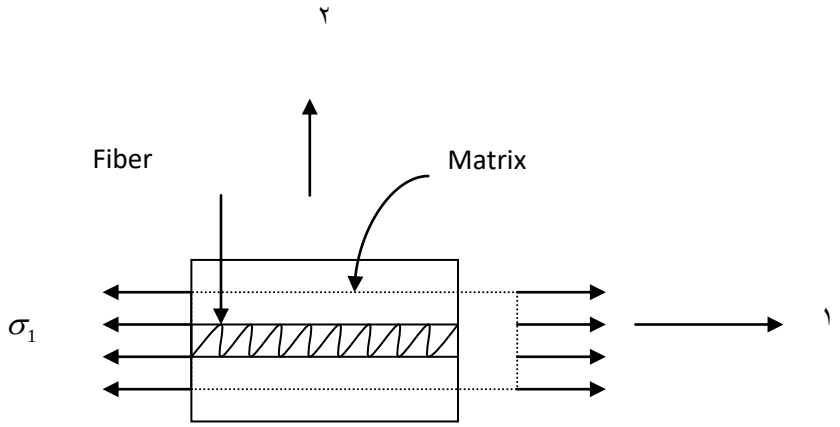

FIG . ٣-٢ Unidirectional Fibrous composite Loaded in ١- direction.

The key properties and strengths of a unidirectional composite material which can be determined by this approach are tabulated in table (٣-٢) below whose informations are gathered from the references referred to besides.

Table ٣-٢ The Properties & Strengths Calculated By

Mechanic of Material Approach to Stiffness [٣ & ٤٣]

Property	Expression	Representative volume element with loading direction
١. E_1 Longitudinal young modulus	$E_1 = E_f \nu_f + E_m \nu_m$ Rule of mixtures	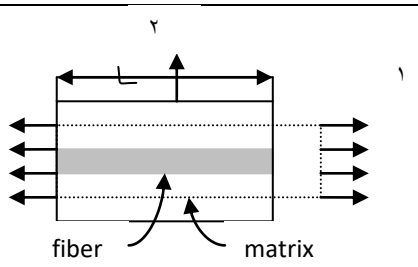
٢. E_2	$E_2 = \frac{E_m * E_f}{V_m * E_f + V_f * E_m}$	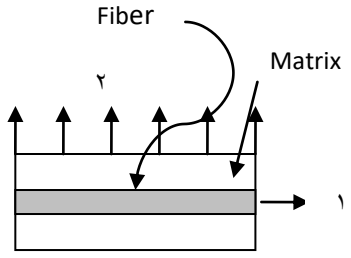

٣. ν_{12} Poisson's Ratio	$\nu_{12} = \nu_f * V_F + \nu_m * V_m$ Rule of mixture	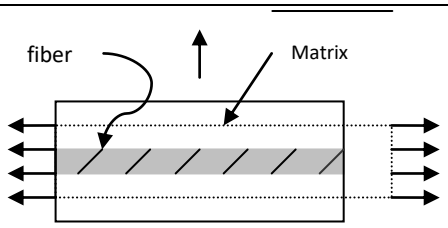
٤. G_{12} Shear modulus	$G_{12} = \frac{G_m G_f}{G_f V_m + G_m V_f}$	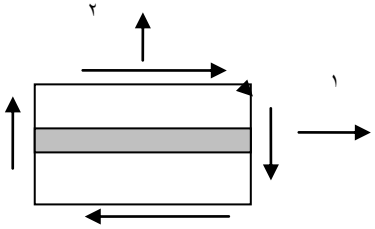
٥. σ_c	$\sigma_c = \sigma_f V_f + \sigma_m V_m$ Rule of mixtures	Similar to E_1
6.ρ_c	$\rho_c = \rho_f V_f + \rho_m V_m$	=
٧. ν_{21}	$\nu_{21} E_1 = \nu_{12} E_2$	

-

- Mechanics of materials Approach to Strength :

When a unidirectional continuous fiber reinforced composite material is loaded in a fiber direction, the stress induced in the composite follows the rule of mixtures, that is:

$$\sigma_c = \sigma_f V_f + \sigma_m V_m \qquad \text{--------- (٣-١٨)}$$

As $V_f + V_m = 1$ ---------- (٣-١٩)

Eq.(٣-١٨) can be put in the form :

$$\sigma_c = \sigma_f V_f + \sigma_m \left(1 - V_f\right) \qquad \text{---------- (٣-٢٠)}$$

Certain restrictions on (V_f) can be put in order to have real reinforcement . For this a composite must have a certain minimum fiber volume fraction, $V_{\min}$, which can be defined as [١&٢]: the fiber volume fraction less than which, the composite will not fracture at a stress predicted by the following Eq. :

$$\sigma_{cu} = \sigma_{fu} V_f + \left(\sigma_m\right)_{\varepsilon_f^*} \left(1 - V_f\right) \qquad \text{-------- (٣-٢١)}$$

Where :

σ_{cu} : is the ultimate strength of the composite.

σ_{fu} : is the ultimate strength of the fibers.

$\left(\sigma_m\right)_{\varepsilon_f^*}$: is the matrix stress at the fiber fracture strain ε_f^*

There is also V_{crit} , the critical volume fraction of fibers, that must be exceeded for strengthening, which can be calculated as :

$$V_{crit} = \frac{\sigma_{mu} - (\sigma_m)_{\varepsilon_f^*}}{\sigma_{fu} - (\sigma_m)_{\varepsilon_f^*}} \qquad \text{---------- (٣-٢٢)}$$

Where, σ_{mu} is the ultimate strength of the matrix. At these volume fractions, the fibers are in effective in restraining the matrix elongation.

٣.٣.٢ Elasticity Approach:

The second approach of the micromechanics is the elasticity approach whose subdivisions are mentioned previously. The bounding technique focuses on the upper & lower limits of the properties of the composite and does not predict the properties directly. The property is only determined when the upper and lower limits are coincident. Frequently, they are well separated [٤٤].

The exact solution method is suitable for indicating the types of solutions that are available and to compare them with the results of mechanics of materials.

An interesting approach to more realistic fiber-matrix interaction is the contiguity approach. Also, the Halpin – Tsai equations are widely used in literatures [٣].

– Elasticity Solutions With Contiguity :

From an analytical viewpoint, a linear combination of:

- A solution in which all fibers are isolated each other and
- A solution in which all fibers contact each other provides the correct modulus .

If C denotes degree of contiguity, then C = ٠ corresponds to non-contiguous (isolated fibers) and C = ١ refers to perfectly contiguous fibers, (all fibers are in contact). Naturally, with high volume fractions of fibers C would be expected to approach unity (i.e. C=١) [١].

In this work, the fibers are assumed to be isolated from each others thus, C=٠.

Tsai obtained expressions to calculate the modulus transverse to the fibers direction considering the contiguity factor which can be found in many various literatures. According to the assumption above , C is put zero in Tsai equations already mentioned to be [٤٤] :

$$E_2 = 2[1-\nu_f+(\nu_f-\nu_m)V_m][\frac{K_f(2K_m+G_m)-G_m(K_f-K_m)V_m}{(2K_m+G_m)+2(K_f-K_m)V_m}] \qquad \text{--------- (٣-٢٣)}$$

For ν_{12}, Tsai also obtained (taking c = ٠) :

$$\nu_{12} = \frac{K_f\nu_f(2K_m+G_m)V_f+K_m\nu_m(2K_f+G_m)V_m}{K_f(2K_m+G_m)-G_m(K_f-K_m)V_m} \qquad \text{--------- (٣-٢٤)}$$

And for $G_{١٢}$ (when c = o) [١]:

$G_{12} = \frac{G_m[2G_f - (G_f - G_m)V_m}{2G_m + (G_f - G_m)V_m}$ --------- (٣-٢٥)

Where :

$K_f = \frac{E_t}{2(1-\nu_f)}$

$K_m = \frac{E_m}{2(1-\nu_m)}$

$G_f = \frac{E_f}{2(1+\nu_f)}$

$G_m = \frac{E_m}{2(1+\nu_m)}$ ---------- (٣-٢٦)

- **The Halpin – Tsai Equations :**

Halpin & Tsai had put an interpolation procedure that is an approximate representation of more complicated micromechanics results reduces the solution to the approximate form [٣].

$E_1 \approx E_f V_f + E_m V_m$ ---------- (٣-٢٧)

$\nu_{12} \approx \nu_f V_f + \nu_m V_m$ ---------- (٣-٢٨)

And :

$\frac{M}{M_m} = \frac{1+\xi\eta V_f}{1-\eta V_f}$ ---------- (٣-٢٩)

Where :

$$\eta = \frac{(M_f / M_m) - 1}{(M_f / M_m) + \xi} \qquad \text{---------- (٣-٣٠)}$$

M = composite modulus (E_2 , G_{12} or ν_{23}) .

M_f = corresponding fiber modulus.

M_m= corresponding matrix modulus.

And ξ is a measure of fiber reinforcement of the composite which depends on the fiber geometry, packing geometry & loading conditions. The value of ξ can be obtained by comparing Eqns. (٣-٢٩ & -٣٠) with exact elasticity solutions using curve fitting technique, which seems to be difficult.

The term η is called reduced factor and its value $\leq$ ١. Morever, it is apparent from Eq. (٣-٣٠) that η is affected by the constituent materials properties as well as by the reinforcement geometry factor (ξ).

In the present work stresses, strains and displacements will be analyzed in a unidirectional fiber reinforced composite beam subjected to transversely bending loads using the method of unit cells in micromechanical stress analysis in composite materials, adapting the finite element formulation as a numerical solution approach for the problem manipulation. The assumptions in the section ٣.١ are considered in the present work. The solution of the problem is performed through the following steps:

- Specifying composite type, geometry, layout and dimensions.
- Specifying loading and supporting conditions.
- Selecting of the proper type of fiber-matrix packing system idealization, hence the suitable unit cell can be adopted.

- Discritization and meshing the beam in the longitudinal and transverse directions (i.e. the unit cell) .
- Formulation of stiffness, displacement and force matrices and vectors .
- Insertion of the relevant boundary conditions in the equations system obtained from the finite element analysis.
- Adopting a suitable means for the solution algorithm to get the field quantities (i.e. stresses, strains & displacements).
- Insertion the above quantities in one of the failure criteria.
- Investigating effects of fibers and matrix type, fiber cross section, fibers volume fraction and distribution on the stresses, strains and displacements on the unit cell under consideration and then on the entire composite .

٣.٤ Theory Of Beams:

In the analytical approach there are three steps or stages to perform a proper component design. First of them is to identify and establish the pertinent mathematical expressions as discussed in the previous sections. Beams perhaps are the most widely used structures in engineering [٣], so it is useful to review some relations of interest about beams analysis. For example, for a simply supported isotropic beam subjected to bending by a uniformly distributed load of intensity (q) as shown in figure (٣-٤) [٤٥ & ٤٦], the boundary conditions at the upper and lower edges are :

$$(\tau_{xy})_{y=+c} = 0 \qquad (\sigma_y)_{y=+c} = 0 \qquad (\sigma_y)_{y=-c} = q \qquad \text{---------- (٣-٣١)}$$

From theory of elasticity, it is found that [٤٦]:

$$\sigma_x = -\frac{q}{2I}(x^2 y - \frac{2}{3}y^3)$$ ---------- (٣-٣٢)

$$\sigma_y = -\frac{q}{2I}\left(\frac{1}{3}y^3 - c^2 y + \frac{2}{3}c^3\right)$$ ---------- (٣-٣٣)

$$\tau_{xy} = -\frac{q}{2I}(c^2 - y^2)x$$ ---------- (٣-٣٤)

Where I is the moment of inertia of a rectangular cross-sectional area of unit width .

The deflection δ can be given by [٣ & ٤٥] :

$$\delta = \frac{5}{24} * \frac{ql^4}{EI}\left[1 + \frac{12}{5}\frac{c^2}{l^2}(\frac{4}{5} + \frac{\nu}{2})\right]$$ ---------- (٣-٣٥)

The curvature $(\frac{d^2 v}{dx^2})$ is given in the form of [٣ & ٤٦]:

$$\left(\frac{d^2 v}{dx^2}\right)_{y=0} = \frac{q}{EI}\left[\frac{l^2 - x^2}{2} + c^2\left(\frac{4}{5} + \frac{\nu}{2}\right)\right]$$ ---------- (٣-٣٦)

Certain other relations are put for the displacements u &v in the x- and y-directions respectively, from which the normal and shearing strains in x-y plane can be obtained as [٤٦]:

$$\varepsilon_x = \frac{\partial u}{\partial x} \quad , \quad \varepsilon_y = \frac{\partial v}{\partial y} \quad \& \quad \gamma_{xy} = \frac{\partial u}{\partial y} + \frac{\partial v}{\partial x}$$ ---------- (٣-٣٧)

In case of anisotropic beam the solution may be obtained by introducing the stiffness along the axis of the beam into the above expressions such that they are turned to be valid for composites.

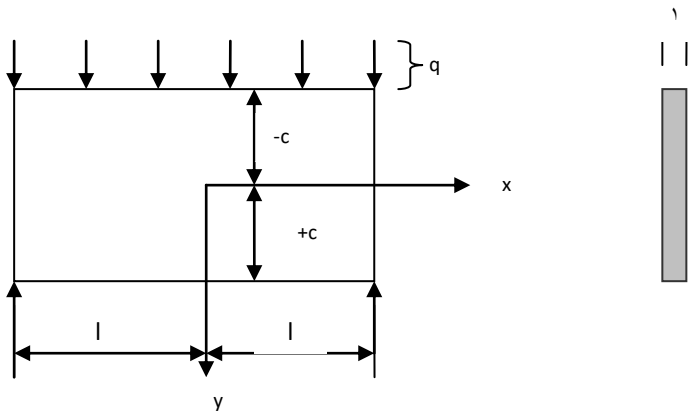

Fig. ٣-٤ Simply supported beam subjected to bending by uniform distributed load .

٣.٥ Unit Cell Method in Micromechanical Analysis:

The unit cell method in micromechanical stress analysis may be briefly described as a method in which the composite is idealized by a regular fiber-matrix packing arrangement in either square or hexagonal layout such that a periodical element composed of a fiber surrounded by a matrix represents the overall composite cross-section engineering characteristics throughout the whole cross-section of the component. A stress analysis over this periodical repetitive element which is called hereafter "The Unit Cell", can determine, by virtue of the symmetries existed in the system and stress mapping techniques, the field quantities such as stresses, strains and displacements everywhere in the cross-section of the composite component or structure, as well as the effective elastic properties of the composite can also be determined from such an analysis [٥&١٣].

The unit cell method is coupled with the finite element method formulation (FEMF) using a suitable engineering package as a solution means will give more accurate results than other numerical methods used in micromechanical stress analysis of composites. The engineering packages

usually employed in such applications are abundant like ANSYS, ABAQUS or NASTRAN, etc. [٤٧]. This method is explained in more details through chapter ٤, the next.

Chapter Four

Mathematics and Computerizing of the Unit Cell Method

٤.١ Introduction:

It is approved to put introductory concepts about the unit cell method to reveal the main scope of which and to be familiar with the analysis reviewed later.

An appropriately introduced representative unit cell is the first step. A common practice is to assume an idealized regular arrangement of fiber-matrix packing system [١٢]. For UDFRC the frequently employed idealized fiber-matrix packing systems are the square and hexagonal arrangements. The most important feature and difference between the two systems is the "Transverse Isotropy" which is existed and preserved by the hexagonal one. The second step is the symmetries presented in the system. For any body in three-dimension there are three types of symmetries can be found, namely:

١. Reflection in a plane or mirror reflection denoted as "$\sum$" or more specifically as "$\sum_x$" if the plane is normal to x-axis.

٢.Rotation through an angle about an axis, noted as (C'^{n}) if the angle is ($٢\pi/n$) or(C^{n}_{x}) if the axis is the x-axis. $C^{٢}$ in particular is sometimes termed as reflection in a line, skew-symmetry, inversion symmetry or polar symmetry.

٣. Translational symmetry, denoted by (T^{Δ}) if the translation is Δ or by ($T_x^{\Delta x}$) if the translation is Δx along x-axis. Such a symmetry may occur only when the body is of infinite extent in the chosen direction [٤٨]. Using different symmetries results in different unit cells geometries and the more symmetries in a unit cell the more efficient one. The boundary conditions established depend chiefly on the type of symmetry in the unit cell, usually it is reflectional or rotational and also on the specific loading conditions. Some analyses have dealt separately with particular cases of loading such as transverse or longitudinal tension, compression or shear, others have dealt individually with every single component or a limited combination of macroscopic stresses or strains as loads and then by superposition principle the total effect of these cases entirely can be found specially for linear problems where in non-linear ones this principle is inapplicable. An other advantage of the unit cell so derived is that it is capable for accommodating irregularly shaped fibers cross-sections and even allowing the existence of imperfections, such as local debonding and micro-cracks provided that the regularity of the fiber-matrix arrangement, the uniformity of the fiber cross-section and imperfections distribution are maintained uniform throughout the material, in other words, they allow "regular irregularities" throughout a composite cross-section normal to fibers direction. This pattern extends and is repeated along the fiber length. The square and hexagonal systems can be visualized as shown in Figs. ٤-١ & ٤-٢ respectively.

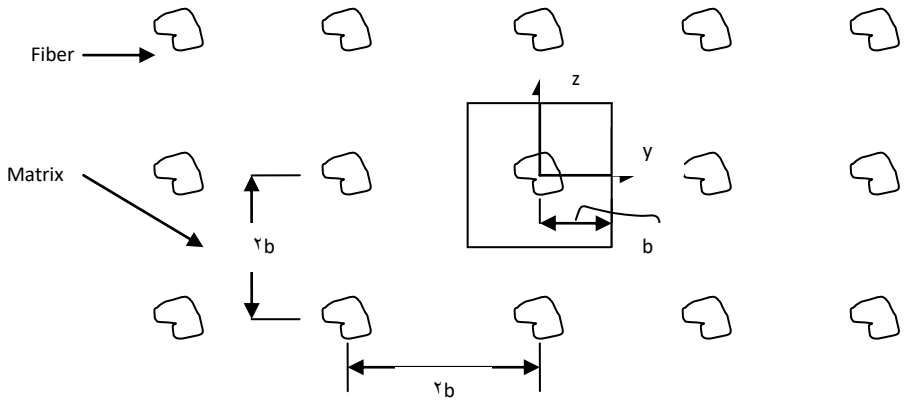

Fig. ٤-١ Square fiber-matrix packing system and the square unit cell

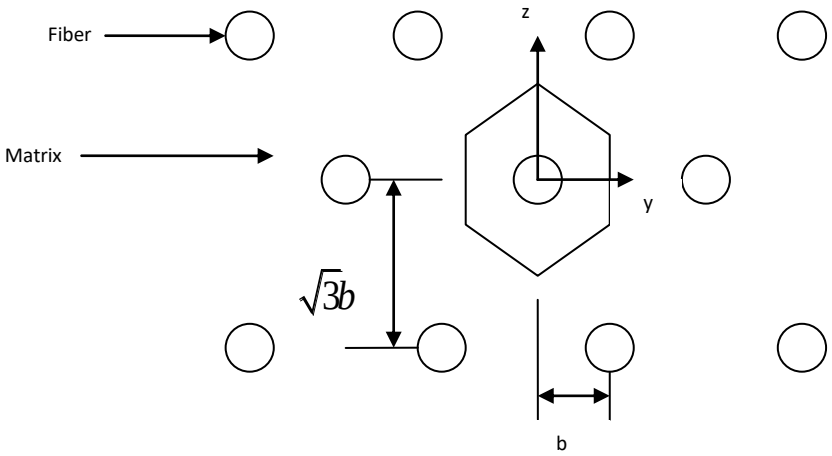

Fig. ٤-٢ Hexagonal fiber-matrix packing system and the hexagonal unit cell.

٤.٢ Finite Element Formulation:

Consider a composite beam of length (l) and a circular cross-section of diameter (d). This beam is pinned at both ends and transversely loaded by two

normal concentrated forces equi-spaced from both ends and from each other as shown in figure ٤-٣:

B

Displacement approach of the finite element is adopted to formulate the problem. The stiffness matrix of the beam element under consideration which is flexurally excited can be shown to be [٤٢]:

$$[K_e] = \frac{E_1 I_c}{l_e^3} \begin{bmatrix} 12 & 6l_e & -12 & 6l_e \\ & 4l_e^2 & -6l_e & 2l_e^2 \\ symmt. & & -12 & -6l_e \\ & & & 4l_e^2 \end{bmatrix} \qquad \text{--------- (٤-١)}$$

Where, Ic: moment of inertia of the composite beam cross-section determined by using parallel axis theorem and the transformed (equivalent) section [٤٩].

E_1: composite Young's modulus of elasticity in a direction perpendicular to that of fibers, for UDFRCM it is given by:

$$E_1 = E_f V_f + E_m V_m \qquad \text{--------- (٤-٢)}$$

l_e : element length.

The load vector (for external applied loads only) for an individual element flexurally excited can be in the form of :

$$\{\overrightarrow{f_e}\} = \begin{bmatrix} p_1 & p_2 & p_3 & p_4 \end{bmatrix}^T \qquad \text{--------- (٤-٣)}$$

The respective displacement vector may be given by:

$$\left\{\overrightarrow{u_e}\right\} = \begin{bmatrix} u_1 & u_2 & u_3 & u_4 \end{bmatrix}^T \qquad \text{--------- (٤-٤)}$$

The various components of the load and displacement are shown in figure (٤-٤) below [٥٠]:

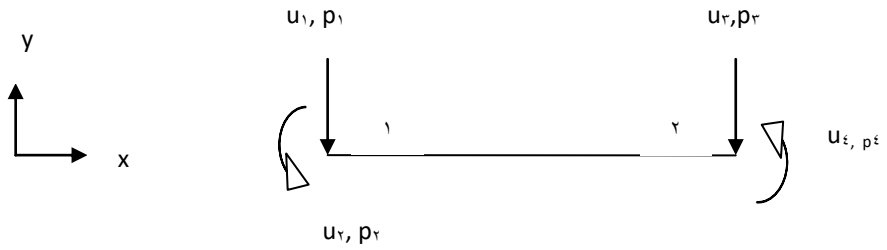

Fig. ٤-٤ Nodal displacement and loads (only externally applied)

For the specific nodal displacements and load components, $u_١$ and $u_٣$ are vertical displacements or deflections while $u_٢$ & $u_٤$ are rotations or slopes, $p_١$ & $p_٣$ are vertical components and $p_٢$ & $p_٤$ are moments. The positive directions are towards the positive y-direction for linear directions, the counterclockwise for the angular quantities. The internal forces at nodes ١ & ٢ are found as:

$$\left\{S^e\right\} = \begin{Bmatrix} Sh_1^e \\ M_1^e \\ Sh_2^e \\ M_2^e \end{Bmatrix} = \left[K^e\right] * \left\{U^e\right\} \qquad \text{---------- (٤-٥)}$$

The shear forces Sh_1^e and Sh_2^e and moments M_1^e & M_2^e are acting at the nodes ١ & ٢ as shown in Fig. (٤-٥) and calculated for an individual element, in other words they have different values at different elements.

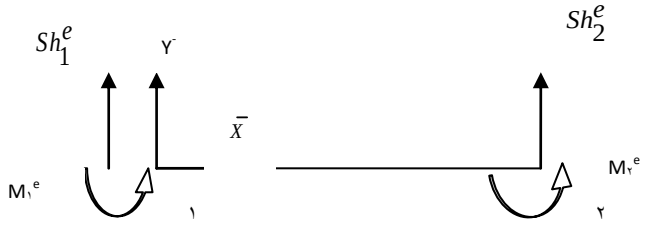

Fig. ٤-٥ Internal shear forces and moments acting at the two nodes.

٤.٣ Discritization and Numbering Scheme:

The beam should be first longitudinally discritized into three elements and numbered according to the following guidelines of nodes location [٥١ & ٥٢]:

Nodes are generally positioned at:

١. Each end of the beam.
٢. Each external support.

٣. Wherever the section property (EI) changes.

٤. Wherever there is a concentrated moment.

٥. Wherever there is a concentrated force.

٦. Wherever the value of the deflection is needed.

٧. Wherever beam or section geometry changes.

Accordingly, the beam can be discritized and numbered as shown in figure (٤-٦) below:

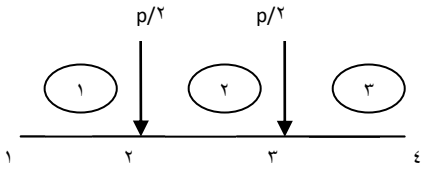

Fig. ٤-٦ The beam is discritized into ٣ elements with ٤ nodes.

The encircled numbers refer to element number, while uncircled numbers refer to those of nodes.

A connectivity or local-global correspondence table may be constructed to be made use of in assembling the elements and then the overall structural matrices as in the following manner:

Table (٤-١) Connectivity or local-global correspondence table [٥٢]

Element no.	First Node	Second Node
١	١	٢
٢	٢	٣
٣	٣	٤

As mentioned above there are two degrees of freedom permitted per each node, translational and rotational

٤.٤ Formulation of Stiffness Matrices:

For element-١ the stiffness matrix can be formulated to be:

u١ u٢ u٣ u٤ global

$$[k_{e1}]=\frac{E_1 I_c}{(l_{e1})^3}\begin{bmatrix} 12 & 6l_{e1} & -12 & 6l_{e1} \\ & 4l_{e1}^2 & -6l_{e1} & 2l_{e1}^2 \\ & & 12 & -6l_{e1} \\ & & & 4l_{e1}^2 \end{bmatrix} \qquad \text{---------- (٤-٦)}$$

For element-٢:

u٣ u٤ u٥ u٦ global

$$[k_{e2}]=\frac{E_1 I_c}{(l_{e2})^3}\begin{bmatrix} 12 & 6l_{e2} & -12 & 6l_{e2} \\ & 4l_{e2}^2 & -6l_{e2} & 2l_{e2}^2 \\ symm. & & 12 & -6l_{e2} \\ & & & 4l_{e2}^2 \end{bmatrix} \qquad \text{---------- (٤-٧)}$$

For element-٣:

u٥ u٦ u٧ u٨ global

$$[K_e]=\frac{E_1 I_c}{l_{e3}^3}\begin{bmatrix} 12 & 6l_{e3} & -12 & 6l_{e3} \\ & 4l_e^2 & -6l_{e3} & 2l_{e3}^2 \\ symmt. & & -12 & -6l_{e3} \\ & & & 4l_{e3}^2 \end{bmatrix} \qquad \text{---------- (٤-٨)}$$

Where l_{e1}, l_{e2}, l_{e3} are the lengths of elements ١, ٢ and ٣ respectively which are equal in length and having the same properties. Combining these three matrices to get the overall structural stiffness matrix of the beam using direct stiffness method. The resulting matrix is a square one of size (٨*٨) [٤٢ & ٥٠]

$$
\begin{array}{c}
\begin{matrix} u١ & u٢ & u٣ & u٤ & u٥ & u٦ & u٧ & u٨ \end{matrix} \\
[K]_t = \frac{E_1 I_c}{l^3}
\begin{bmatrix}
12 & 6l & -12 & 6l & 0 & 0 & 0 & 0 \\
 & 4l^2 & -6l & 2l^2 & 0 & 0 & 0 & 0 \\
 & & 24 & 0 & -12 & 6l & 0 & 0 \\
 & & & 8l^2 & -6l & 2l^2 & 0 & 0 \\
 & & & & 24 & 0 & -12 & 6l \\
 & & & & & 8l^2 & -6l & 2l^2 \\
 & & & & & & -12 & -6l \\
symm. & & & & & & & 4l^2
\end{bmatrix}
\end{array}
\qquad \text{------ (٤-٩)}
$$

Figure ٤-٧ below shows the overall representation of the nodal displacements and force (load) vector components of the entire beam structure:

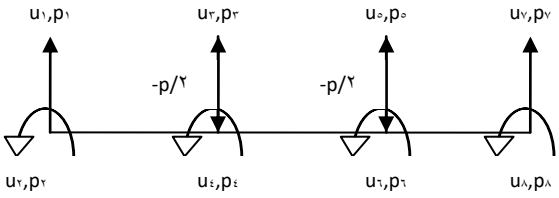

Fig. ٤-٧ The various nodal displacements and load components of the composite beam structure

The load vectors of the various elements can be formulated as follows:

$$\{f_{e1}\} = \begin{Bmatrix} p_1 \\ p_2 \\ p_3 \\ p4 \end{Bmatrix} \begin{matrix} 1 \\ 2 \\ 3 \\ 4 \end{matrix}$$

$$\{f_{e2}\} = \begin{Bmatrix} p_3 \\ p_4 \\ p_5 \\ p_6 \end{Bmatrix} \begin{matrix} 3 \\ 4 \\ 5 \\ 6 \end{matrix}$$

$$\{f_{e3}\} = \begin{Bmatrix} p5 \\ p6 \\ p7 \\ p8 \end{Bmatrix} \begin{matrix} 5 \\ 6 \\ 7 \\ 8 \end{matrix}$$

---------- (٤-١٠)

The assembly of the elemental load vectors into the global load vector is performed in a similar manner to that of stiffness matrices assembly. Using the principle of minimization of potential energy yields [٥٣]:

$$[K] \times \{u\} = \{f\}_t$$ ----------(٤-١١)

Expanding equation (٤-١١) above yields:

$$\frac{E_1 I_c}{l^3} \begin{bmatrix} 12 & 6l_1 & 12 & 6l & 0 & 0 & 0 & 0 \\ & 4l^2 & -6l & 2l & 0 & 0 & 0 & 0 \\ & & 24 & 0 & -12 & 6l & 0 & 0 \\ & & & 8l^2 & -6l & 2l^2 & 0 & 0 \\ & & & & 24 & 0 & -12 & 6l \\ & \text{Symm.} & & & & 8l^2 & -6l & 2l^2 \\ & & & & & & -12 & -6l \\ & & & & & & & 4l^2 \end{bmatrix} \begin{Bmatrix} u_1 \\ u_2 \\ u_3 \\ u_4 \\ u_5 \\ u_6 \\ u_7 \\ u_8 \end{Bmatrix} = \begin{Bmatrix} p_1 \\ p_2 \\ p_3 \\ p_4 \\ p_5 \\ p_6 \\ p_7 \\ p_8 \end{Bmatrix}$$

---------- (٤-١٢)

The boundary conditions of a beam subjected to bending load with both ends are simply supported like the one under consideration, for displacements and force vectors respectively are:

$u_1=u_7=0$ ---------- (٤-١٣)

$p_1=p_2=p_4=p_6=p_7=p_8=0$ ---------- (٤-١٤)

$p_3=p_5=p/2$ ---------- (٤-١٥)

Insertion the boundary conditions above and the elimination principle is adopted as a solution approach [٥٣] leads to omitting of the first and seventh rows and columns of each of the global stiffness matrix, displacement and force vectors, all of which are then called the reduced ones, resulting into the following set of equations:

$$\frac{E_1 I_c}{l^3}\begin{bmatrix} 4l^2 & -6l & 2l & 0 & 0 & 0 \\ -6l & 24 & 0 & -12 & 6l & 0 \\ 2l^2 & 0 & 8l^2 & -6l & 2l^2 & 0 \\ 0 & 12 & -6l & 24 & 0 & 6l \\ 0 & 6l & 2l^2 & 0 & 8l^2 & 2l^2 \\ 0 & 0 & 0 & 6l & 2l^2 & 4l^2 \end{bmatrix} * \begin{Bmatrix} u_2 \\ u_3 \\ u_4 \\ u_5 \\ u_6 \\ u_8 \end{Bmatrix} = \begin{Bmatrix} 0 \\ -p/2 \\ 0 \\ -p/2 \\ 0 \\ 0 \end{Bmatrix} \quad \text{------ (٤-١٦)}$$

The bending stress σ can be given as:

Where l: is the element length which is the same for all of the elements and equal to L/٣ (one third of the beam length).

P: the total force exerted on the beam which can be treated as static. From Eq. ٤-١٦ the displacement u_1 through u_8 can be found.

The shape functions of a beam element are listed below expressed I terms of intrinsic (natural) coordinate system (ξ–η coordinate system) as following [٥٣]:

$$N_1 = \frac{1}{4}\left(2 - 3\xi - \xi^3\right)$$
$$N_2 = \frac{1}{4}\left(1 - \xi - \xi^2 + \xi^3\right)$$
$$N_3 = \frac{1}{4}\left(2 + 3\xi - \xi^3\right)$$
$$N_4 = \frac{1}{4}\left(-1 - \xi + \xi^2 + \xi^3\right)$$

---------- (٤-١٧)

Thus the displacement can be represented in terms of the natural coordinate system (ξ–η coordinate system), for a beam element in a matrix form as:

$\{u\} = [N_1 \ N_2 \ N_3 \ N_4] \{u_i\}$ ---------- (٤-١٨)

Where N_1 through N_4: are the shape functions of a beam element Eqs. ٤-١٧.

u_i: is a displacement vector components.

From the basic bending theory, the bending moment (M) is given by [٥٤]:

$$M = EI \frac{d^2u}{dx^2}$$ ---------- (٤-١٩)

The shear load (V) is:

$$V = \frac{dM}{dx} = \frac{d}{dx}\left[EI \frac{d^2u}{dx^2} \right] = EI \frac{d^3u}{dx^3}$$ ---------- (٤-٢٠)

The bending stress σ can be given as:

$$\sigma = E_1 y \frac{d^2 u}{dx^2} \qquad \text{---------- (٤-٢١)}$$

The shearing stress τ will then be:

$$\tau = \frac{E_1 I_C}{A}\left(\frac{d^3 u}{dx^3}\right) \qquad \text{---------- (٤-٢٢)}$$

(du/dx) can be found using chain rule of differentiation [٥٢]:

$$\frac{du}{dx} = \frac{du}{d\xi} \cdot \frac{d\xi}{dx} \qquad \text{---------- (٤-٢٣)}$$

It is known that from the basics of finite elements principles of one-dimensional element of linear type that [٤٢]:

$$\frac{d\xi}{dx} = \frac{2}{l} \qquad \text{--------- (٤-٢٤)}$$

$$\frac{du}{d\xi} = \frac{d}{d\xi}\begin{pmatrix} N_1 & N_2 & N_3 & N_4 \end{pmatrix}\{u_i\} \qquad \text{---------- (٤-٢٥)}$$

Where l is the element length, substituting Eqs. (٤-٢٤ & ٤-٢٥) results in:

$$\frac{du}{dx} = \frac{2}{l} \cdot \frac{d}{d\xi}\begin{pmatrix} N_1 & N_2 & N_3 & N_4 \end{pmatrix}\{u_i\} \qquad \text{---------- (٤-٢٦)}$$

And:

$$\frac{d^2 u}{dx^2} = \frac{4}{l^2} * \frac{d^2}{d\xi^2}\begin{pmatrix} N_1 & N_2 & N_3 & N_4 \end{pmatrix}\{u_i\} \qquad \text{---------- (٤-٢٧)}$$

Similarly:

$$\frac{d^3u}{dx^3} = \frac{8}{l^3} \frac{d^3}{d\xi^3}\begin{pmatrix} N_1 & N_2 & N_3 & N_4 \end{pmatrix}\{u_i\} \qquad \text{---------- (٤-٢٨)}$$

Consequently the bending moment (M) can be put (by substitution Eq. ٤-٢٧ in Eq. ٤-١٩) as:

$$M = \frac{4E_1 I_C}{l^3}\left[\frac{d^2}{d\xi^2}\{N_I(\xi)\}^T \{u_i\}\right] \qquad \text{---------- (٤-٢٩)}$$

And the bending stress is given (by substitution Eq. ٤-٢٧ in Eq. ٤-٢١) as:

$$\sigma = \frac{4E_1 y}{l^3}\left[\frac{d^2}{d\xi^2}\{N_i(\xi)\}^T \{u_i\}\right] \qquad \text{---------- (٤-٣٠)}$$

The shear load V may be given (by substitution Eq. ٤-٢٨ in Eq. ٤-٢٠) as:

$$V = \frac{8E_1 I_c}{l^3}\left[\frac{d^3}{d\xi^3}\{N_i(\xi)\}^T \{u_i\}\right] \qquad \text{---------- (٤-٣١)}$$

The shear stress τ can be given (by substitution Eq. ٤-٢٨ in Eq. ٤-٢٢) as::

$$\tau = \frac{8E_1 I_c}{l^3 A}\left[\frac{d^3}{d\xi^3}\{N_i(\xi)\}^T \{u_i\}\right] \qquad \text{---------- (٤-٣٢)}$$

Where E١: elastic modulus in a direction parallel to that of fibers.

I_c: composite beam section moment of inertia (or second moment of area).

y: distance from the neutral axis of the beam to the layer at which the stresses to be found.

٤.٥ Stress Analysis Through Beam Cross-Section:

An other additional necessary analysis across the beam cross-section is to investigate and detect the stress state transversely induced in the beam material using the unit cell method in micromechanical analysis which forms the essence of the presented work.

The hexagonal fiber-matrix packing system is adopted for the idealization of the material of the composite beam under consideration due to its advantages over other systems including the square packing one. These advantages can be listed below, [١٢]:

١. The hexagonal packing system with trapezoidal unit cell has more symmetry transformations.

٢. It preserves the property of transverse isotropy whilst others don't.

٣. It is characterized by its compactness compared with other packing systems, in other words the fibers occupy a lesser space for the same volume fractions of other layouts. The layout of the cross-section of the beam under consideration can be visualized as a form like that shown in figure ٤-٨ below:

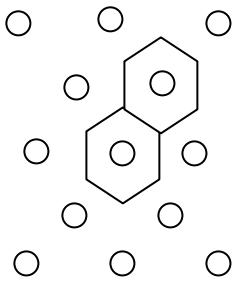

Fig. ٤-٨ The hexagonal fiber-matrix packing system with hexagonal unit cell.

٤. This fiber-matrix packing system and the associated unit cell are formulated such that they are capable of accommodating the irregular fiber cross-sections and imperfections asymmetrically distributed around fibers such as micro-cracks and local debonding.

٥. The unit cell is such fabricated that it can be subjected to arbitrary combinations of macroscopic stresses or strains unlike to most available unit cells in literatures.

The hexagonal layout has what so called the periodic element translations of which in y- and z-direction can cover the whole area of the cross-section. The size of this periodic element can be reduced to quarter of it, called hereafter the quarter model which can also be further reduced to a unit cell size by virtue of the translational and reflectional symmetry transformations existed in the system. These concepts could be shown in figure ٤-٩ [٥].

The unit cell so obtained carries the elastic properties of the composite material it represents, so a stress analysis by finite element method can well capture the overall structural status from both mechanical loading and stress distribution viewpoints.

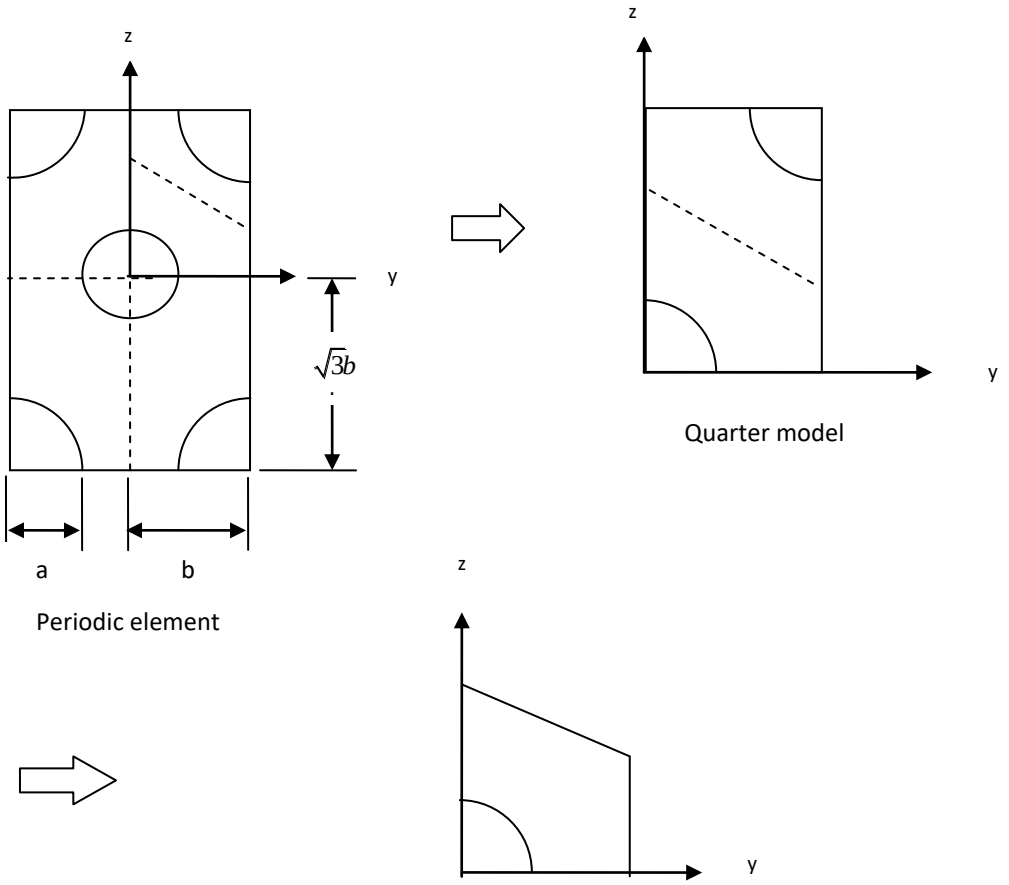

Figure ٤-٩ Periodical element, quarter model

And the unit cell obtained from the hexagonal system

٤.٦ Determination of The Effective Properties of The Unit Cell:

A three-dimensional model is designated for the unit cell representing the composite material under consideration and the properties given to the unit cell as a small element or portion of the beam are the effective elastic properties of E-glass/polyester calculated by the rule of mixture and Halpin-Tsai equation (Eqns. ٣-٢٩ & ٣-٣٠) as mentioned below [٣]:

$$E_1 = E_f V_f + E_m V_m \qquad \text{------ (٤-٣٣)}$$

$$E_2 = \frac{E_f E_m}{E_f V_m + E_m V_f} \qquad \text{------ (٤-٣٤)}$$

$$\nu_{12} = \nu_f V_f + \nu_m V_m \qquad \text{------ (٤-٣٥)}$$

$$G_{12} = \frac{G_f G_m}{G_f V_m + G_m V_f} \qquad \text{------ (٤-٣٦)}$$

For ν_{23} & G_{23} the Halpin-Tsai Eq. is used such that E_2 can be determined from Eq. ٤-٣٤ above, then inserted in Eq. ٣.٢٩ to find the term of ηV_f , the term of ξ can determined using equation of Hewitt & Malherbe [١] :

$$\xi = 1 + 40\, V_f^{10} \qquad \text{------ (٤-٣٧)}$$

Thus, ν_{23} is found. G_{23} is calculated using the relation [١٣]:

$$G_{23} = \frac{E_2}{2(1+\nu_{23})} \qquad \text{------ (٤-٣٨)}$$

The results of Eqns. ٤.٣٣ through ٤.٣٨ for E-glass/polyester for various fiber volume fractions with the properties of the constituent materials are listed in the tables of appendix-C.

٤.٧ Calculation of The Areas and Forces Applied on The Unit Cells:

A unit cell of trapezoidal geometry shown in Fig. ٤.٩ is chosen at the node possessing the maximum longitudinal (bending) stresses throughout the beam. This unit cell can be chosen everywhere else in order to perform a desired micromechanical analysis at that position to capture the variation and/or distribution of the field parameters (stress, strain and displacement) their. Appendix-D contains the tables of the ٣-dimensional stresses and

displacements and the nodal elastic strains of the unit cells as determined by ANSYS-v٥.٤ [٥٨]. Areas of various sides of the unit cells in the directions of x, y and z (Fig. ٤.٩) are calculated as following [١٣]: (The area A_x lies in the plane perpendicular to x-axis, so as all other areas with their respective axes).

$$A_x = \frac{b}{\sqrt{3}} * l$$

$$A_y = b * l$$

$$A_z = \frac{\sqrt{3}}{2} b^2 \qquad \text{------ (٤-٣٩)}$$

The term (b) can be found using the relation [١٢]:

$$V_f = \frac{\pi a^2}{2\sqrt{3}\, b^2} \qquad \text{------ (٤-٤٠)}$$

Where V_f: fiber volume fraction of the material represented by the unit cell.

a: fiber radius.

Then, the forces applied on the various sides due to the stresses are:

$$F_x = \sigma_x * A_x$$
$$F_y = \sigma_y * A_y \qquad \text{------ (٤-٤١)}$$
$$F_z = \sigma_z * A_z$$

The unit cell referred to above is descritized and meshed by the ٣-dimensional element of the type of ٨-node brick element known as solid-٤٥ in the ANSYS program default as shown in Figs. ٤.١٠ through ٤.١٢

Appendix-E contains the tables of the various fiber volume fractions with the corresponding dimension (b), areas, stresses and the forces applied on the unit cell.

٤.٨ Calculation of the Micro-stresses of The Fibers and Matrix:

The micro stresses of the fibers and matrix for the various cases can be determined by using the principle of equating the elastic strains in the composite material with those in the matrix and fibers to avoid the state of debonding as referred to in the assumptions of §٣.١, this means [٦١]:

$$\varepsilon_c = \varepsilon_f = \varepsilon_m \qquad \text{------ (٤-٤٢)}$$

Then, using Hook's law in ٣-dimensional state of stress to calculate the normal microstresses in terms of their corresponding normal elastic strains, since both fibers and matrix are assumed isotropic, homogeneous and linearly elastic. Thus for normal stresses of fibers and matrix [٤٥ & ٥٤]:

$$\begin{Bmatrix} \sigma_x \\ \sigma_y \\ \sigma_z \end{Bmatrix} = \begin{bmatrix} \lambda + 2G & \lambda & \lambda \\ \lambda & \lambda + 2G & \lambda \\ \lambda & \lambda & \lambda + 2G \end{bmatrix} \begin{Bmatrix} \varepsilon_x \\ \varepsilon_y \\ \varepsilon_z \end{Bmatrix} \qquad \text{------ (٤-٤٣)}$$

Where:

$$\lambda = \frac{\nu E}{(1+\nu)(1-2\nu)}$$

$$G = \frac{E}{2(1+\nu)} \qquad \text{------ (٤-٤٤)}$$

Therefore, for matrix and fibers whose engineering properties listed in appendix-c respectively using Eq. ٤-٤٤ :

$(\lambda+2G)_m$ = ٥.٣٧٥GPa and λ_m =٣.٠٢٥ GPa

$(\lambda+2G)_f$ = ٨٠ GPa and λ_f =٢٠ GPa

The results of microstresses of fibers and matrix and for the unit cells are listed in appendix-D. These values are chosen at the nodes mentioned in the tables, because those nodes represent the midpoints between the fiber and its surrounding matrix and the direct next fibers from all directions Fig. ٤.١٣.

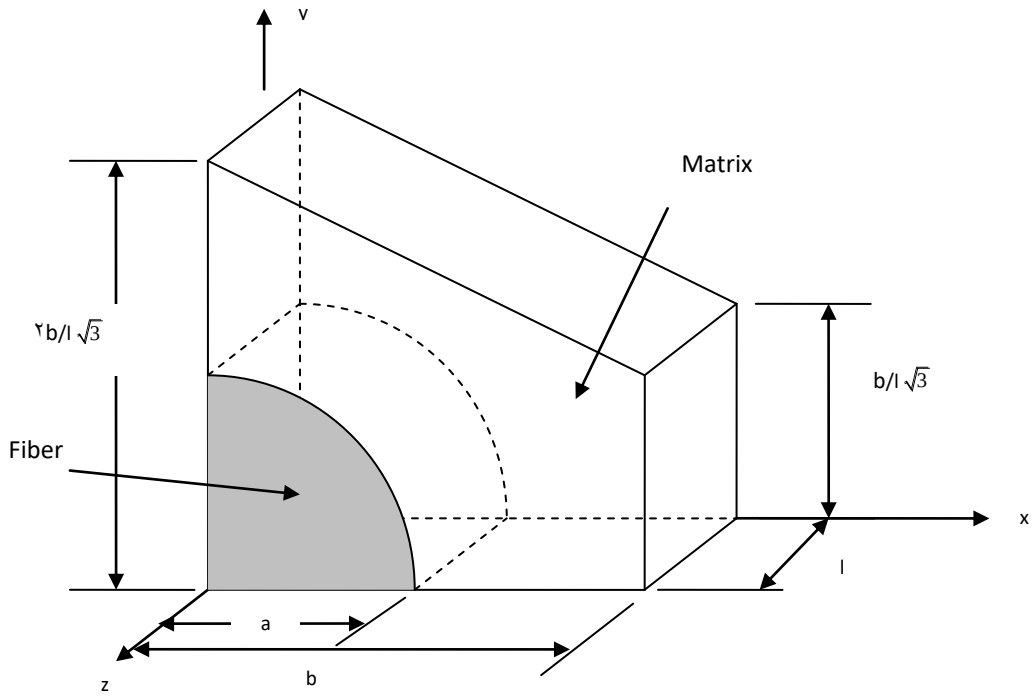

Fig. ٤.٩: The three-dimensional unit cell in a quarter model.

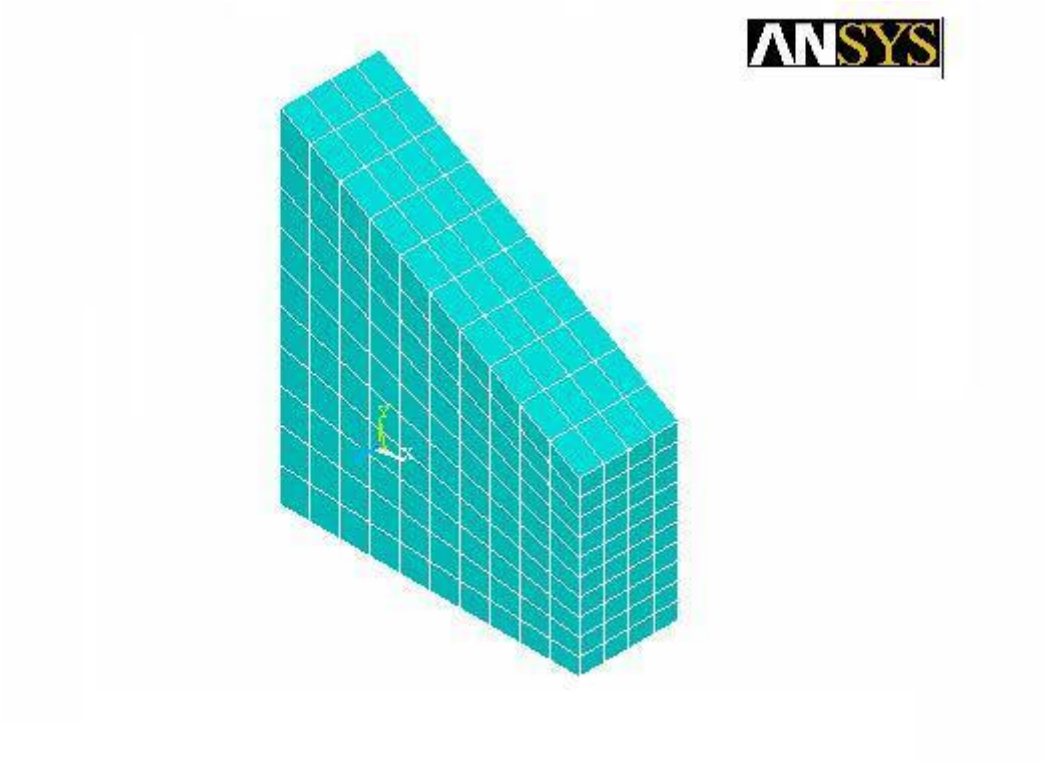

Fig. ٤.١٠: Descritization of the trapezoidal Unit Cell.

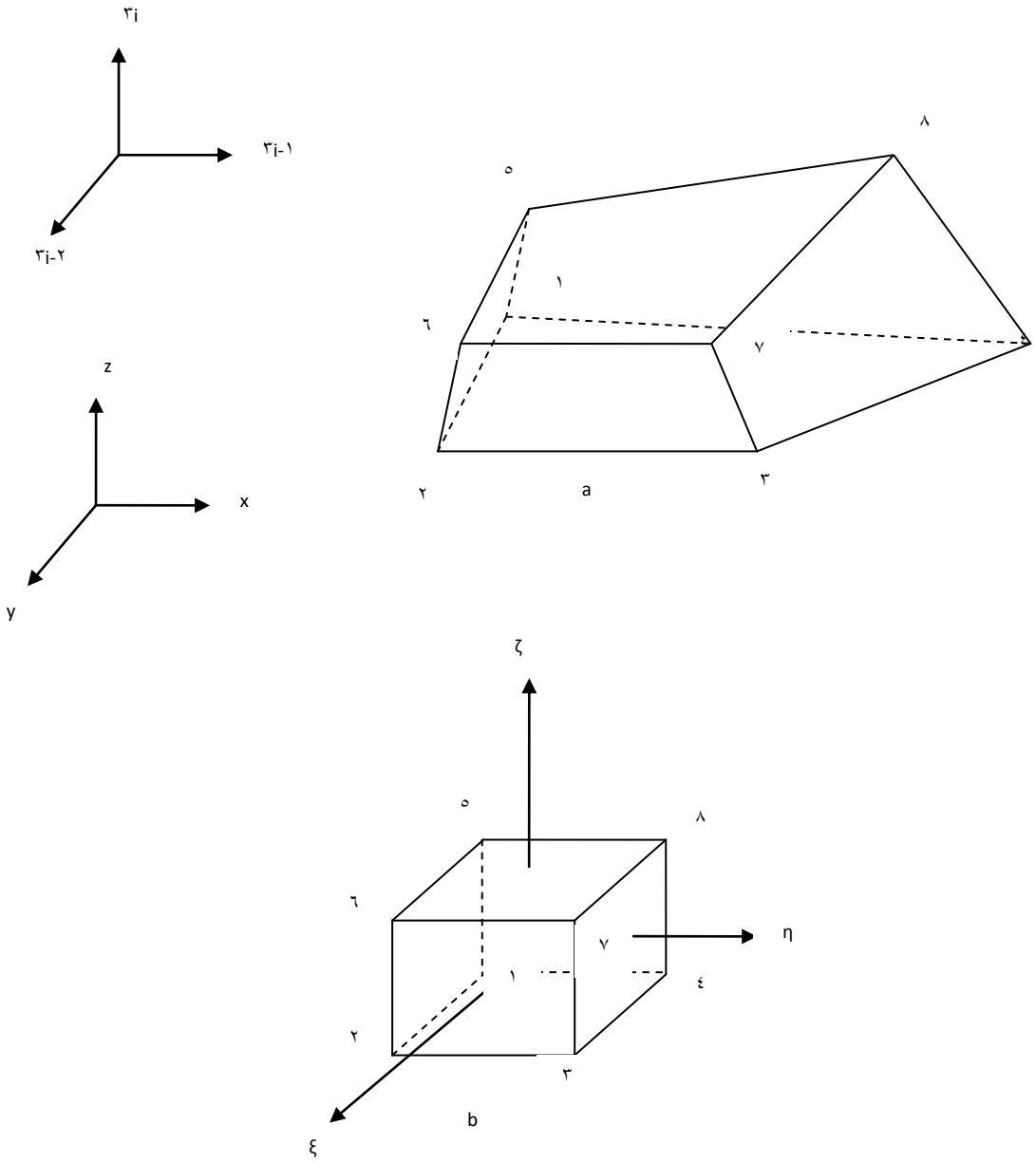

Fig.٤.١١: The geometry of the hexahedral ٨-nodes brick element and node numbering scheme. (a) the general shape. (b) the master hexahedral brick element

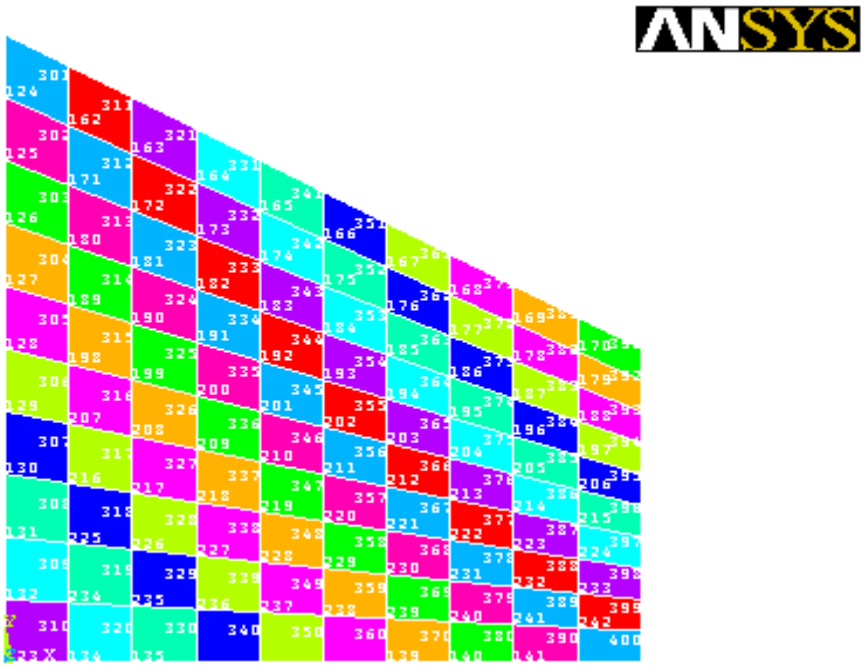

Fig. ٤.١٢: The front view of the unit with elements numbers.

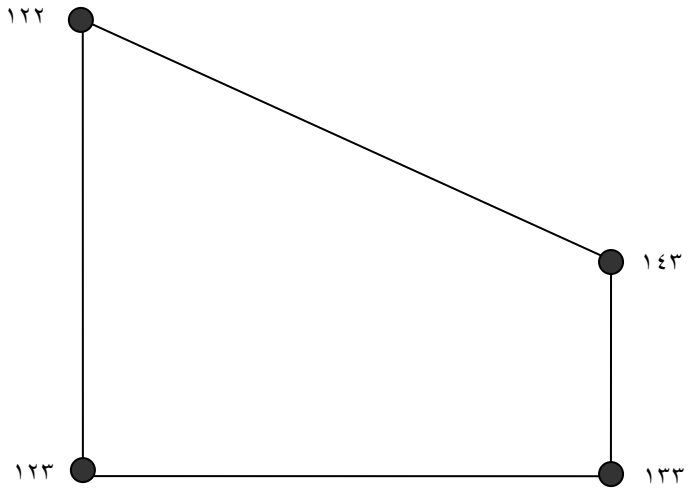

Fig. ٤.١٣: Specification of the corner nodes of the unit cell at which the elastic strains are taken for microstresses calculation.

٤.٩ Finite element Formulation and Mesh Generation of The Unit Cell:

The mesh which can be made for the unit cell cited above and the type or types of the elements adopted for this application may take various shapes or geometries, but the preferred one for the problem of plane strain state may be the quadratic (higher order) quadrilateral and triangular elements due to their better accuracy over other types since they have eight and six nodes respectively resulting in more precise stress distribution detection. Figure ٤-١٤ shows a proposed meshing of a unit cell of a unidirectional fiber-reinforced composite of fiber volume fraction of (٦٠٪) (V_f =o.٦) discritized into ٧٢ elements from both types mentioned above (in case of ٢-dim. problems) plotted by the program of AUTOCAD ٢٠٠٤ [٥٢]. The shape functions of both types of elements are listed below [٤٢]:

١. for quadratic triangular ٦ nodes elements:

$$
\begin{aligned}
N_1 &= \xi(2\xi - 1) \\
N_2 &= \eta(2\eta - 1) \\
N_3 &= \zeta(2\zeta - 1) \\
N_4 &= 4\xi\eta \\
N_5 &= 4\zeta\eta \\
N_6 &= 4\xi\zeta
\end{aligned}
\qquad \text{---------- (٤-٤٥)}
$$

Where $\zeta = 1 - \xi - \eta$

The general shape of this respective triangular element and the associated node numbering scheme are shown in figure ٤-١١.

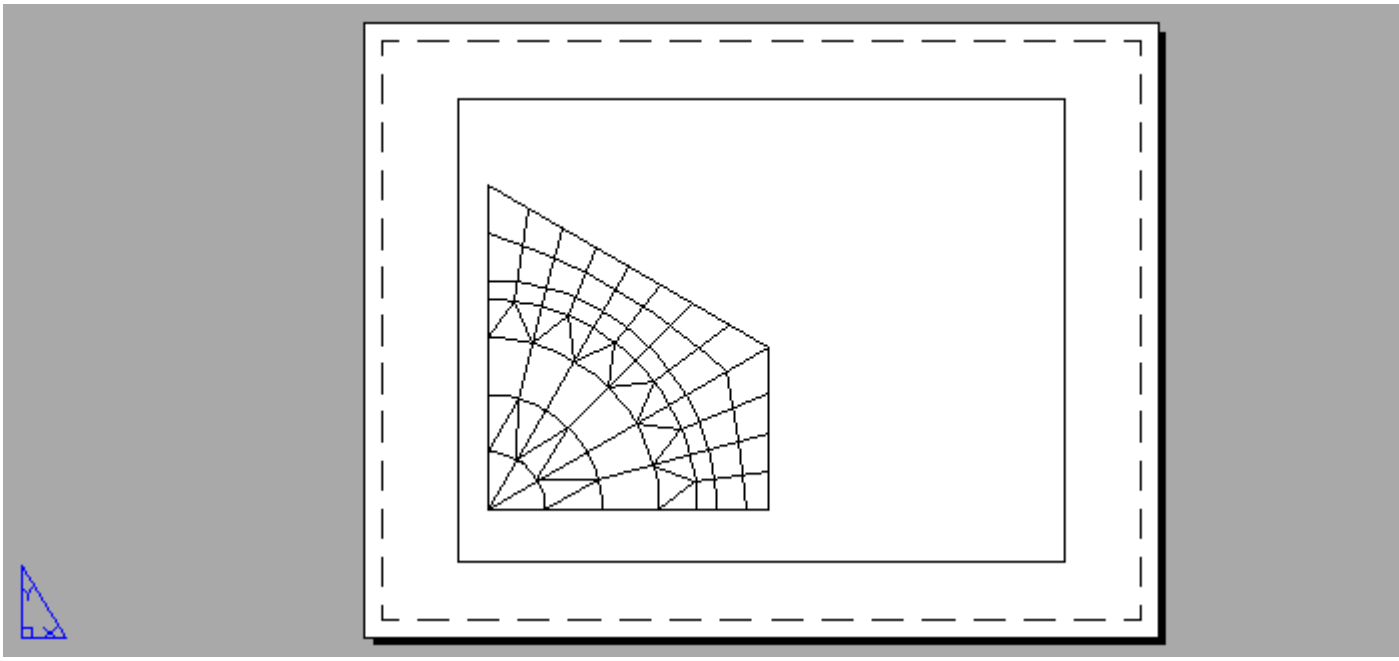

Figure ٤-١٤ the proposed mesh of the unit cell of a UFRCM. used in Matlab.

For the quadratic quadrilateral element, the shape functions and numbering scheme can be listed and shown in figure ٤-١٢ respectively as following [٤٢ & ٥١]:

$$N_1 = -\frac{1}{4}(1-\xi)(1-\eta)(1+\xi+\eta)$$

$$N_2 = -\frac{1}{4}(1+\xi)(1-\eta)(1-\xi+\eta)$$

$$N_3 = -\frac{1}{4}(1+\xi)(1+\eta)(1-\xi-\eta)$$

$$N_4 = -\frac{1}{4}(1-\xi)(1+\eta)(1+\xi-\eta)$$

$$N_5 = \frac{1}{2}(1-\xi^2)(1-\eta)$$

$$N_6 = \frac{1}{2}(1+\xi)(1-\eta^2)$$

$$N_7 = \frac{1}{2}(1-\xi^2)(1+\eta)$$

$$N_8 = \frac{1}{2}(1-\xi)(1-\eta^2) \qquad \text{---------- (٤-٤٦)}$$

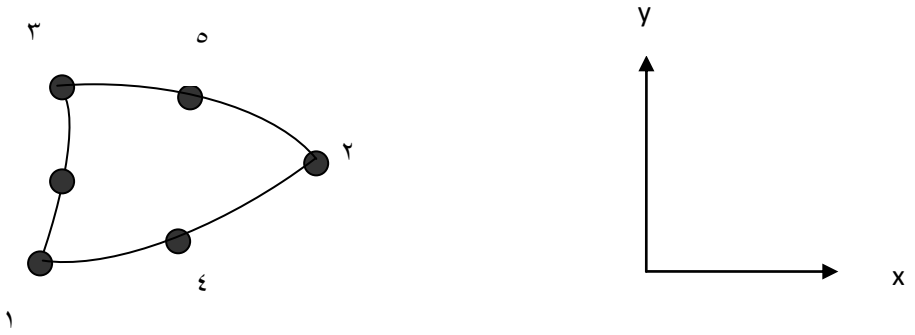

Fig. ٤.١٥: The six node higher order triangular element

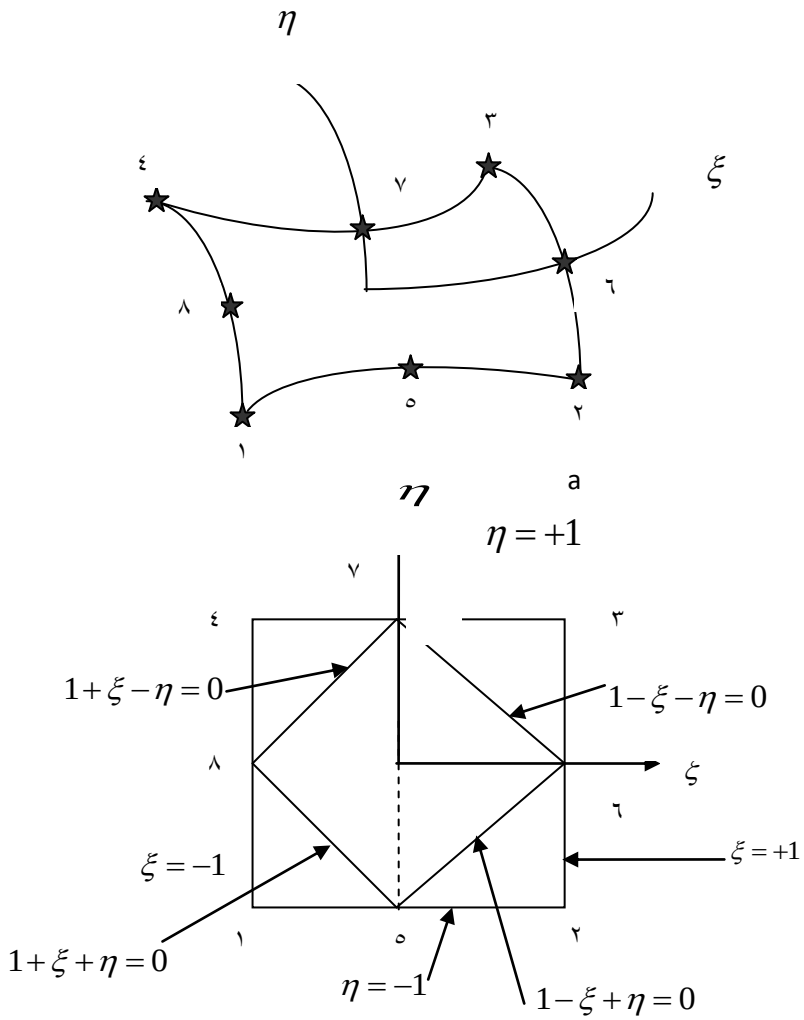

Figure ٤-١٦ Eight-node quadratic quadrilateral

(a) in x-y plane, (b) in $\xi-\eta$ plane

٤.١٠ Formulation of Element Stiffness Matrix:

Stiffness matrix of a six-node triangular element can be computed by using Gauss-Legender numerical integration method which can be expressed by [٤٢ & ٥٠]:

$$[k_e] = t_e \int_A \int [B]^T [D][B] \det J \; d\xi \, d\eta \qquad \text{---------- (٤-٤٧)}$$

Where t_e : is the element thickness.

The above integrand of Eq. ٤-٤٧ can be evaluated through the following summation:

$$\int_A \int f(\xi,\eta) \, d\xi \, d\eta = \sum_{i=1}^{n} w_i f(\xi_i, \eta_i) \qquad \text{---------- (٤-٤٨)}$$

Where n is the number of Gaussian points over which the integration is performed.

[B] is the strain-displacement matrix calculated by the following formula:

[B] = [A] × [G] ---------- (٤-٤٩)

Where:

$$[A] = \frac{1}{\det J} \begin{bmatrix} J_{22} & -J_{12} & 0 & 0 \\ 0 & 0 & -J_{21} & J_{11} \\ -J_{21} & J_{11} & J_{22} & -J_{12} \end{bmatrix}$$

[G]: matrix of the partial derivatives of the shape functions given as:

$$[G] = \begin{bmatrix} \frac{\partial N_1}{\partial \xi} & 0 & \frac{\partial N_2}{\partial \xi} & 0 & \frac{\partial N_3}{\partial \xi} & 0 & \frac{\partial N_4}{\partial \xi} & 0 & \frac{\partial N_5}{\partial \xi} & 0 & \frac{\partial N_6}{\partial \xi} & 0 \\ \frac{\partial N_1}{\partial \eta} & 0 & \frac{\partial N_2}{\partial \eta} & 0 & \frac{\partial N_3}{\partial \eta} & 0 & \frac{\partial N_4}{\partial \eta} & 0 & \frac{\partial N_5}{\partial \eta} & 0 & \frac{\partial N_6}{\partial \eta} & 0 \\ 0 & \frac{\partial N_1}{\partial \xi} & 0 & \frac{\partial N_2}{\partial \xi} & 0 & \frac{\partial N_3}{\partial \xi} & 0 & \frac{\partial N_4}{\partial \xi} & 0 & \frac{\partial N_5}{\partial \xi} & 0 & \frac{\partial N_6}{\partial \xi} \\ 0 & \frac{\partial N_1}{\partial \eta} & 0 & \frac{\partial N_2}{\partial \eta} & 0 & \frac{\partial N_3}{\partial \eta} & 0 & \frac{\partial N_4}{\partial \eta} & 0 & \frac{\partial N_5}{\partial \eta} & 0 & \frac{\partial N_6}{\partial \eta} \end{bmatrix}$$

det J: is the determinant of the Jacobean matrix defined as:

$$[J]=\begin{bmatrix}\frac{\partial x}{\partial \xi} & \frac{\partial y}{\partial \xi}\\ \frac{\partial x}{\partial \eta} & \frac{\partial y}{\partial \eta}\end{bmatrix}=\begin{bmatrix}J_{11} & J_{12}\\ J_{21} & J_{22}\end{bmatrix} \qquad \text{---------- (٤-٥٠)}$$

x & y are obtained as functions of ξ & η through the isoparametric representation of the problem then differentiated with respect to ξ & η as shown in the manner below:

$$x = N_1x_1 + N_2x_2 + N_3x_3 + \ldots\ldots\ldots\ldots + N_6x_6 \qquad \text{---------- (٤-٥١)}$$

$$y = \sum_{i=1}^{6} N_i y_i \qquad \text{---------- (٤-٥٢)}$$

Thus:

$$\frac{\partial x}{\partial \xi}=\frac{\partial}{\partial \xi}(N_1x_1 + N_2x_2 + N_3x_3 + N_4x_4 + N_5x_5 + N_6x_6) \qquad \text{---------- (٤-٥٣)}$$

$$\frac{\partial x}{\partial \eta}=\frac{\partial}{\partial \eta}\left(\sum_{i=1}^{6} N_i x_i\right) \qquad \text{---------- (٤-٥٤)}$$

The same holds for y. The [D] is known as the material properties matrix for an orthotropic material under plain strain condition in ٢-٣ plane figure (٤-١٣) [٥٠, ٥١ & ٥٢]:

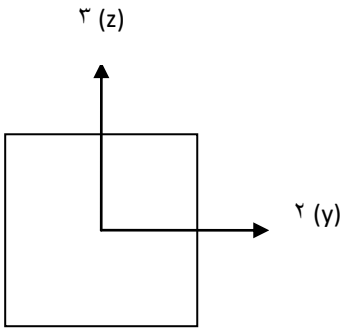

Figure ٤-١٧ A plane area under plane strain condition in ٢-٣ plane where ١-direction towards the viewer

$$[D] = \begin{bmatrix} Q_{11} & Q_{12} & 0 \\ Q_{12} & Q_{22} & 0 \\ 0 & 0 & Q_{66} \end{bmatrix} \qquad \text{---------- (٤-٥٥)}$$

Where:

$$Q_{11} = \frac{1 - \nu_{23}\nu_{32}}{E_2 E_3 \Delta} = \frac{E_1}{1 - \nu_{21}\nu_{12}}$$

$$Q_{12} = \frac{\nu_{21} + \nu_{31}\nu_{32}}{E_2 E_3 \Delta} = \frac{\nu_{12} + \nu_{13}\nu_{32}}{E_1 E_3 \Delta}$$

$$or \; Q_{12} = \frac{\nu_{12} E_2}{1 - \nu_{21}\nu_{12}}$$

$$Q_{22} = \frac{1 - \nu_{31}\nu_{13}}{E_1 E_3 \Delta} = \frac{E_2}{1 - \nu_{21}\nu_{12}}$$

$$Q_{66} = \frac{1}{G_{12}}$$

The [A] and [G] matrices are of size (٣×٤) and (٤×١٢) respectively, thereby [B] will be of size of (٣×١٢) consequently the elemental stiffness matrix [K_e] will be of size of (١٢×١٢) whose all elements are functions of both ξ and η. The superscript n in the summation equation ٤-٤٨ represents the number of the Gaussian points over which the numerical integration is performed, w_i is the weight of approximation and ξ_i and η_i are the locations of the Gaussian points. In the present work n = ٣ is considered since this value is frequently adopted in structural engineering applications otherwise, it can be found using the following relation [٥٠]:

٢n-١ = highest power of ξ ---------- (٤-٥٦)

For the quadratic quadrilateral element the same concepts discussed above are used to formulate its stiffness matrix except that [G] will defined as:

$$[G]=\begin{bmatrix} \frac{\partial N_1}{\partial \xi} & 0 & \frac{\partial N_2}{\partial \xi} & 0 & \frac{\partial N_3}{\partial \xi} & 0 & \frac{\partial N_4}{\partial \xi} & 0 & \frac{\partial N_5}{\partial \xi} & 0 & \frac{\partial N_6}{\partial \xi} & 0 & \frac{\partial N_7}{\partial \xi} & 0 & \frac{\partial N8}{\partial \xi} & 0 \\ \frac{\partial N_1}{\partial \eta} & 0 & \frac{\partial N_2}{\partial \eta} & 0 & \frac{\partial N_3}{\partial \eta} & 0 & \frac{\partial N_4}{\partial \eta} & 0 & \frac{\partial N_5}{\partial \eta} & 0 & \frac{\partial N_6}{\partial \eta} & 0 & \frac{\partial N_7}{\partial \eta} & 0 & \frac{\partial N_8}{\partial \eta} & 0 \\ 0 & \frac{\partial N_1}{\partial \xi} & 0 & \frac{\partial N_2}{\partial \xi} & 0 & \frac{\partial N_3}{\partial \xi} & 0 & \frac{\partial N_4}{\partial \xi} & 0 & \frac{\partial N_5}{\partial \xi} & 0 & \frac{\partial N_6}{\partial \xi} & 0 & \frac{\partial N_7}{\partial \xi} & 0 & \frac{\partial N_8}{\partial \xi} \\ 0 & \frac{\partial N_1}{\partial \eta} & 0 & \frac{\partial N_2}{\partial \eta} & 0 & \frac{\partial N_3}{\partial \eta} & 0 & \frac{\partial N_4}{\partial \eta} & 0 & \frac{\partial N_5}{\partial \eta} & 0 & \frac{\partial N_6}{\partial \eta} & 0 & \frac{\partial N_7}{\partial \eta} & 0 & \frac{\partial N_8}{\partial \eta} \end{bmatrix}$$

And also again:

$$x = \sum_{i=1}^{8} N_i x_i \qquad \text{---------- (٤-٥٧)}$$

$$y = \sum_{i=1}^{8} N_i y_i \qquad \text{---------- (٤-٥٨)}$$

Therefore the stiffness matrix for such element will be of size of (١٦x١٦) and it is a symmetric one.

Furthermore, Eq. ٤-٣٤ is calculated for the two dimensional quadratic quadrilateral element as:

$$[k_e] = t_e \int_A \int [B]^T [D][B] \det J \; d\xi \, d\eta \qquad \text{---------- (٤-٥٩)}$$

The integral above is solved numerically by using Gauss-Legender numerical technique in two dimensions expressed as:

$$I = \int_{-1}^{1}\int_{-1}^{1} f(\xi,\eta)\, d\xi \, d\xi = \sum_{i=1}^{n}\sum_{j=1}^{m} w_i w_j f(\xi_i, \eta_j) \qquad \text{---------- (٤-٦٠)}$$

Where n, m are the numbers of Gaussian points over which the integration is achieved while w_i & w_j are weights of approximation and ξ_i & η_j are the locations of the Gaussian points.

To specify the number of the Gaussian points (n) or (m) which are frequently taking the same value, it is sometimes resorted to the following expressions:

$2n-1$ = highest power of η ---------- (٤-٦١)

$2m-1$ = highest power of ξ ---------- (٤-٦٢)

For two-dimensional problems values of ξ_i & η_j are taken equal [٥٣]. The mesh of the quarter of the unit cell of the composite beam cross-section of interest is shown in Fig. ٤-١٠. Calculations of stiffness matrices of the various elements are performed by a Matlab program. With the results obtained are all shown throughout the next section.

Assemblage of the overall global structural stiffness matrix is achieved by accumulating the corresponding elements in the individual elemental stiffness matrices according to the local-global correspondence table (connectivity table) analogous to table ٤.١. The method of assembly can be referred to and reviewed in many respective textbooks. Mapping of stresses, strains and displacements will be according to the bending of orthotropic beams theory relations. The formulation above can analogously be extended for the three-dimensional problems in order to comprehensively capture the various field parameters distribution throughout any required domain as performed in the current study.

Chapter Five

Results and Discussion

٥.١ Introduction

In this chapter the presented results are obtained from the finite element formulation (FEF) for a unidirectional fiber-reinforced composite beam (UDFRCB) using a matlab program and ANSYS v-٥.٤ for analyzing the macro- and microstresses induced in the beam alluded to above when subjected to a four-points-bending state of stress with the following two types of supports:

١. Both ends are clamped (built-in beam case).

٢. Both ends are pinned (simply supported beam case).

For each of the above cases of supports, different fiber volume fractions of the composite material are considered to study their effect on the beam response and stresses induced. The effect of variation of fibers and matrices materials on the beam behavior is also investigated. The effect of increasing of the applied loads on the beam deflection and stresses will also be discussed. All of these parameters will be investigated on both macro- and microscopic levels using the method of unit cell in micromechanical stress analysis of UDFRCM. A unit cell is selected at the cross-section containing the maximum stresses at different fiber volume fractions and different loads with different fiber sizes and analyzed for the responses and the stresses induced to assign the effect of these parameters. The elastic properties of the composites and their constituent materials adopted in this work are as tabulated in the following tables. These properties are calculated by using the rule of mixtures for $E_{١}$, $E_{٢}$, $G_{١٢}$ and ν_{12} and Halpin-Tsai equation for $G_{٢٣}$ and ν_{23}. The variation of the effective elastic properties of the composite material adopted is based on the variation of both fibers and matrices materials. First, fibers variation is considered.

Variation of the composite elastic properties is based on extra types of Kevlar-٤٩ [٥٤] with Polyester as a matrix at a given fiber volume fraction (V_f) of ٥٠٪ . Results are listed in appendix-C

٥.٢ Macromechanical Analysis:

Using ANSYS V-٥.٤ to solve for the beam response and stresses. The beam is of circular cross-section of diameter of (٥٠ mm) reinforced by unidirectional fibers with different volume fractions and subjected to two bending forces of different values according to the assumptions mentioned earlier in §٣.١. The forces are equispaced from both ends of the beam and from each other. The type of the element by which the cylindrical beam under consideration longitudinally meshed in ANSYS is (solid ٩٥)[٥٨] and in MATLAB [٥٩ & ٦٠] is the linear one-dimensional.

٥.٢.١ Effect of Variation of Fiber Volume Fractions On Beam Responses and Stresses:

When the applied load is kept constant at (١٥٠٠N) and the fiber volume fraction is changed, the results obtained are as listed in table C.١.٥ containing beam deflections and the stresses induced for E-Glass/Polyester in case of both ends clamped. When the force is increased to ٣٠٠٠N for the same set of fiber volume fractions for the same composite, the results obtained as shown in table C.١.٦ in appendix-C. The results at ٦٠٠٠N are tabulated in table C.١.٧.

At ١٢٠٠٠N, the tests show the set of readings for the deflections and the stresses as arranged in table C.١.٨. It is obviously seen from these tables that

the normal and shear stresses induced in the beam material keep higher levels when the beam is being too stiff (i.e. of high fiber volume fraction) and too soft (i.e. of low fiber volume fraction),while these stresses having their minimum levels at the intermediate fiber volume fractions (٤٠٪ & ٥٠٪). Also, it is clearly seen that the stresses in the direction of the fibers represents the maximum values among them due to the nature of the bending state of stress the beam undergoes, for the same reason, the longitudinal shear stresses represent the minimum values among them, which the case coincides with both simple and thick beam theories. Figures ٥.١ and ٥.٢ graphically and clearly show the stresses and deflection of the beam under bending forces of ١٥٠٠N at different fiber volume fractions (V_f). As mentioned above, the values of ٤٠٪ and ٥٠٪ seem to be the optimum values of reinforcement from the viewpoint of the stresses induced in beam material. With respect to the deflection, the situation is rather different, such that it is inversely proportional to the increase in V_f (Fig. ٥.٢). When the applied loads are doubled, the overall behavior of the beam is unaltered, but the values of the stresses and deflections are approximately doubled by the same factor as it is clearly seen from Figs. ٥.٣ through ٥.٦ & ٥.٩. Figure ٥.٧ shows that the variation of transverse normal stresses (σ_x & σ_y), such that σ_x is of slightly more variation than σ_y and both of them has its minimum limit at a V_f of about ٥٠٪ and have no considerable variations with fiber volume fractions. Fig.٥.٨ shows no variation of the longitudinal normal stress σ_z with V_f.

This may be attributed to the high tensile strength of the fibers which is about (٣٤٥٠ MPa) [٤٥].

٥.٢.٢ Effect of Matrix Material on Beam Deflection and Stresses:

When the matrix material is changed, the magnitudes of beam deflection and stresses will inevitably be changed in a certain manner. The results obtained are as listed in table C.١.٩. Beam deflection and stresses are calculated at a given fiber volume fraction of ٤٠%, the fiber material chosen is Kevlar-٤٩ [٤٥] where the applied load is ٣٠٠٠N. These results are graphically displayed in Figs. ٥.١٠ through ٥.١٣, such that Fig. ٥.١٠ discloses the variation of transverse normal stresses σ_x and σ_y with matrix Young's modulus (E_m) (in GPa).

σ_y which is directed upwards can reasonably be considered as insensitive to the variation of matrix Young's modulus Fig. ٥.١٠, while σ_x which is directed perpendicularly to σ_y (towards the viewer) has rather little variation and directly proportional to E_m. This may be justified by the beam is responding downward due to the applied load hence, the internal stresses induced in that direction will not be highly excited, while there is no response or deflection by the beam or in other words the beam is not allowed to deflect or respond towards x-axis, thus, the beam material exerts an equivalent resistance in that direction to the applied load. The longitudinal stress σ_z shows an inverse proportionality to E_m (Fig. ٥.١١), so is to the longitudinal shear stress τ_{yz} with respect to the shear modulus of the matrix G_m up to a limit of ١.٥ GPa (Fig. ٥.١٢). Fig. ٥.١٣ illustrates that the deflection is decreased with the increase of matrix Young's modulus.

٥.٢.٣ Effect of Fibers Materials on Beam Deflections and Stresses:

Different fiber materials are chosen such as E-Glass, kevlar-٤٩ & carbon fibers to analyze their effects on beam behavior and stresses at predefined

matrix material which is taken to be polyester and V_f of ٥٠٪ subjected to a bending load of ٣٠٠٠N. The results obtained using ANSYS^R V-٥.٤ are as shown in table C.١.١٠.

These readings are graphically represented through Figs. ٥.١٤ to ٥.١٧ to demonstrate the beam behavior as the fibers materials changed. The following remarks can be drawn when observing the figures referred to above:

١. In fig. ٥.١٤ it is clearly seen that σ_y is not significantly fluctuated with fibers elastic modulus and can be considered insensitive to it within this loading range, while σ_x has more variation with fibers elastic modulus than σ_y but of lesser values because the load is fully applied in the direction of (y).

٢. In fig. ٥.١٥ it is clearly seen that the longitudinal normal stress (bending stress) is also approximately insensitive to the fibers elastic modulus, this may be attributed to the very high tensile strength of the fibers.

٣. In fig. ٥.١٦ it is clearly seen that the longitudinal shear stress shows an inverse relationship to the shear modulus of the fibers where it decreases with its increasing.

٤. In fig. ٥.١٧ it is clearly seen that the max. beam deflection decreases with E_f increase due to increasing of composite elastic modulus $E_١$.

٥.٣ Effect of Composite Elastic Properties on Beam Stresses and Deflection:

Variation of beam stresses (σ_x & σ_y) is studied against variation of Poisson's ratio ($\nu_{١٢}$) of the composite material of the beam so as the maximum deflection occurred. Other than this, the effect of variation of the longitudinal

shear modulus (G_{12}) on the magnitude of the stress (τ_{12}) formation is also discussed. The obtained results are listed in their respective table (Appendix C.١.١١) and graphically represented in Figs. ٥.١٨ through ٥.٢٠.

It is apparently seen that the transverse normal stress σ_x does not vary as uniformly as the deflection with the composite Poisson's ratio ν_{12} or as it varies with composite elastic modulus E_1, this may be attributed to the direct affecting of σ_x by E_1 and the dependency of ν_{12} on E_1 in addition to the nature of state of stress which the beam undergoes.

The transverse normal stress σ_y due to its direction with respect to the applied load it generally shows a direct proportionality with decreasing of ν_{12} values up to ٠.٢٣٤ where it up rises, because of the respectively large drop of ν_{12} with respect to it's previous values. The deflection displays a more specified relation with drop of ν_{12} such that it is directly proportional to it.

The longitudinal shear stress τ_{yz} which is due to coincidence of material principal directions with the geometric coordinates and when the equilibrium equations are considered equal to τ_{12} exhibits an inverse relation with G_{12} increasing up to ٢.٧٥٥ from which it starts to increase, this can be interpreted by the physical meaning or explanation of stress formation and induction inside the stressed materials [٤٦ & ٥٤].

٥.٤ Micromechanical Analysis of Clamped-Ends-Beam:

In this section, a micromechanical analysis is carried out by considering a critical cross-section which is the one containing the maximum bending stress induced in the beam material and it is found located at the support region. The unit cell method and the finite element technique are used to find the stresses, strains and displacement around and at the fibers and the matrix. Through this

analysis the effect of the following parameters is investigated on the beam stresses and deflection:

١. Fiber volume fraction.

٢. Fiber diameter.

The geometry of the fiber cross-section is assumed to be circular. Within the first parameter the fiber diameter is assumed constant at (٠.٢٥ mm), then different fiber volume fractions are considered (٠.٩, ٠.٦, ٠.٥, ٠.٤, ٠.٣ and ٠.١). The applied bending load is kept constant at ٣٠٠٠N. Through the second parameter, the fiber volume fraction and the applied load are kept at ٤٠٪ and ٣٠٠٠N respectively while the fiber diameter will be varied over the range of (٠.٩, ٠.٦, ٠.٤ and ٠.٢٥mm) to search their influence on the unit cell size and consequently the responses resulted in it.

٥.٤.١ Discussion of Macro- and Microscopic Results of Unit Cell:

It is clearly seen from observation of the pertinent figures that the unit cells of fiber volume fraction of ٤٠-٥٠٪ represent the minimum values of field parameters. These results are then compared with those of simply supported case

to establish the effect of support type on the stresses induced level and beam deflection.

Fig. ٥.٢١ shows that the macroscopic normal stresses (σ_x, σ_y and σ_z) are approximately directly proportional to fiber volume fraction but σ_z has the lowest affecting among them. A reversed situation holds with respect to the macroscopic displacement of the unit cell, such that, they are decreasing with the increase of fiber volume fraction (Figs. ٥.٢٢ & ٢٣). Figs. ٥.٢٤ and ٢٥ show

the effect of fiber volume fraction on micro stresses of matrix and fibers respectively.

The effect of fiber diameter at constant fiber volume fraction on the maximum unit cell normal stresses, matrix and fiber microstresses is displayed in

Figs. ٥.٢٦ through ٥.٢٩ respectively. The overall indication that can be drawn is the inverse proportionality of these stresses and displacements with the increase of fiber diameter.

٥.٥ Analysis of Simply Supported-Ends Beam:

In this section the effect of the second type of support on the stresses and displacements in the beam is investigated on both macro- and microscopic levels considering the influence of fiber volume fraction, fiber diameter and the applied load on the field parameters variations.

٥.٥.١ Effect of Fiber Volume Fraction on Macroscopic Beam Responses:

The fiber volume fraction has the results on this beam responses as listed in the tables of appendix-E each at its respective applied bending load and graphically plotted in Figs. ٥.٣٠ and ٥.٣١ for the normal stresses and deflection respectively. It can be observed that the longitudinal bending stress (σ_z) is approximately unaffected by fiber volume fraction changing due to high modulus of elasticity in direction of fibers ($E_١$) of the composite material of the beam with respect to the applied load resulting from the high tensile strength of the fibers (about ٣٤٥٠ GPa), but σ_x & σ_y are fluctuating with fiber volume

fraction having their minimum level at V_f of ٤٠٪. The beam deflection is apparently decreases with increase of fiber volume fraction, and usually increases as the applied load increases so as all the other stress components. A comparison is held between beam responses in each case of supporting to clarify its contribution to the resulting stresses and deflection through a graphical plotting as seen in Figs. ٥.٣٢ & ٥.٣٣ are showing that the deflection is independent to the supporting method. The bending stress σ_z is higher in clamped case than its counterpart in simply supported-ends as well as the transverse normal stresses σ_x and σ_y . Both types of supports keep minimum transverse normal stress (σ_x & σ_y) at fiber volume fraction range ٤٠-٥٠٪.

٥.٥.٢ Micromechanical Analysis of Simply Supported Beam:

In this section the microscopic analysis results are plotted and discussed such that the effect of fiber volume fraction and fiber diameter variation upon macro- and microstresses and displacements are explored. It is observed from Fig. ٥.٣٤ that the macroscopic displacement of the unit cell decreases as the fiber volume fraction increases at constant fiber diameter; this can be attributed to the high moduli of elasticity resulting when increasing the fiber volume fraction. In spite of that ٦٠٪ fiber volume fraction has a lower displacement than that of ٤٠- or ٥٠٪ but the latter are more preferable for many reasons among of which the economic.

For macroscopic stresses (Fig. ٥.٣٥), the fiber volume fraction increasing generally leads to an increasing in the stresses σ_x & σ_y beyond ٤٠٪ volume fraction, before this limit the reverse is occurred for these stresses as the fiber volume fraction raises from ١٠-٤٠٪. Therefore, this limit (٤٠٪) can be

considered as the most appropriate magnitude of reinforcement since the longitudinal bending stress σ_z is not noticeably affected by its variation, this may be interpreted by the very high modulus of elasticity of the fibers, σ_x is the most stress component affected by this factor as shown in Fig. ٥.٣٥. The behavior of the microstresses of the matrix is illustrated in Fig. ٥.٣٦ which shows that all stresses in general have an inverse relation with fiber volume fraction increasing despite that ٤٠٪ is still considered the most preferred one for its applicability, economy and having an intermediate limit of stress. Fig. ٥.٣٧ demonstrates that microstresses of the fibers are increasing from ١٠-٥٠٪ fiber volume fraction at which the peak values of all stress components are occurred afterwards, they start to drop to the min. value at ٩٠٪. The stress σ_z is still the one having the minimum variation.

When the fiber diameter effect is considered on the responses of the unit cell, Fig. ٥.٣٨ refers to that the fiber diameter has no effect on the transverse macro-displacements of the unit cell (U_x & U_y) while the longitudinal component (U_z) increases as the fiber diameter increases from ٠.٢٥-٠.٩ mm. Fig. ٥.٣٩ illustrates that the macro-stresses σ_x, σ_y & σ_z of the unit cell are decreasing with fiber diameter increasing, noting that σ_y is the stress component of the highest level this can be ascribed to the position of the node at which the unit cell is selected is at the support where the vertical degree of freedom is constrained. As a general, the position of the largest elastic displacement is the one of the minimum stress induce and vice versa. Figs. ٥.٤٠ and ٤١ clearly show that the micro stresses of both of matrix and fibers respectively decreases as the fiber diameter increases, thus there are some advantages involved in increasing the fiber diameter can be summarized as:

١. Reducing the stresses induced in both fibers and matrix.

٢. Fewer fibers are needed for the same reinforcing degree.
٣. Easier in molding, fabrication and manufacturing consequently, quicker in production.

٥.٦ Failure Criteria of Composite Materials:

After determination of the maximum stresses induced macro- and microscop-

ically in the composite beam, unit cell, fibers and matrix respectively. Failure criterion should be adopted to check for the safety and failure. The reliable failure criteria for composite materials are [١ & ٣]:

١. Tsai-Hill theory.

٢. Tsai-Wu tensor theory.

In all theories, the material, although orthotropic must be homogeneous. Thus, some of the microscopic failure mechanisms are not inherently accounted for. The applicability and suitability of a certain criterion depends upon a number of

factors among of which is that whether the material of interest is ductile or brittle thus, it is a respective matter. For example, for E-glass/epoxy the Tsai-Hill criterion seems to be the most suitable one to be applied [١], other composites may be better treated with something else. Prior to considering a certain criterion, it is essential to specify the composite yield strengths in x-, y-, z-directions and shear in ١-٢ plane they are X, Y, Z and S respectively. In some cases the strength in the same direction in tension is different to that in compression. These strengths are usually practically measured or determined

therefore, the failure criteria will be in terms of them since there are no experimentations involved in the present work.

٥.٦.١ Tsai-Hill Theory:

It is an extension of Von-Mises theory for isotropic materials stating that [١]:

$$(G+H)\sigma_1^2+(F+H)\sigma_2^2+(F+G)\sigma_3^2-2H\sigma_1\sigma_2-2G\sigma_1\sigma_3-2F\sigma_2\sigma_3$$

$$+2L\tau_{23}^2+2M\tau_{13}^2+2N\tau_{12}^2=1 \quad \text{------ (٥.١)}$$

Where F, G, H, L, M and N are failure strengths parameters. If a three dimensional state of stress is encountered with six stress components, then the failure strengths parameters are related to the composite material failure strengths X, Y, Z and S as [٣]:

$$٢N = \frac{1}{S^2} \quad \text{------ (٥.٢)}$$

$$٢H = \frac{1}{X^2}+\frac{1}{Y^2}-\frac{1}{Z^2} \quad \text{------ (٥.٣)}$$

$$٢G = \frac{1}{X^2}-\frac{1}{Y^2}+\frac{1}{Z^2} \quad \text{------ (٥.٤)}$$

$$٢F = \frac{1}{Y^2}+\frac{1}{Z^2}-\frac{1}{X^2} \quad \text{------ (٥.٥)}$$

$$٢L = \frac{1}{\left(\tau_{23}^*\right)^2} \quad \text{------ (٥.٦)}$$

$$M_{٢} = \frac{1}{\left(\tau_{13}^{*}\right)^{2}} \qquad \text{------ (٥.٧)}$$

Where τ_{23}^{*} and τ_{13}^{*} are the failure shear strengths in ٢-٣ and ١-٣ planes respectively. With respect to the application of the present work only the failure strength parameters of F, G, H and L are considered since the shear stresses in ١-٢ and ١-٣ planes are unconsidered. Therefore, Tsai-Hill equation will be reduced to the following form:

$$(G+H)\sigma_1^2 + (F+H)\sigma_2^2 + (F+G)\sigma_3^2 - 2H\sigma_1\sigma_2 - 2G\sigma_1\sigma_3 - 2F\sigma_2\sigma_3$$

$$\text{------ (٥.٨)} \quad +2L\tau_{23}^2 = 1$$

Where $\sigma_{١}$, $\sigma_{٢}$ and $\sigma_{٣}$ are the three principal stresses respectively.

٥.٦.٢ Tsai-Wu Tensor Theory:

It is more complicated than the previous one; it is of the following tensor form:

$$F_i\sigma_i + F_{ij}\sigma_i\sigma_j = 1 \qquad \text{----- (٥.٩)}$$

Wherein F_i and F_{ij} are stress tensors of the second and forth rank respectively, with usual contracted stress notation is used except that $\sigma_{٤} = \tau_{23}$, $\sigma_5 = \tau_{12}$ & $\sigma_6 = \tau_{12}$. The components of the strength tensors are determined by uniaxial tests in their respective directions for the linear terms. For the quadratic terms such as $F_{١٢}$ or in general form F_{ij} terms, they can be determined by biaxial tests (two dimensional tests) and so on. The tests directions and types

are defined by the stress coefficients conjugated with the failure strength tensors

parameters. For example $F_{11} + F_1 \to \sigma_1$, $F_{22} + F_2 \to \sigma_2$ & $F_{12} \to \sigma_1\sigma_2$, thus these relations can be decided when the tensor is put in its expanded form. Therefore, it is expected to have very complicated and long expressions for various terms and can only be solved via suitable mathematic software, otherwise numerous and accumulative errors will be involved.

٥.٦.٣ Application of Tsai-Hill Theory:

Due to the fact that the fracture limits or fracture strengths of such a material are experimentally determined, so it is resorted to assume them in order to proceed in the application of Tsai-Hill theory on the beam under consideration. Let the clamped case of fiber volume fraction of ٤٠٪ at a load of ١٥٠٠ N of E-glass/polyester be adopted to such application, the effective elastic properties are as in appendix C.١.١. The various fracture strengths of the composite referred to above are assumed to be as under:

X=Y=٢٠ GPa, Z=٥٠ GPa, $S=\tau^*_{١٣}$=١٢ GPa, $\tau^*_{٢٣}$ =١١ GPa.

Using ANSYS V-٥.٤ to solve for the principal stresses and a MATLAB program to solve for the terms of Eqs. ٥.٢ through ٥.٨ give:

$$(G+H)\sigma_1^2 + (F+H)\sigma_2^2 + (F+G)\sigma_3^2 - 2H\sigma_1\sigma_2 - 2G\sigma_1\sigma_3 - 2F\sigma_2\sigma_3$$

$$+2L\tau_{23}^2 = ٨.٢٧٦٠e\text{-}٠٠٦$$

Therefore, it is very safe and reliable for this beam to withstand such a load and

stress. The same procedures can be carried out for the different cases met in practice to check for the safety of the load carrying capacity.

٥.٧ Verification of the Composite Beam Analyses Results:

One of the means adopted to verify the results obtained in the analyses of the composite beam has already been carried out is applying the solution method to a

corresponding isotropic beam, then comparing its results with an exact solution method, the double integration method for example. The results obtained from the solution of an isotropic carbon steel simply supported beam having the following geometric and engineering properties [٦٢ & ٦٣]:

Outer diameter = ٥٠ mm

Beam length = ١٥٠٠ mm

Modulus of elasticity = ٢٠٧ $GN/m^{٢}$

Modulus of rigidity = ٨٠ $GN/m^{٢}$

Poisson's ratio = ٠.٢٩٤

using the double integration method as an exact solution approach [٦٢ & ٦٣] the maximum beam deflection is found to be:

y_{max} = ١.٢٣ mm

Using ANSYS v٥.٤ procedures adopted in the present work, the maximum beam deflection is found to be:

y_{max} = ١.٢٠٥ mm

The results as clearly seen are very close to each other such that the accuracy of the results is ٩٧.٩٦% between ANSYS v٥.٤ and the exact method.

٥.٨ Verification of the Unit cell Analyses Results:

To verify the validity of the unit cell results, a unit cell is arbitrarily chosen among those whose behaviors have already been discussed in this chapter, and then the fibers and matrix are given the same linearly elastic and isotropic properties, one should expect the unit cell to behave as a homogeneous, isotropic and linearly elastic material, e.g. a uniformly uniaxial stress should result in uniform strains in the unit cell related to the applied stress by Hook's law [١٣]. The results of such a unit cell should also be reasonably close to their corresponding in the orthotropic counterpart [١٢]. Accordingly, a unit cell of ٤٠٪ fiber volume fraction is so chosen from the clamped case and given isotropic properties of fibers and subjected to the same state of stress as that of the orthotropic one. The results obtained are as listed in the following table along with those of the orthotropic case for the purpose of comparison:

Table ٥.٧.١: Results of isotropic and orthotropic unit cells

	U_x mm	U_y mm	U_z mm	σ_x GPa	σ_y GPa	σ_z GPa
Isotropic case	٠.٠٠٧	٠.٠١٠٣	٠.٠٠٤	٢٧	٤٠	١٧
Orthotropic	٠.٠١	٠.٠٢	٠.٠٢	٣١	٤٤	٢٢

case						

It is clearly seen that both results are reasonably close to each other, so the analysis is valid and can be accepted.

CHAPTER SIX

CONCLUSIONS AND RECOMMONDATIONS

٦.١ Conclusions:

From the obtained results of the present work, some conclusions can be drawn. These conclusions may be ramified into two types:

١. Macroscopic conclusions.

٢. Microscopic conclusions.

٦.١.١ Macroscopic conclusions:

The following conclusions are some of the first type:

١. The normal stresses σ_x & σ_y decrease as the fiber volume fraction V_f increases from ١٠ – ٤٠٪ afterwards, they start to increase with it, thus, ٤٠٪ V_f represents the optimum limit from this viewpoint. The same holds for the shear stress. The longitudinal (bending) stress is unaffected by this factor (V_f).

٢. Beam deflection is inversely proportional to the fiber volume fraction.

٣. Beam stresses and deflection are linearly increasing with the applied load.

٤. The increase in matrix Poisson's ratio υ_m leads to an increase in the transverse normal stress σ_x and doesn't affect on σ_y and beam deflection.

٥. Fiber Poisson's ratio υ_f inversely influences on the stress component σ_x of the beam, so as on beam deflection. σ_y is still unaffected.

٦.١.٢ Microscopic conclusions:

١. The normal transverse stress σ_x is directly proportional to the elastic modulus of the matrix E_m and inversely to that of fiber E_f, σ_y is markedly unaffected by them, while σ_z, the longitudinal stress is inversely proportional to E_m and unaffected by that of fiber at this loading level.

٢. The longitudinal shear stress τ_{yz} drops with the increase of the matrix shear modulus up to a certain limit after which starts to increase with it.

٣. Beam deflection is inversely proportional to the fiber and matrix elastic moduli.

٤. The increase of V_f has an ascending effect on the normal stresses of the unit cell and an inverse one on its displacements in x, y &z directions at constant fiber diameter, so as on the normal microstresses of the matrix and the fibers

except on fiber longitudinal (bending) stress σ_{zf} which remains approximately constant.

٥. Increase of fiber diameter leads to reducing of the normal stress and displacement of the unit cell, so as with the micro stresses of the matrix and the fibers individually in both types of supports.

٦. Clamping both ends of a beam results in inducing much more bending stresses in the composite material than the simply supported type does, while the beam deflection is not susceptible to the type of support.

These conclusions are traditional and typical such that they are proving the validity of the unit cell method application to the bending state of stress of a unidirectional fiber-reinforced composite beam.

٦.٢ Recommendations for Future Works:

The following recommendations can be introduced for future works:

١. Analysis of the torsional loading case of the UDFRC beam by the method of the current study.

٢. Analysis of the combined stresses case (torsion and bending) of the UDFRC beam by the same method.

٣. Analysis of all the preceding loading cases individually under dynamic loads environment.

٤. Considering the stress concentration factors in the in the analysis of the above cases.

Beam normal & shear stresses MPa

nsidering the case of woven fiber-reinforced composite beams in the analysis discussing fibers orientation angles effects on the beam strengths under various loading conditions.

alysis of particulated-reinforced composite beams discussing the effects rticles size, shape and orientation on the beam strengths under various loading conditions.

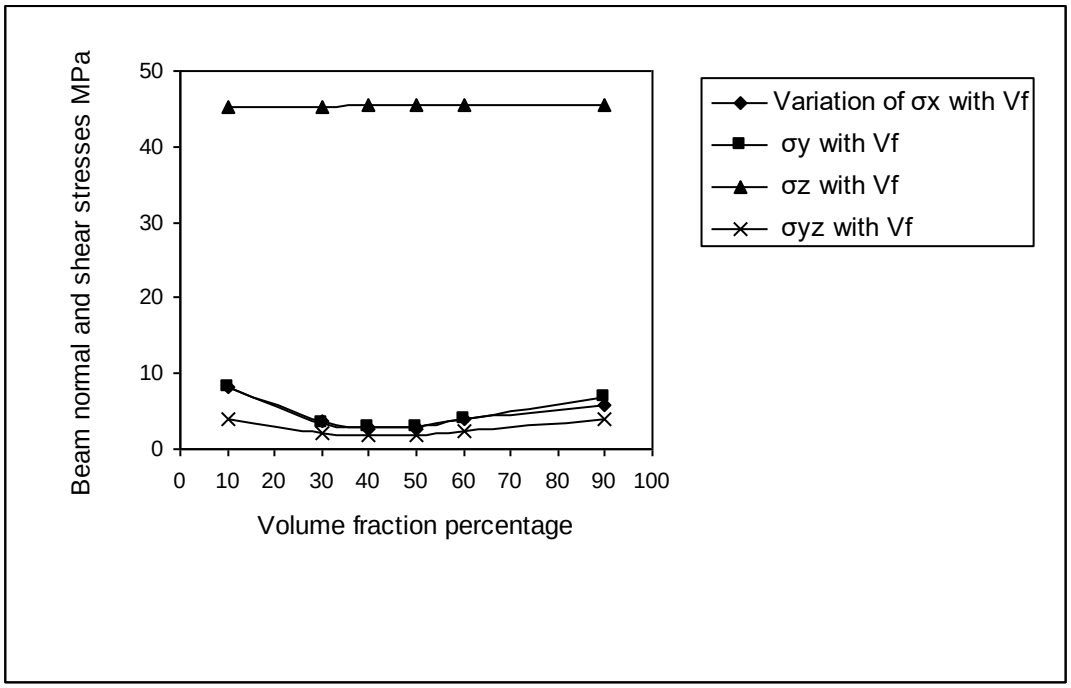

Fig. ٥.١: Variation of normal and shear stresses with fiber volume fraction at ١٥٠٠N for E-Glass/Polyester

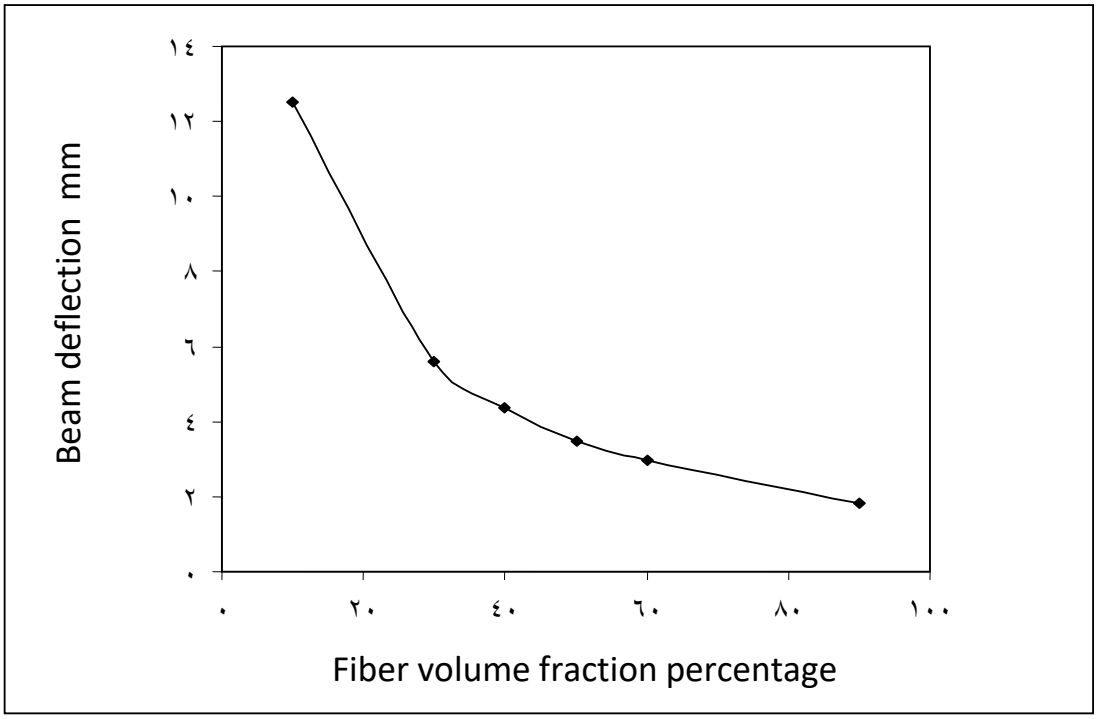

Fig. ٥.٢: Variation of beam deflection with fiber volume fraction at ١٥٠٠N for E-Glass/Polyester of ١٥٠٠mm long

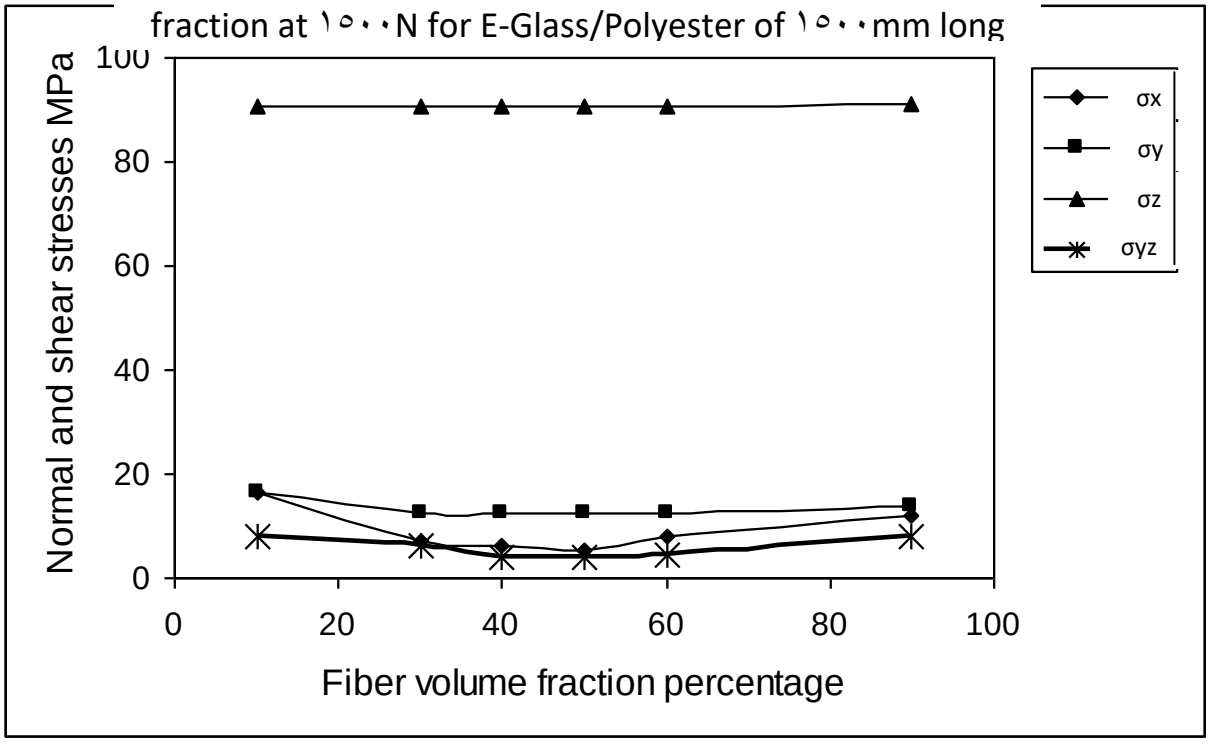

Fig.٥.٣: Variation of normal and shear stresses with fiber volume fraction percentage at ٣٠٠٠N for E-Glass/Polyester

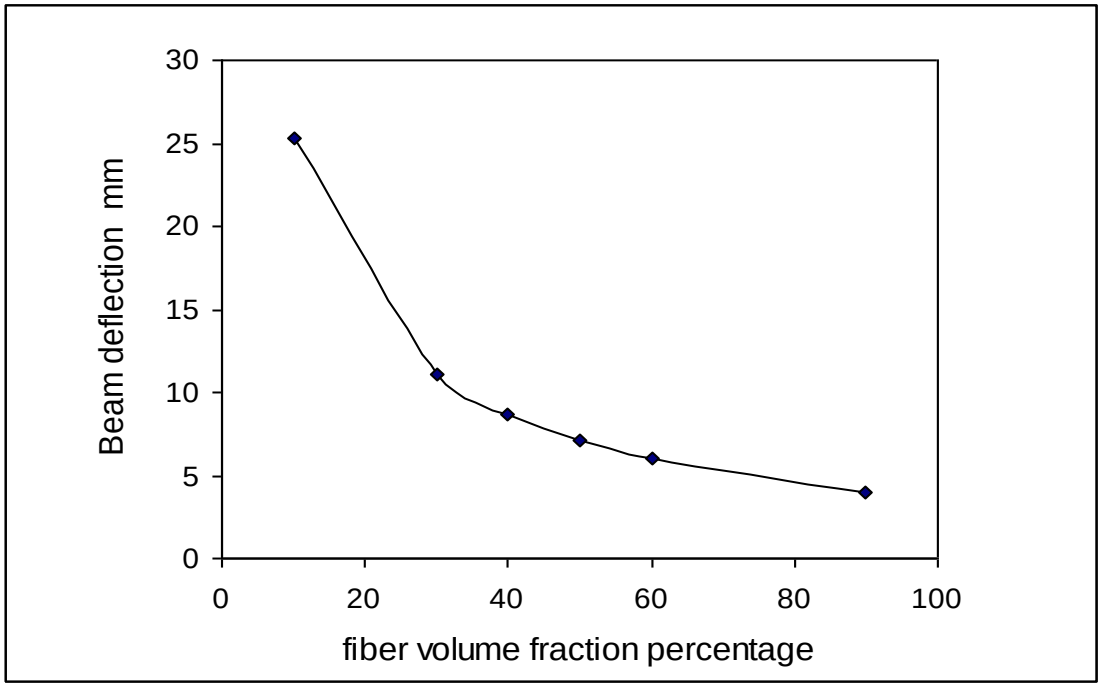

Fig. ٥.٤: Variation of Beam deflection with fiber volume fraction percentage at ٣٠٠٠N for E-Glass/Polyester

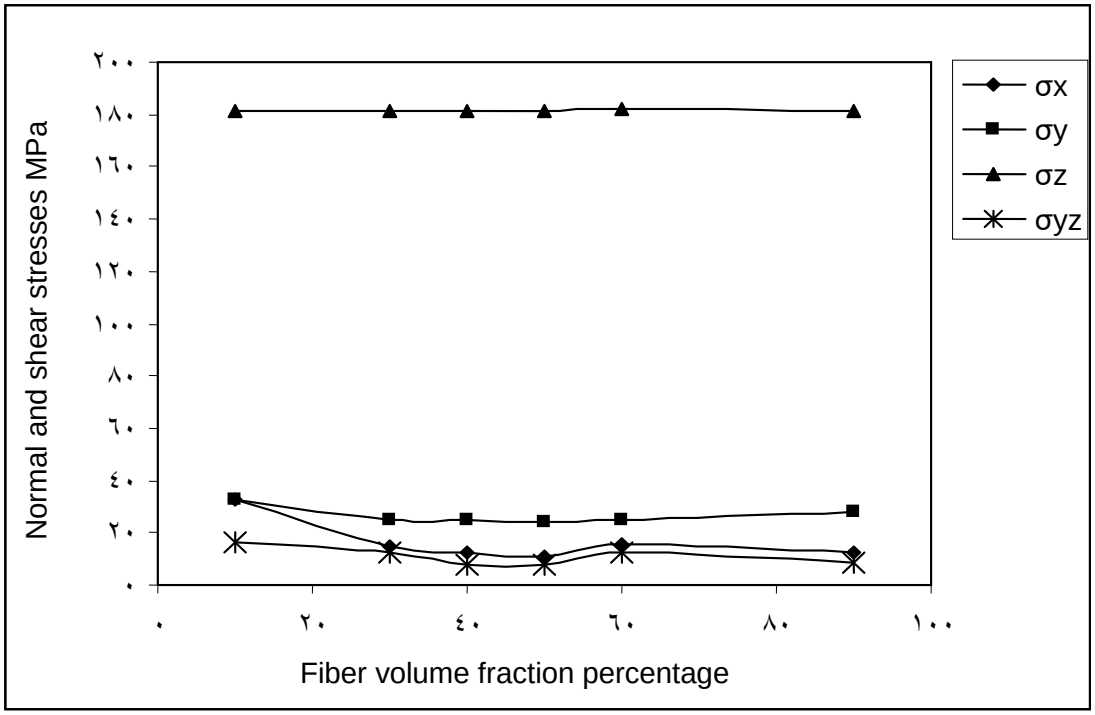

Fig. ٥.٥: Variation of normal and shear stresses of the beam with fiber volume fraction percentage at ٦٠٠٠N of E-Glass/Polyester

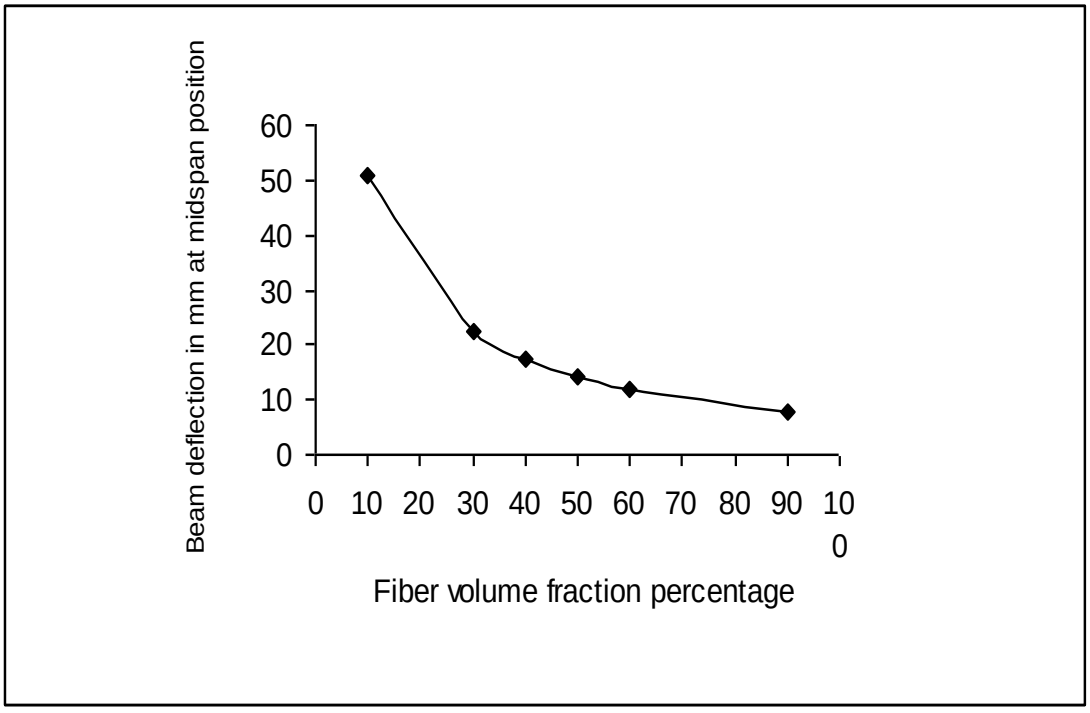

Fig. ٥.٦: Variation of beam deflection with fiber volume fraction percentage at ٦٠٠٠N of E-Glass/Polyester

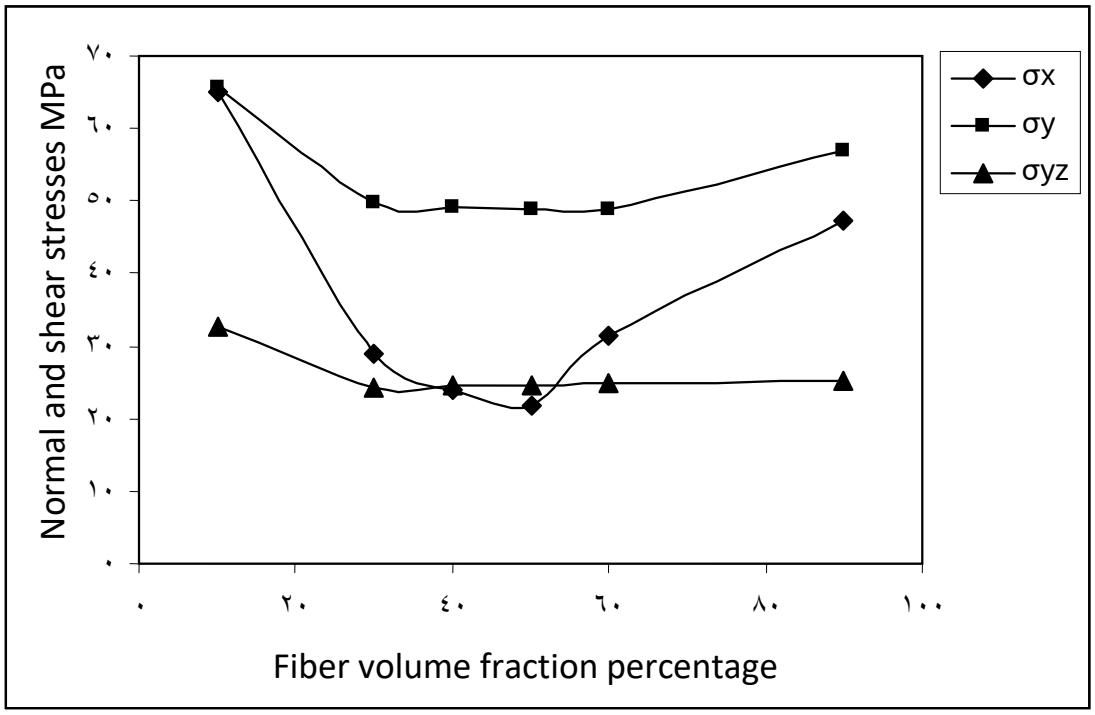

Fig. ٥.٧: Variation of transverse normal and shear stresses of the beam with fiber volume fraction percentage at ١٢٠٠٠N of E-Glass/Polyester (table C.١.٨)

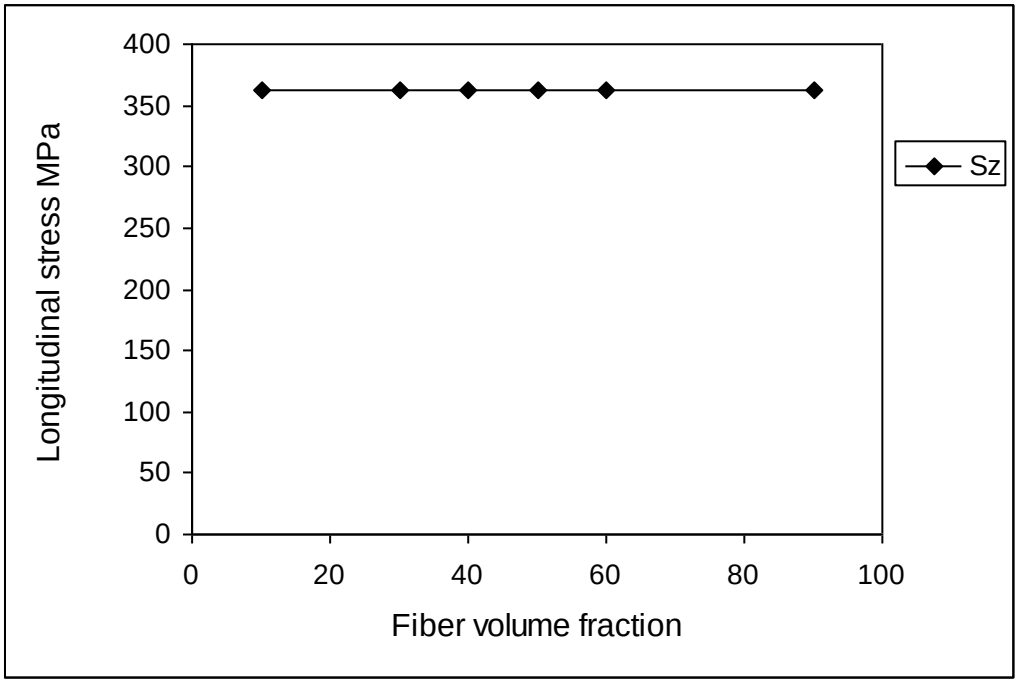

Fig. ٥.٨: Variation of longitudinal bending stress of the beam with fiber volume fraction at ١٢٠٠٠N of E-Glass/Polyester.

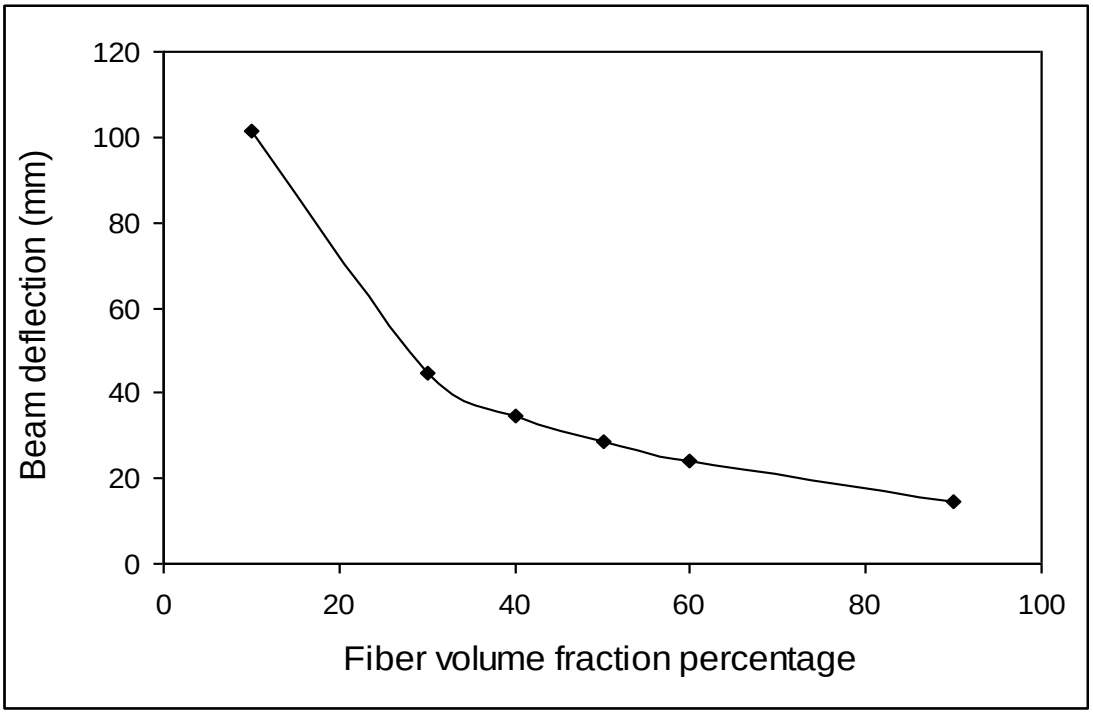

Fig. ٥.٩: Variation of beam deflection with fiber volume fraction percentage at ١٢٠٠٠N of E-Glass/Polyester.

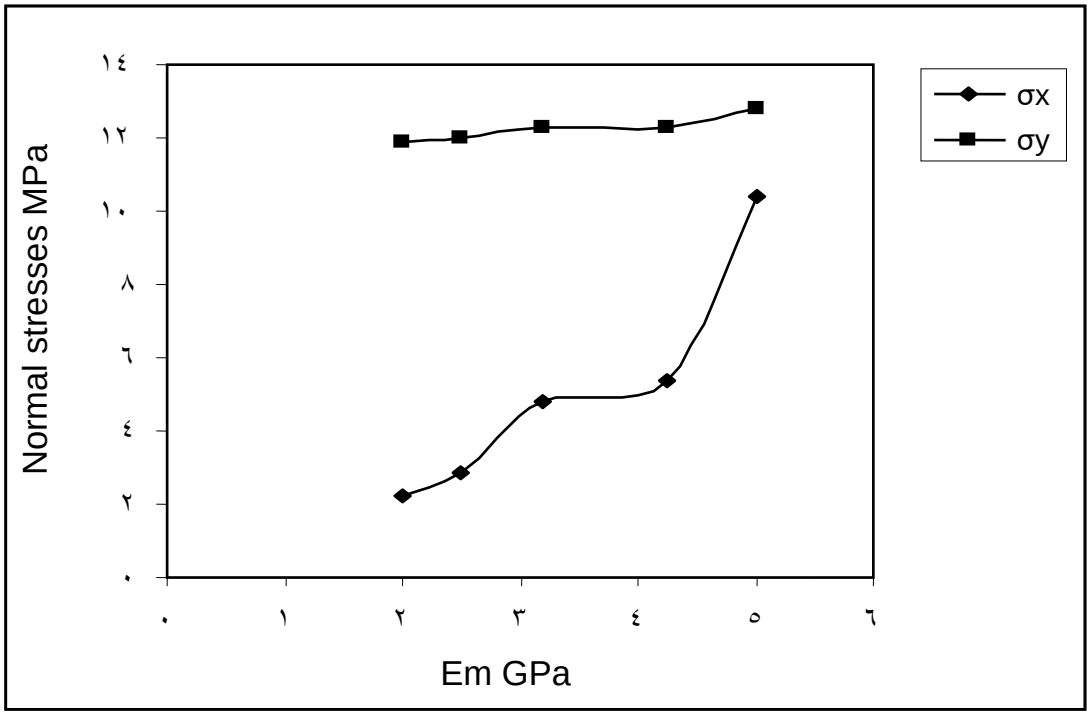

Fig. ٥.١٠: Variation of σ_x and σ_y with matrix elastic modulus

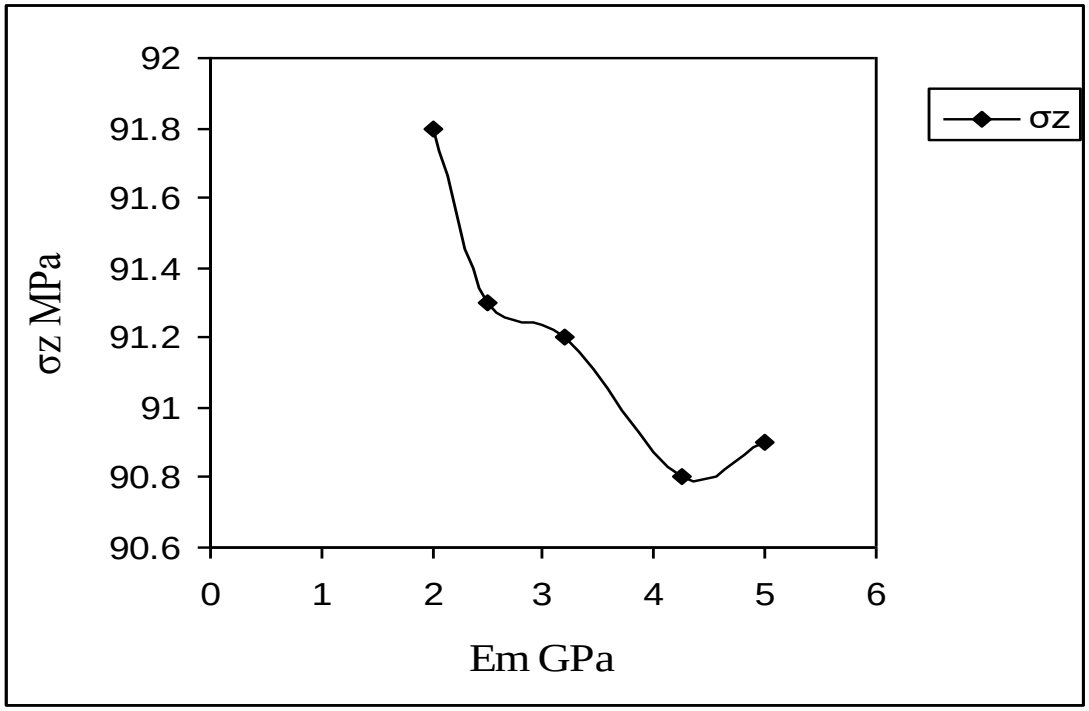

Fig. ٥.١١: Variation of longitudinal stress with matrix elastic modulus.

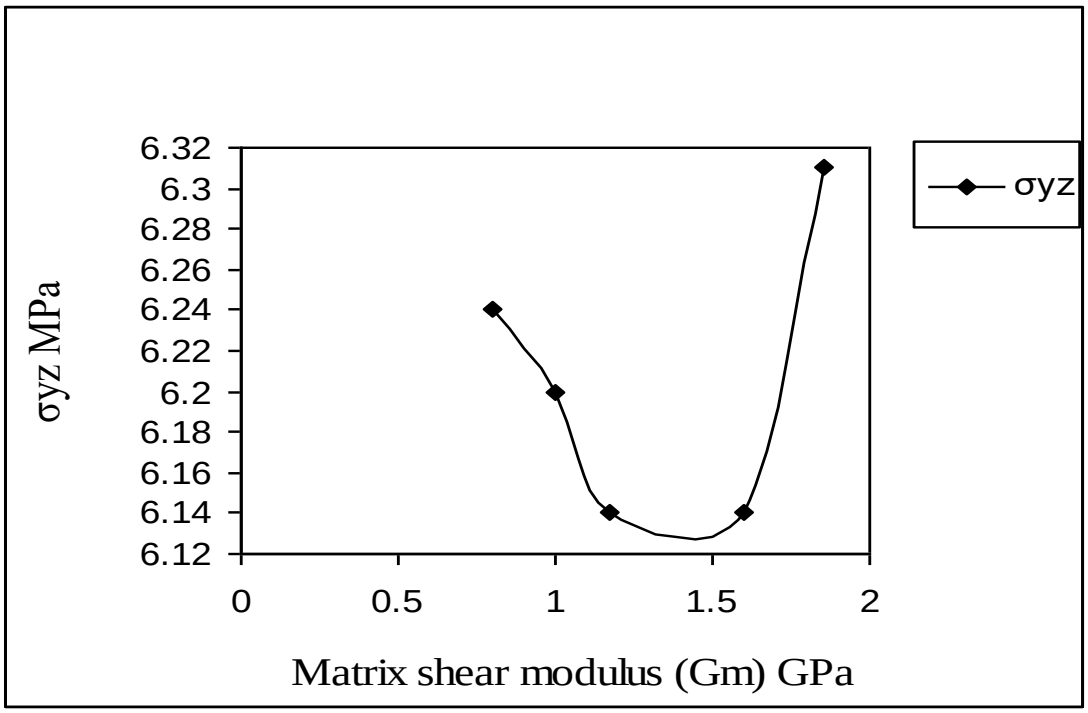

Fig. ٥.١٢: Variation of longitudinal shear stress of the beam with matrix shear modulus

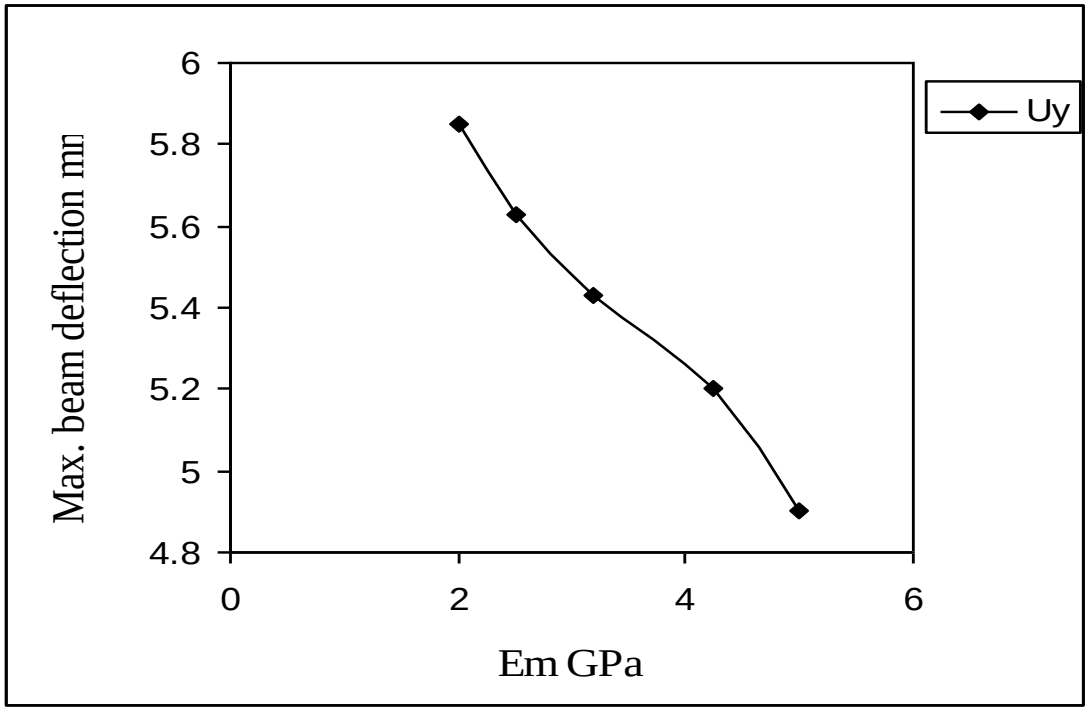

Fig. ٥.١٣: Variation of max. beam deflection with matrix elastic modulus

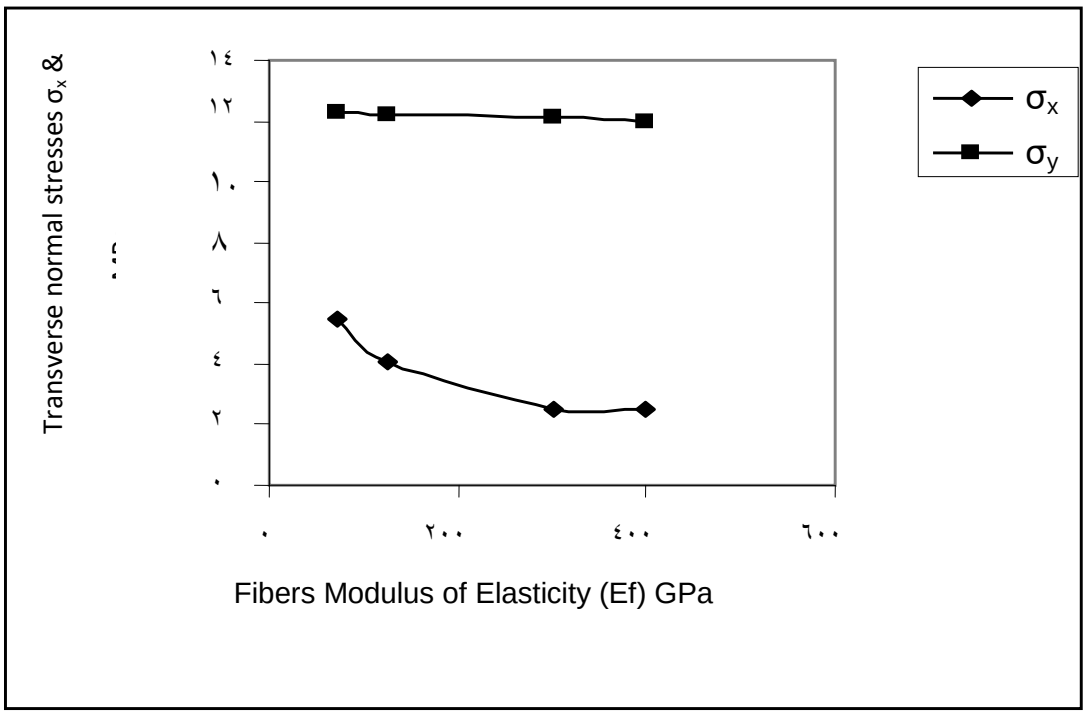

Fig. ٥.١٤: Variation of transverse normal stresses with fibers modulus of elasticity.

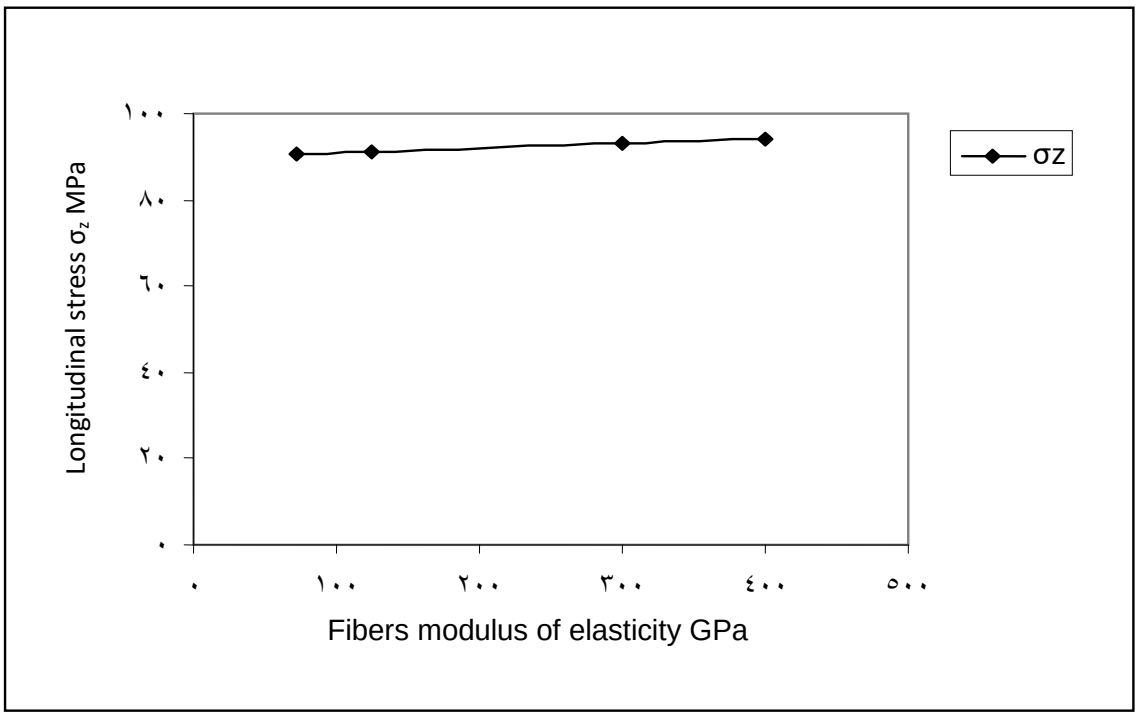

Fig. ٥.١٥: Variation of longitudinal stress σ_z with fibers modulus of elasticity.

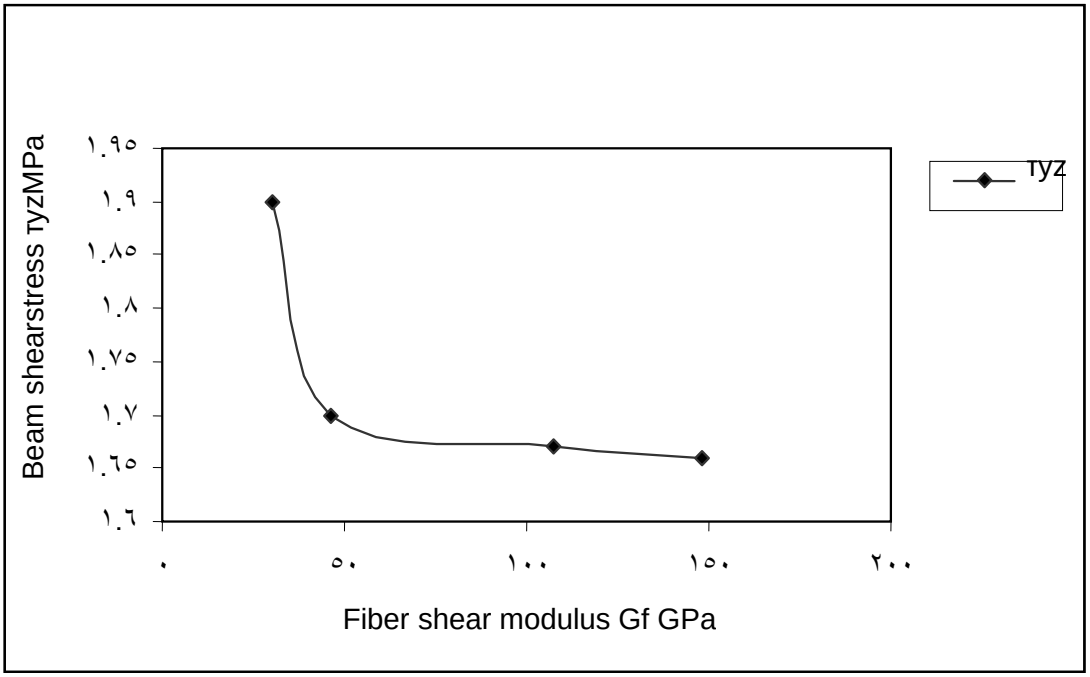

Fig. ٥.١٦: Variation of the longitudinal shear stress τ_{yz} with fibers shear modulus G_f GPa

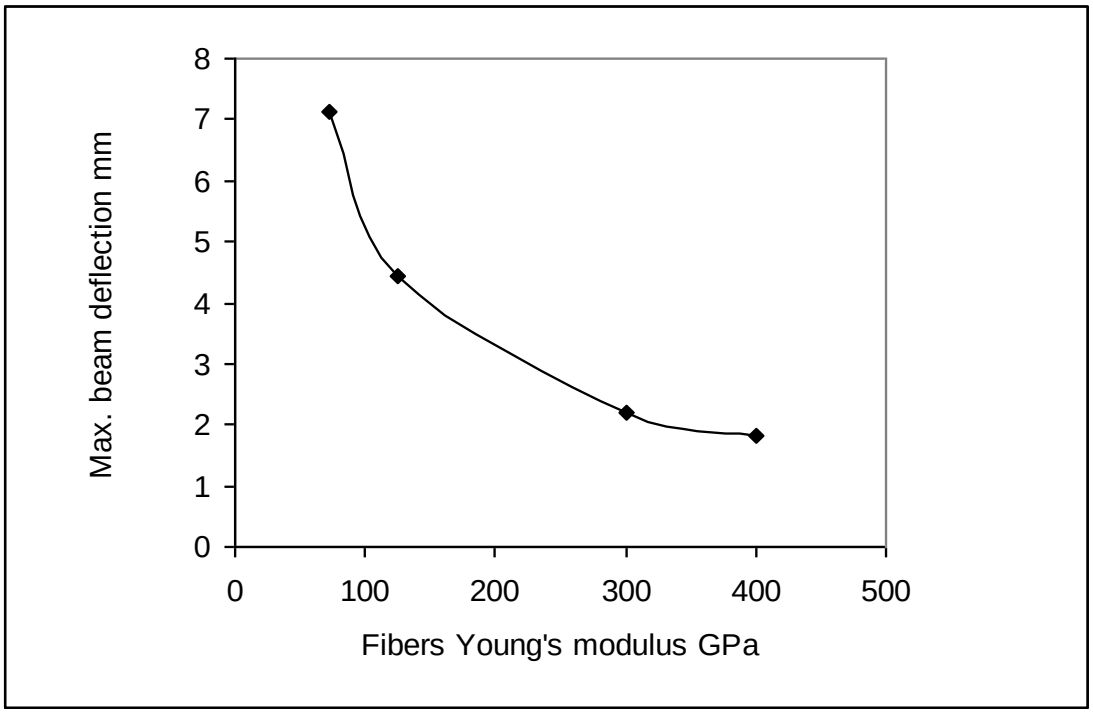

Fig.٥.١٧: Variation of the maximum beam deflection with fibers Young's modulus.

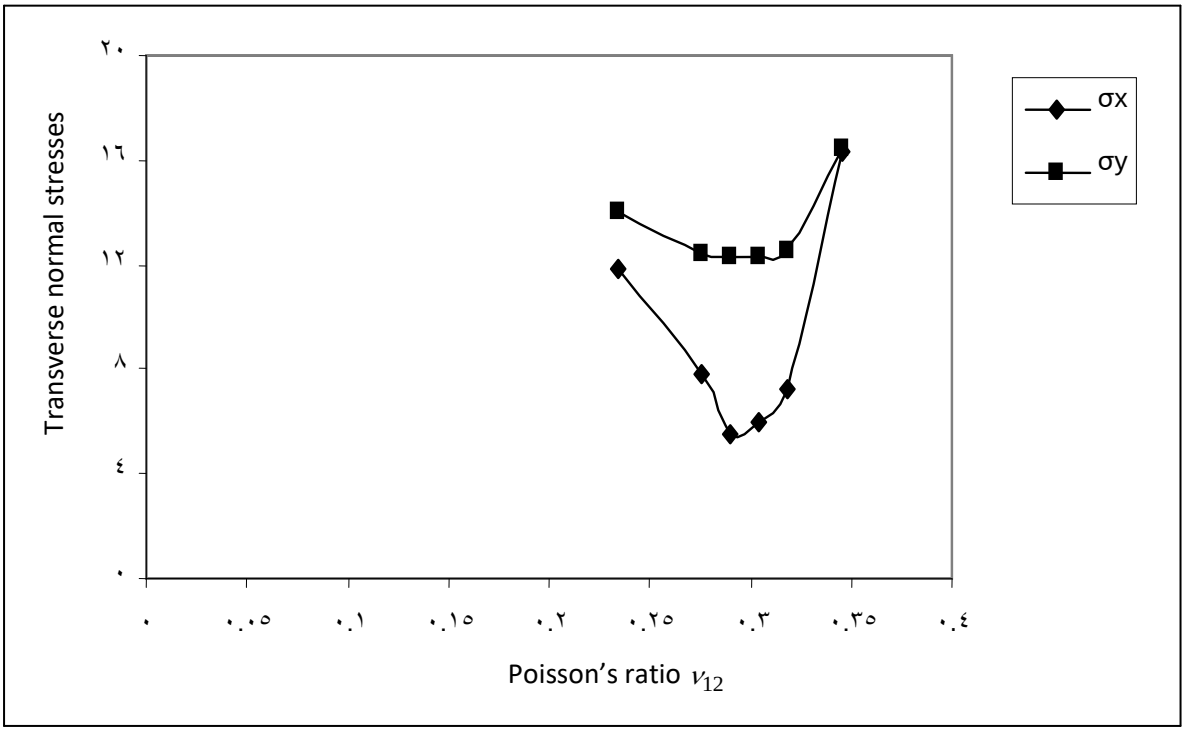

Fig. ٥.١٨: Variation of transverse normal stresses with Poisson's ratio ν_{12}

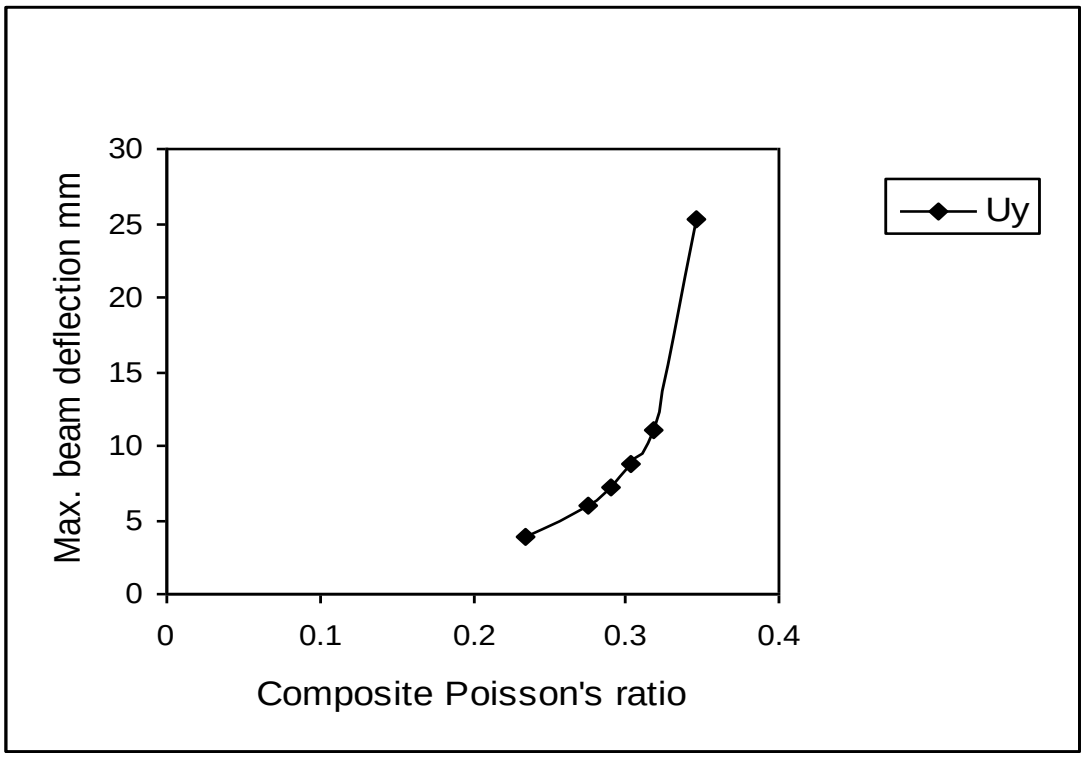

Fig. ٥.١٩: Variation of beam max. deflection with composite Poisson's ratio $v_{١٢}$

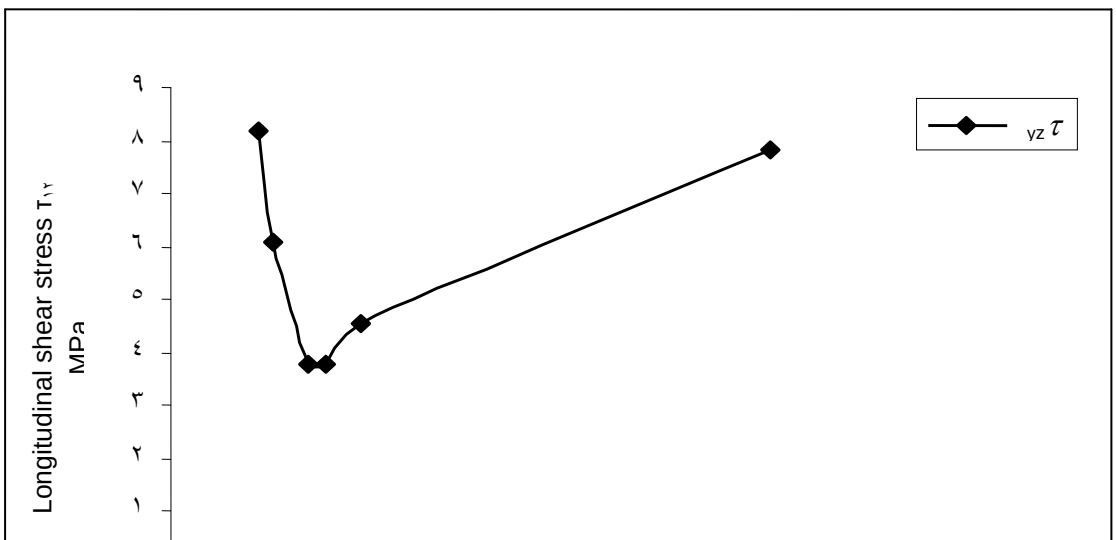

Fig. ٥.٢٠: Variation of longitudinal shear stresses (MPa) with composite shear modulus $G_{١٢}$ (GPa)

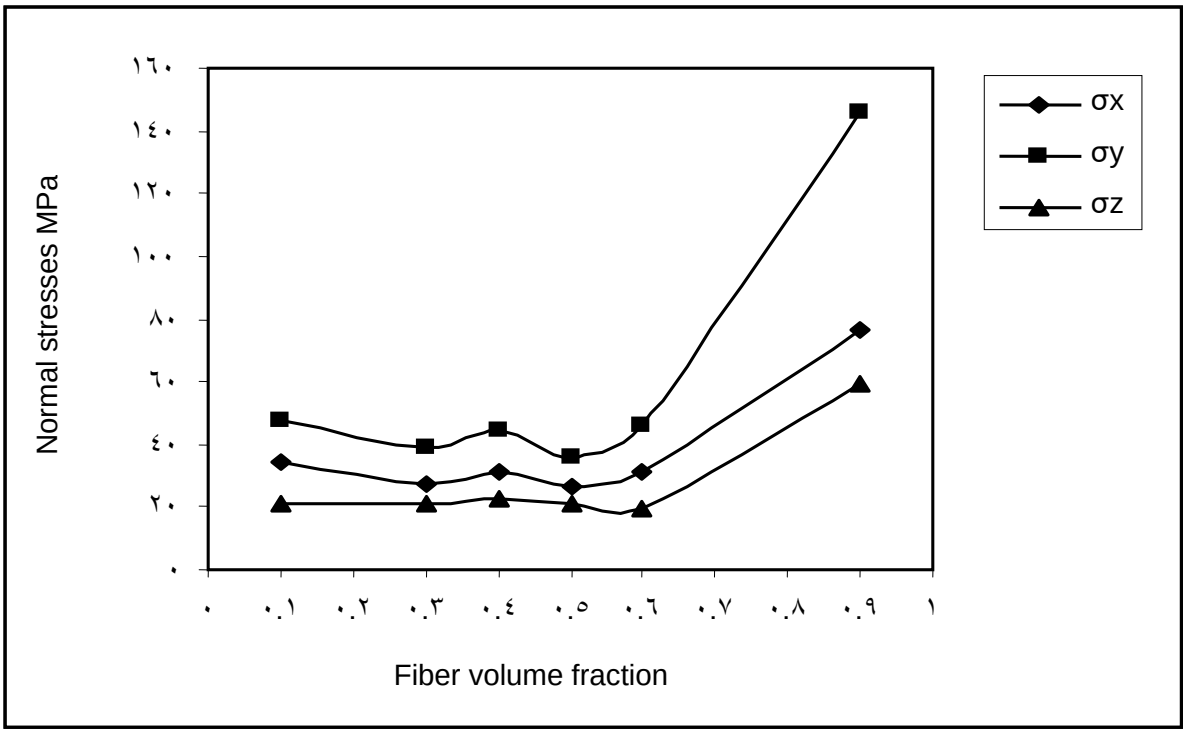
Normal stresses MPa
١٦٠
١٤٠
١٢٠
١٠٠
٨٠
٦٠
٤٠
٢٠
٠
٠
٠.١
٠.٢
٠.٣
٠.٤
٠.٥
٠.٦
٠.٧
٠.٨
٠.٩
١
Fiber volume fraction
σx
σy
σz

Fig. ٥.٢١: Variation of unit cell normal stresses with fiber volume fraction at constant fiber diameter of .٢٥ mm for E-glass/ polyester.

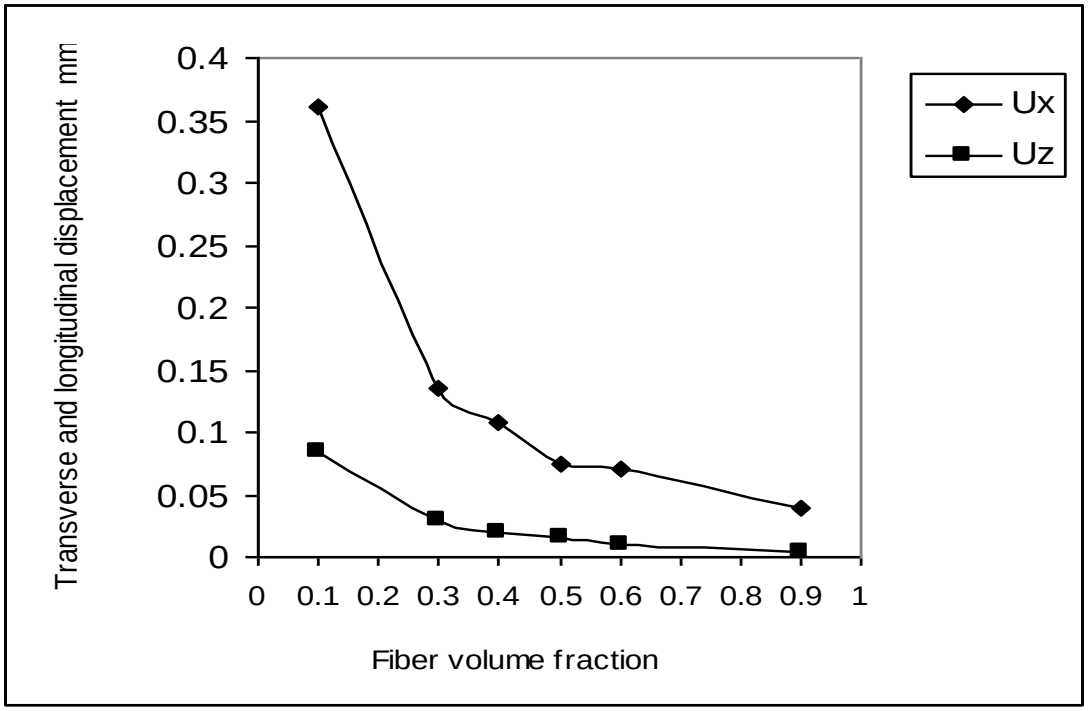

Fig. ٥.٢٢: Fiber volume fraction with transverse and longitudinal displacement of the unit cell of E- glass/polyester at constant fiber diam. of ٠.٢٥mm.

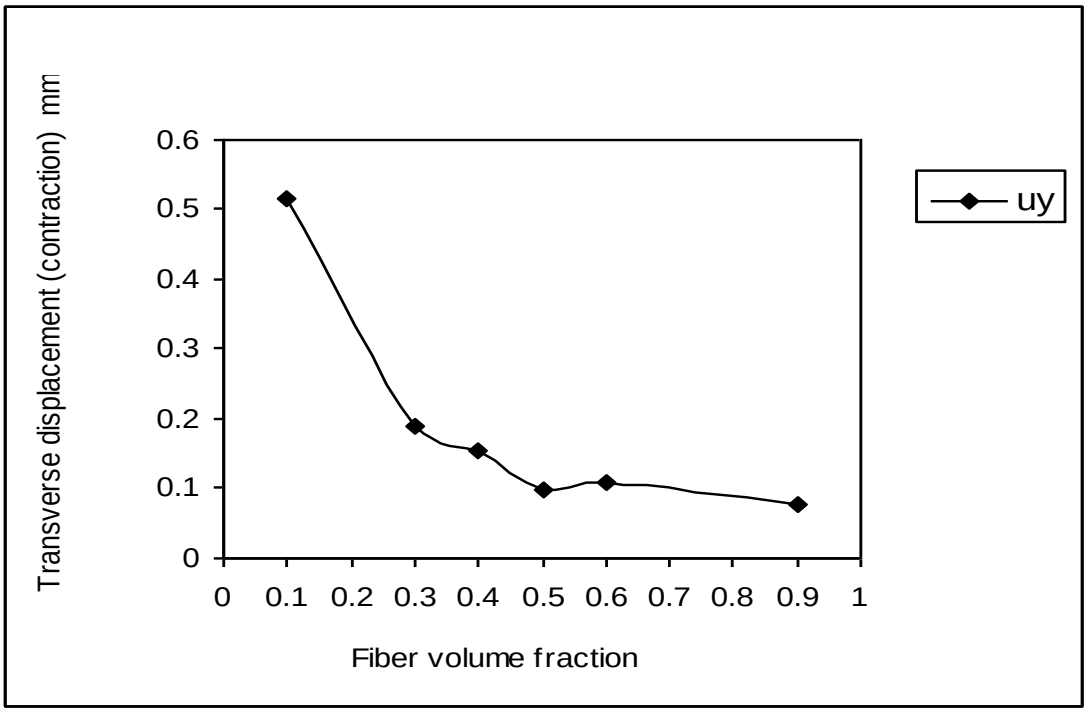

Fig. ٥.٢٣: Variation of the transverse displacement (contraction) U_y with fiber volume fraction for a unit cell of E-glass/polyester of ٤٠٪ fiber volume fraction.

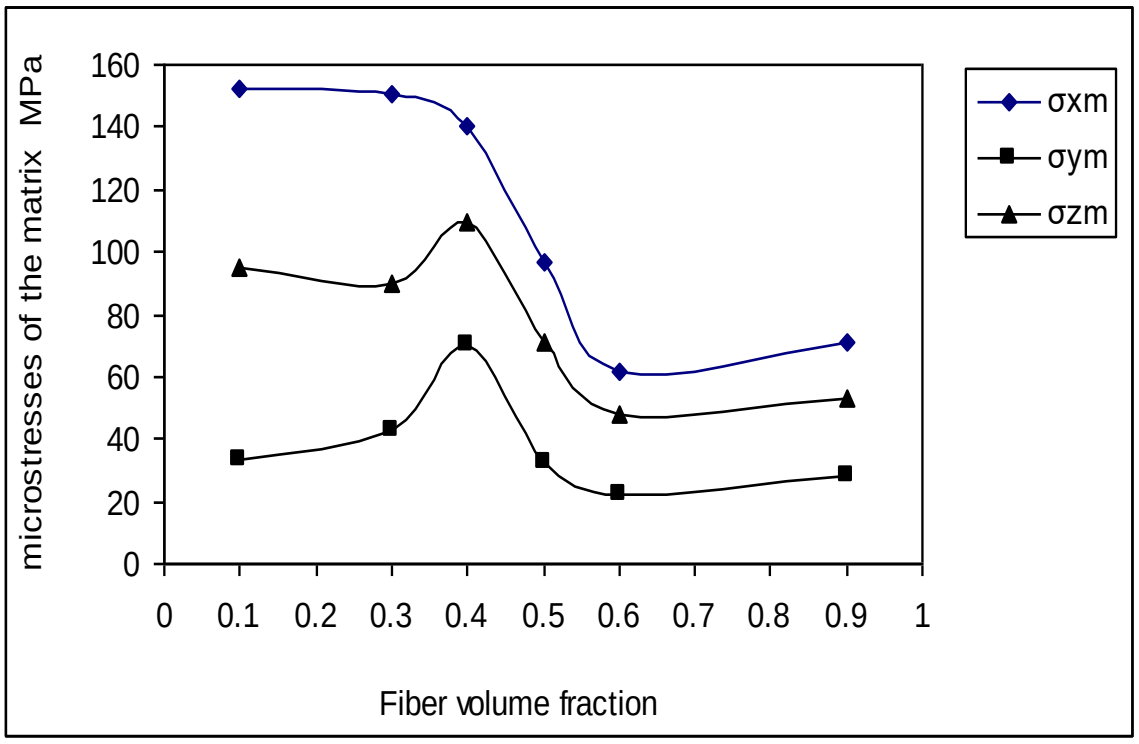

Fig. ٥.٢٤: Variation of the matrix normal stresses with fiber volume fraction at constant fiber diameter for E-glass/polyester.

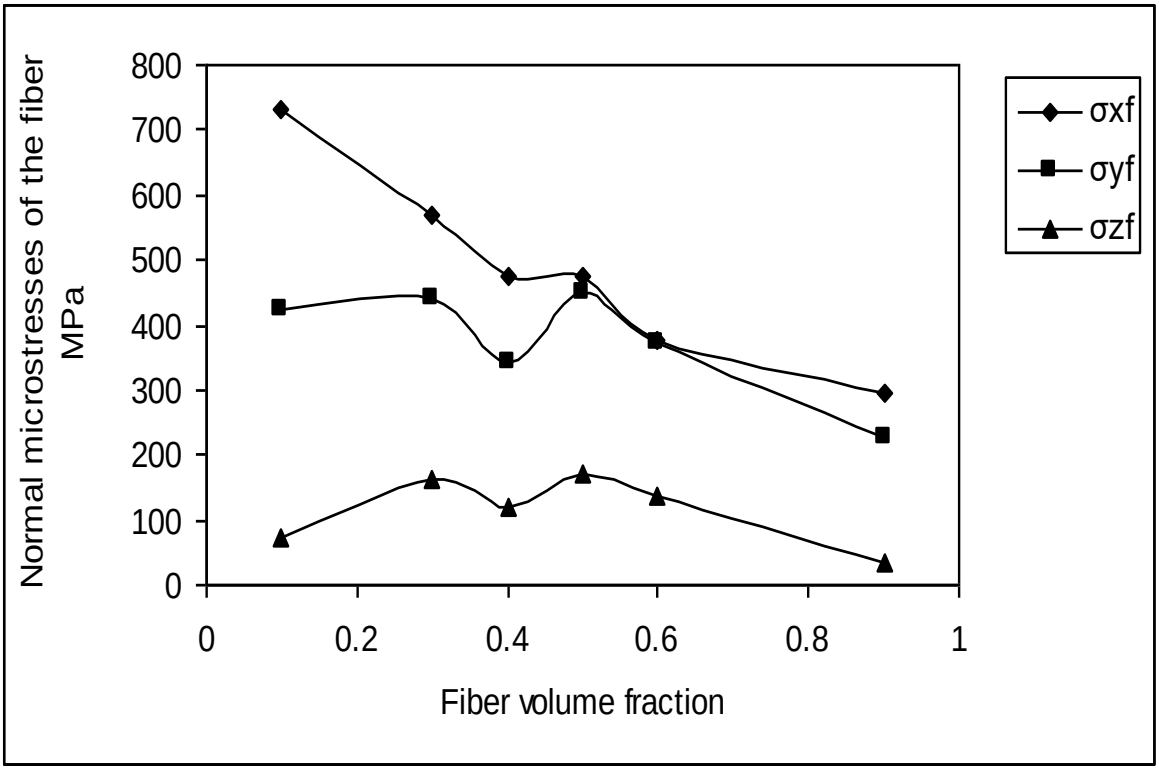

Fig. ٥.٢٥: Variation of fiber normal stresses (MPa) with fiber volume fraction at constant fiber diameter for E-glass/polyester.

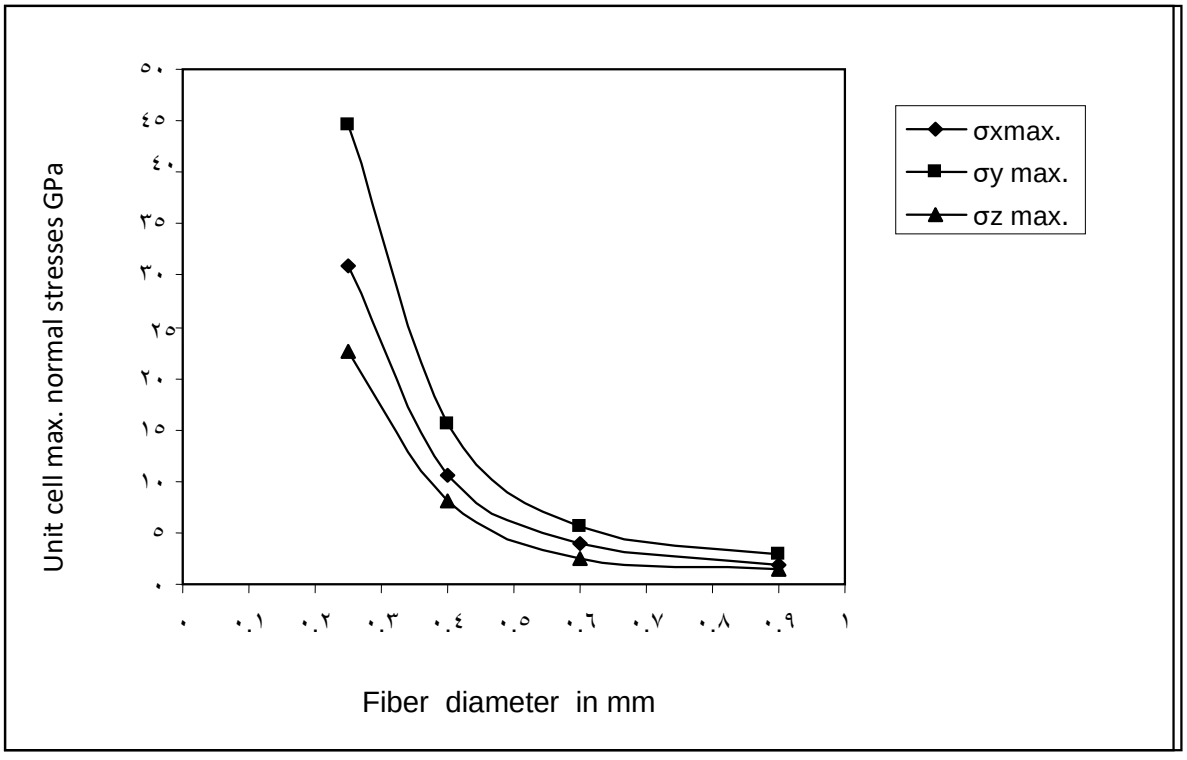

Fig. ٥.٢٦: Variation of unit cell normal stresses with fiber diameter at constant fiber volume fraction of ٤٠٪ for E-glass/polyester.

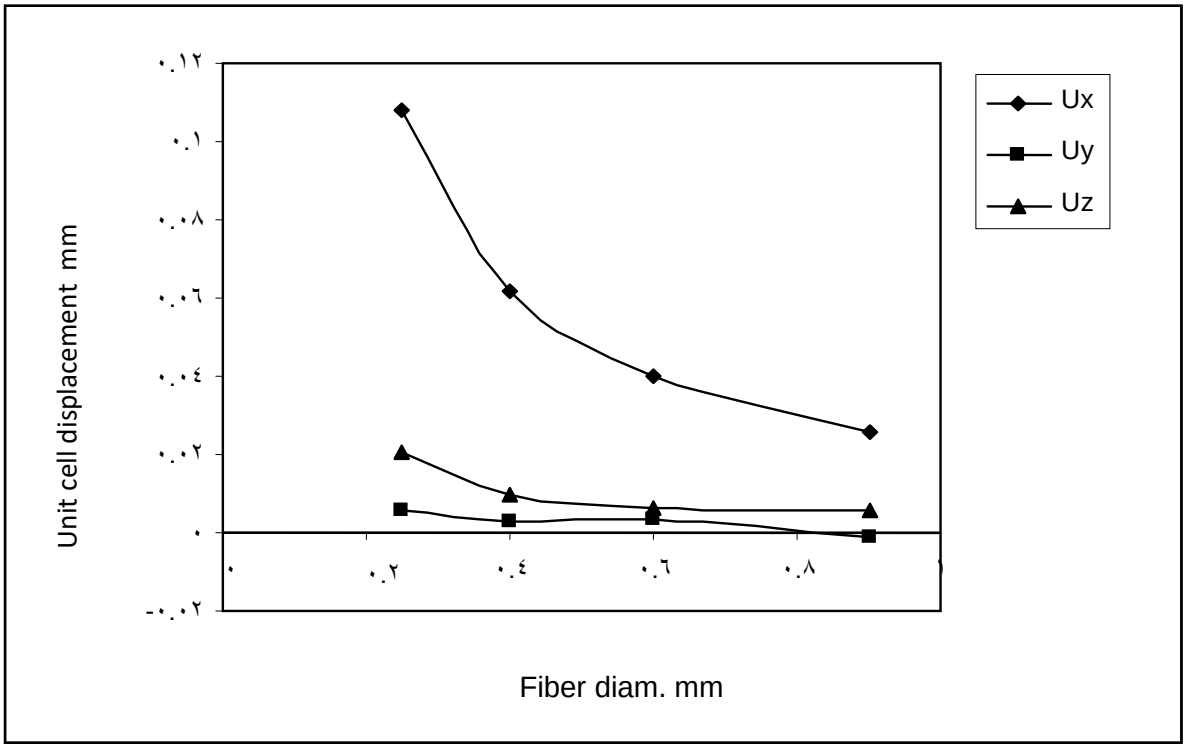

Fig. ٥.٢٧: Variation unit cell displacement in (mm) with fiber diameter at constant fiber volume fraction of ٤٠٪ for E-glass/polyester.

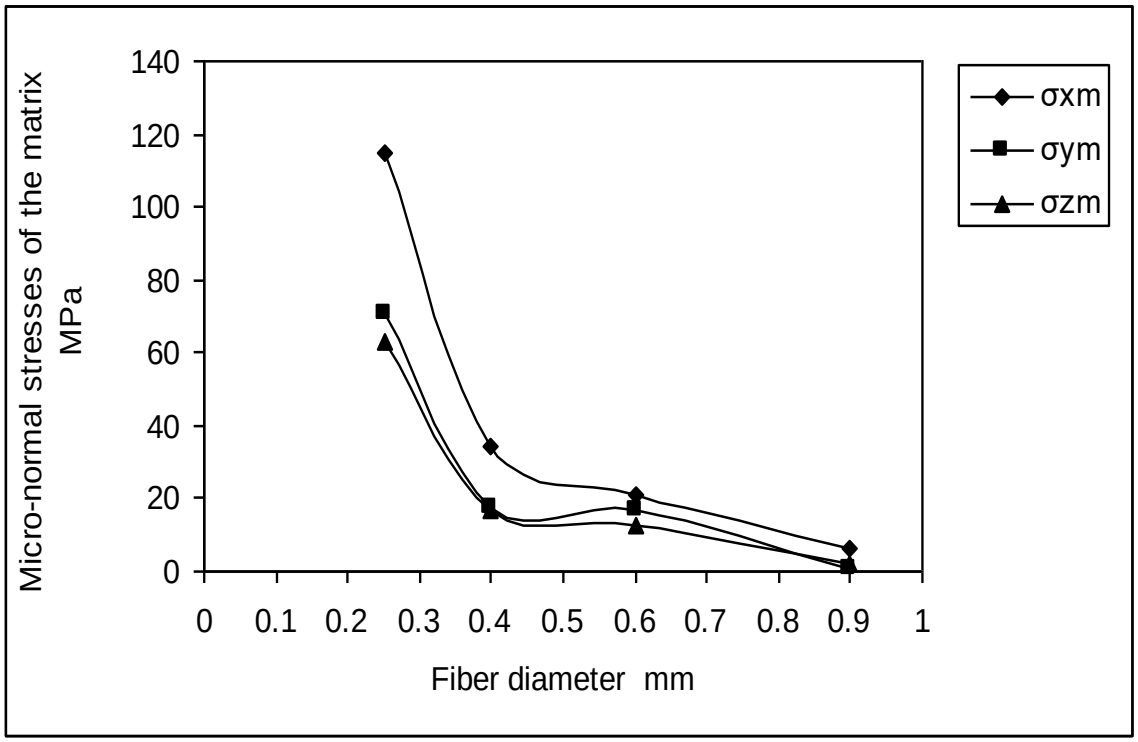

Fig. ٥.٢٨: Variation of matrix normal stresses with fiber diameter at constant fiber volume fraction of ٤٠٪ for E-glass/polyester

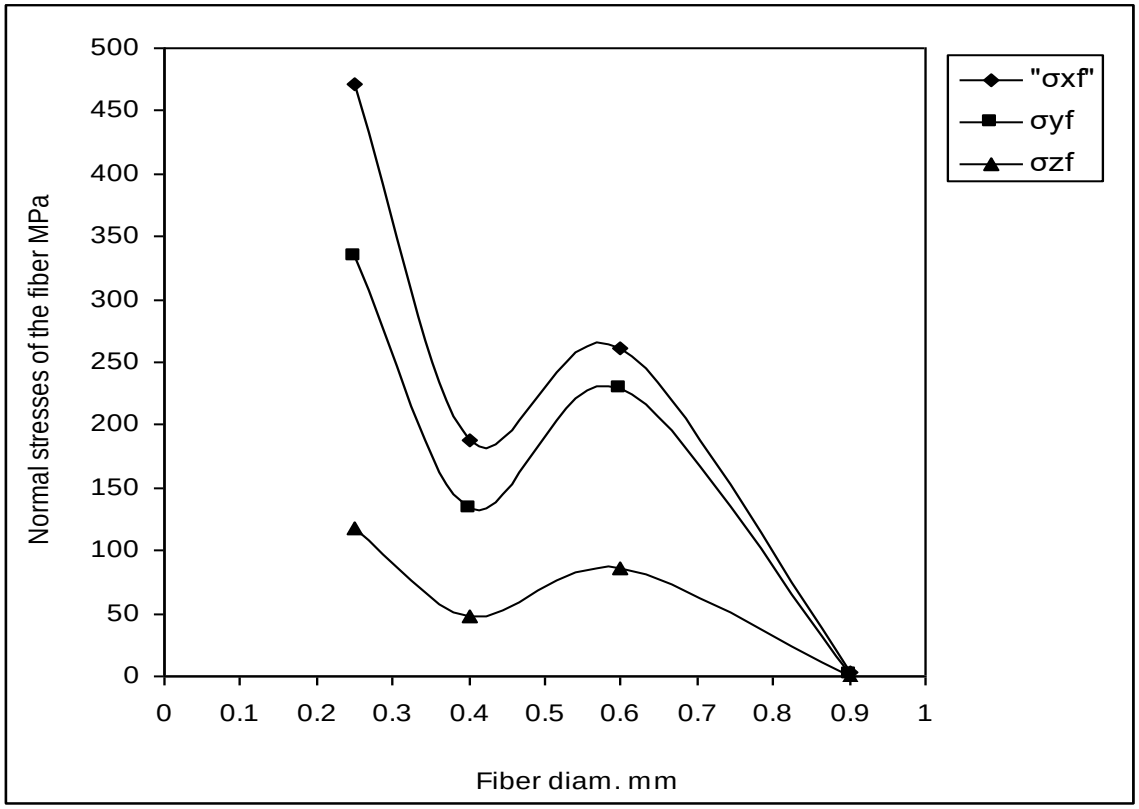

Fig. ٥.٢٩: Variation of fiber normal stresses with fiber diameter at constant fiber volume fraction of ٤٠٪ for E-glass/polyester

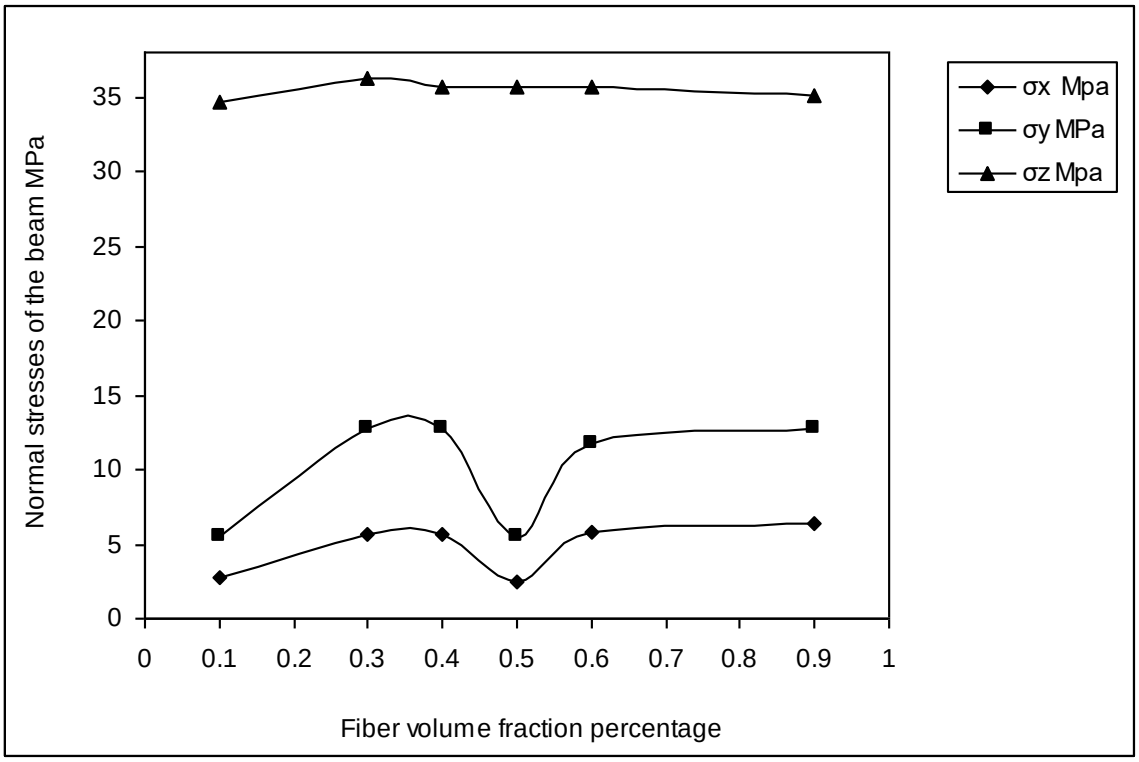

Fig. ٥.٣٠ Variation of normal stresses induced in a simply supported E-glass/polyester composite beam.

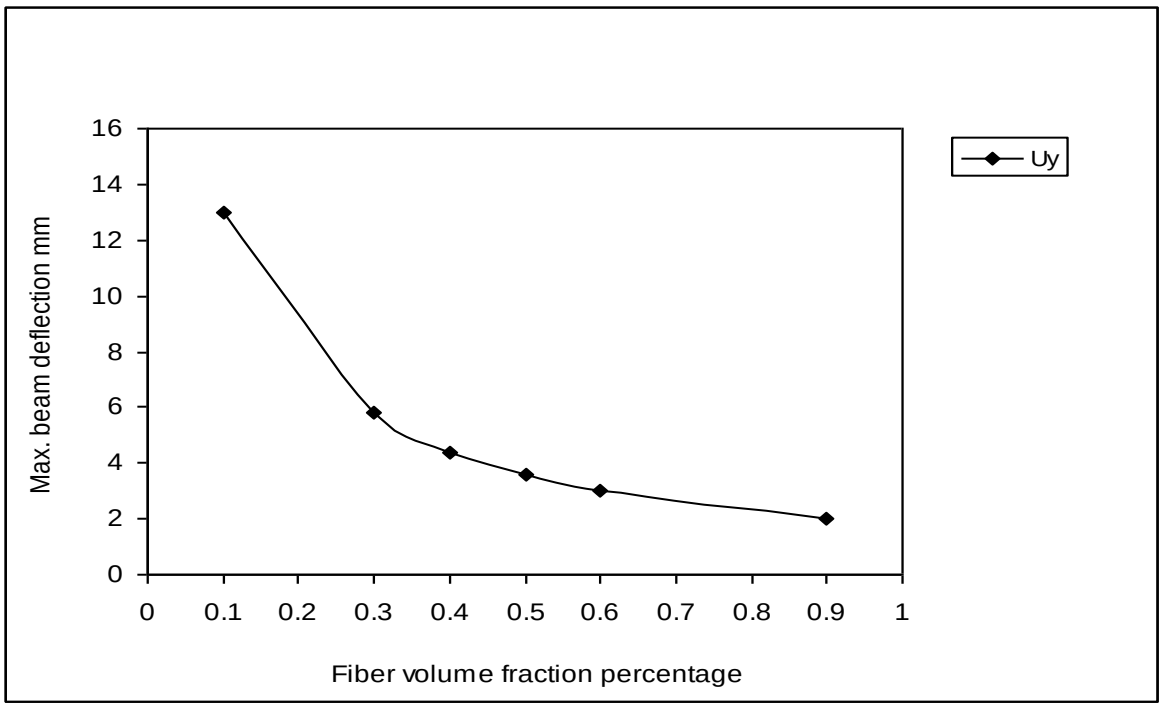

Fig. ٥.٣١: Effect of fiber volume fraction on beam deflection in case of simply supported ends for E-glass/polyester.

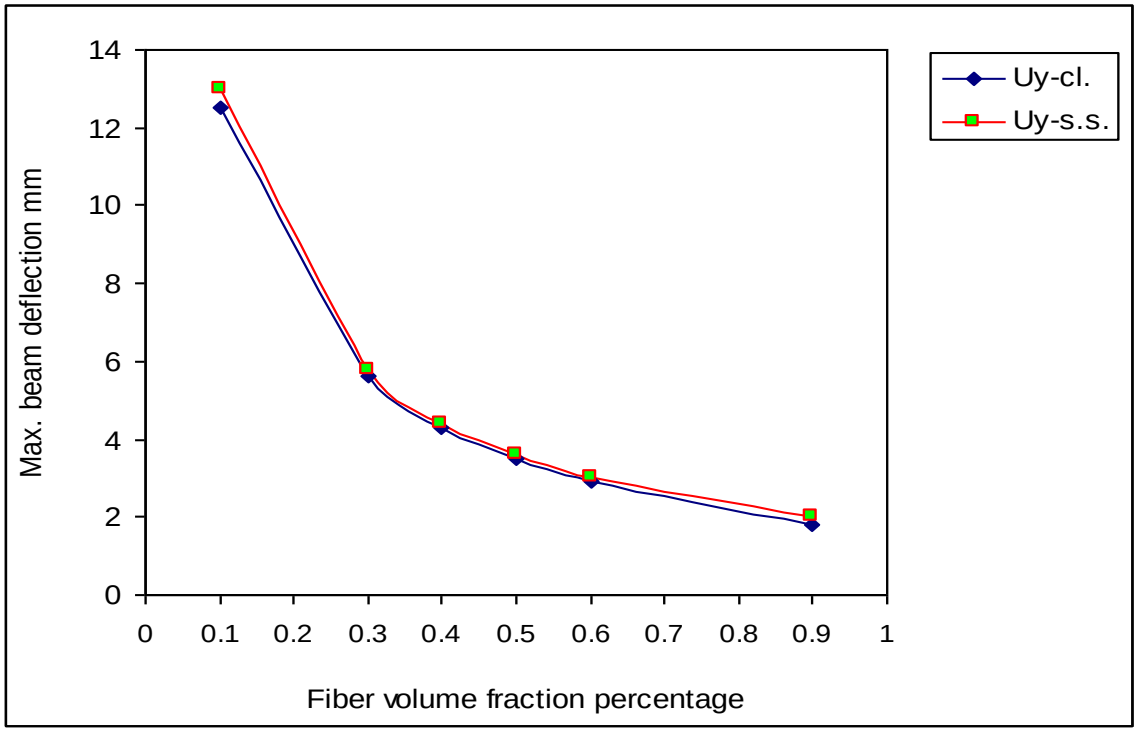

Fig. ٥.٣٢: Effect of type of support on beam deflection for E-glass/polyester.

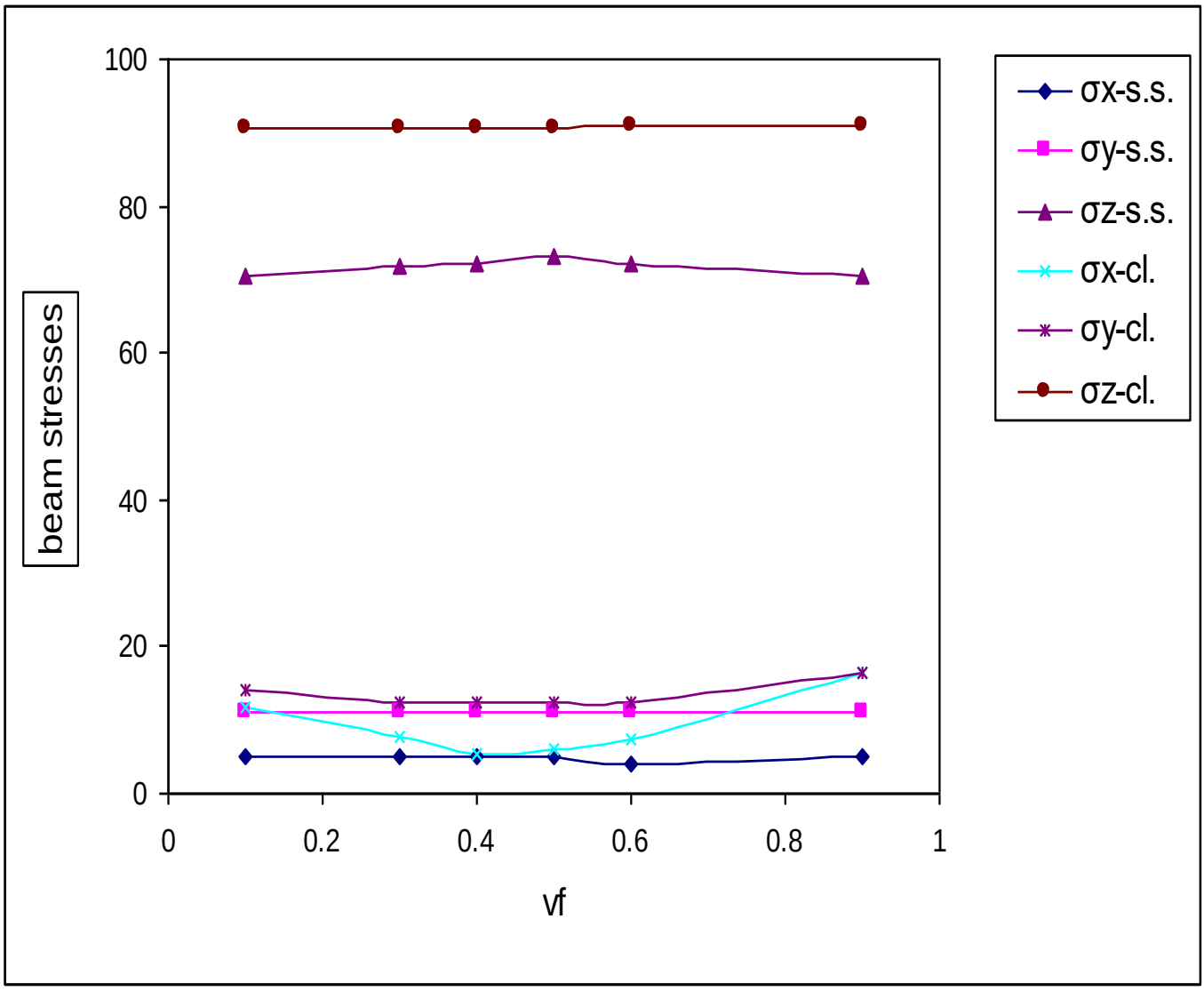

Fig. ٥.٣٣: Effect of type of support on beam normal stresses in MPa for E-glass/polyester at ٣٠٠٠N at the support and at the mid-span regions of the clamped and simply supported cases respectively.

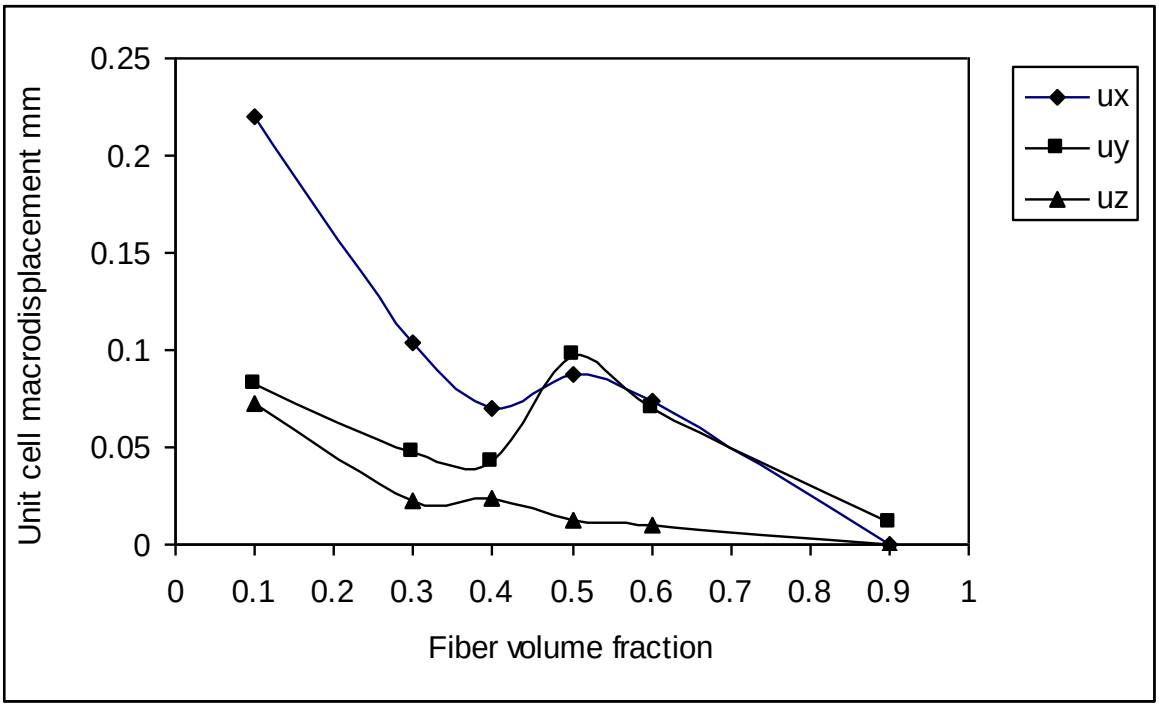

Fig. ٥.٣٤: Effect of fiber volume fraction on the macroscopic displacement of the unit cell in mm for the simply supported E-glass/polyester composite beam.

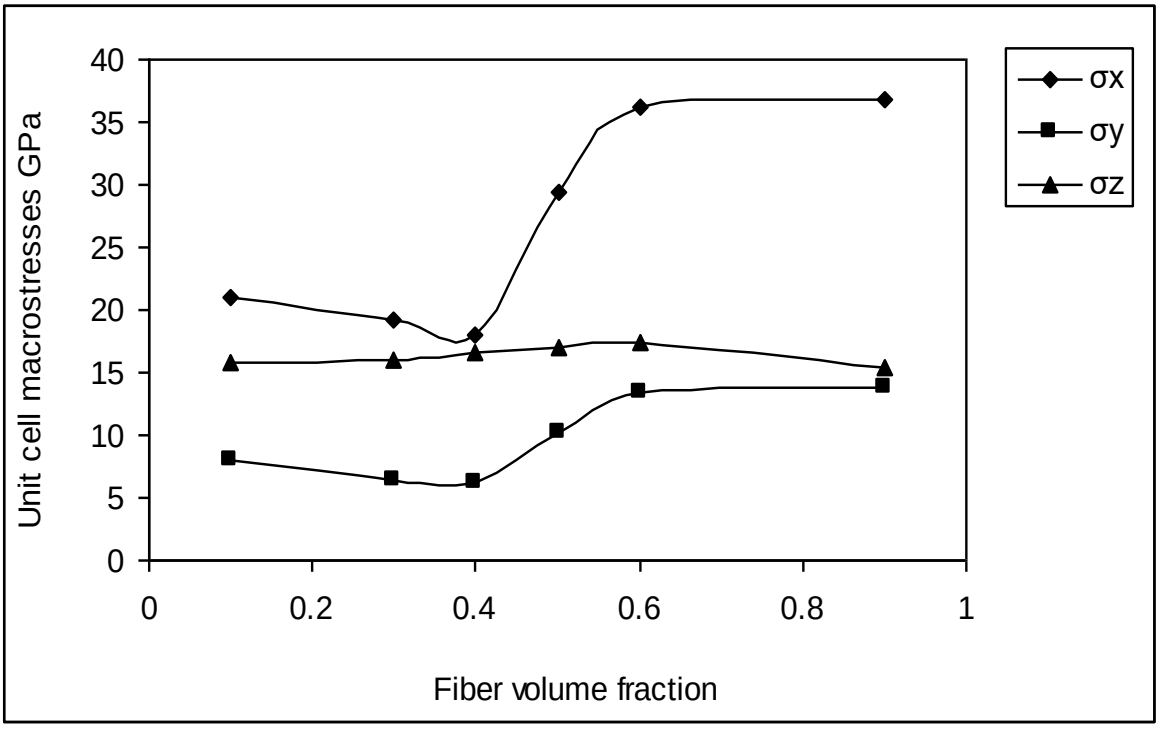

Fig. ٥.٣٥: Effect of fiber volume fraction on unit cell macro stresses in a simply supported E-glass/polyester composite beam.

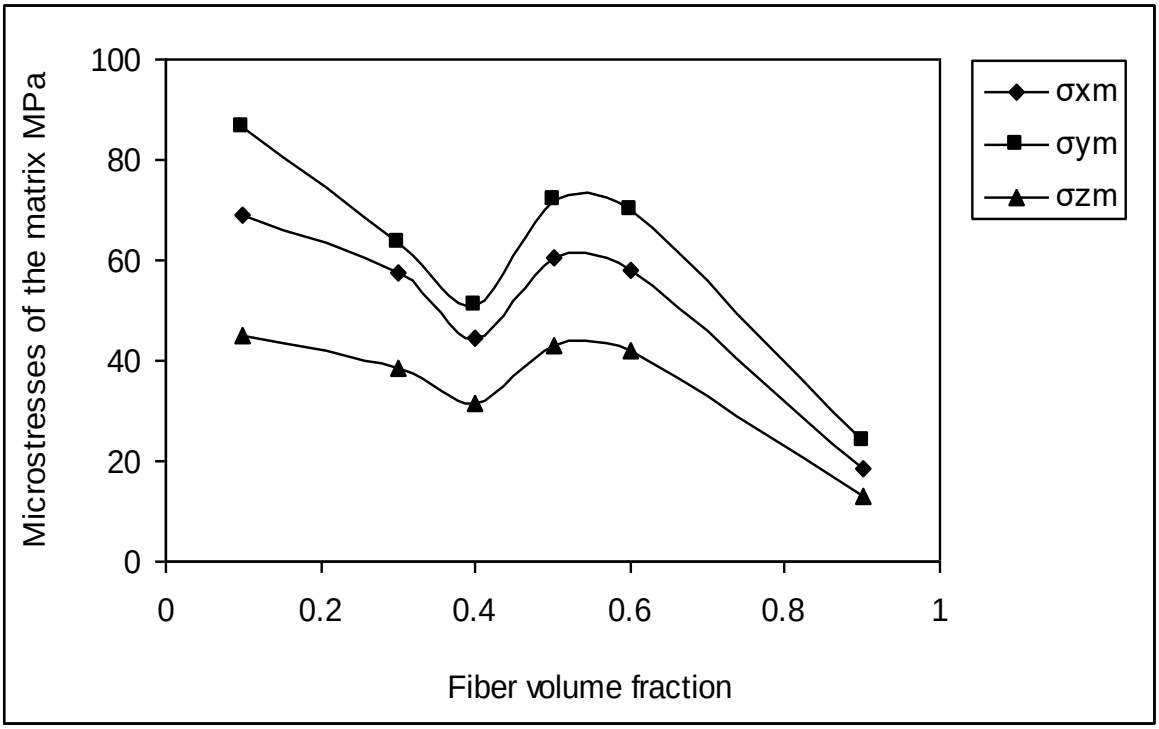

Fig. ٥.٣٦: Effect of fiber volume fraction on matrix micro stresses at constant fiber diameter for simply supported E-glass/polyester composite beam.

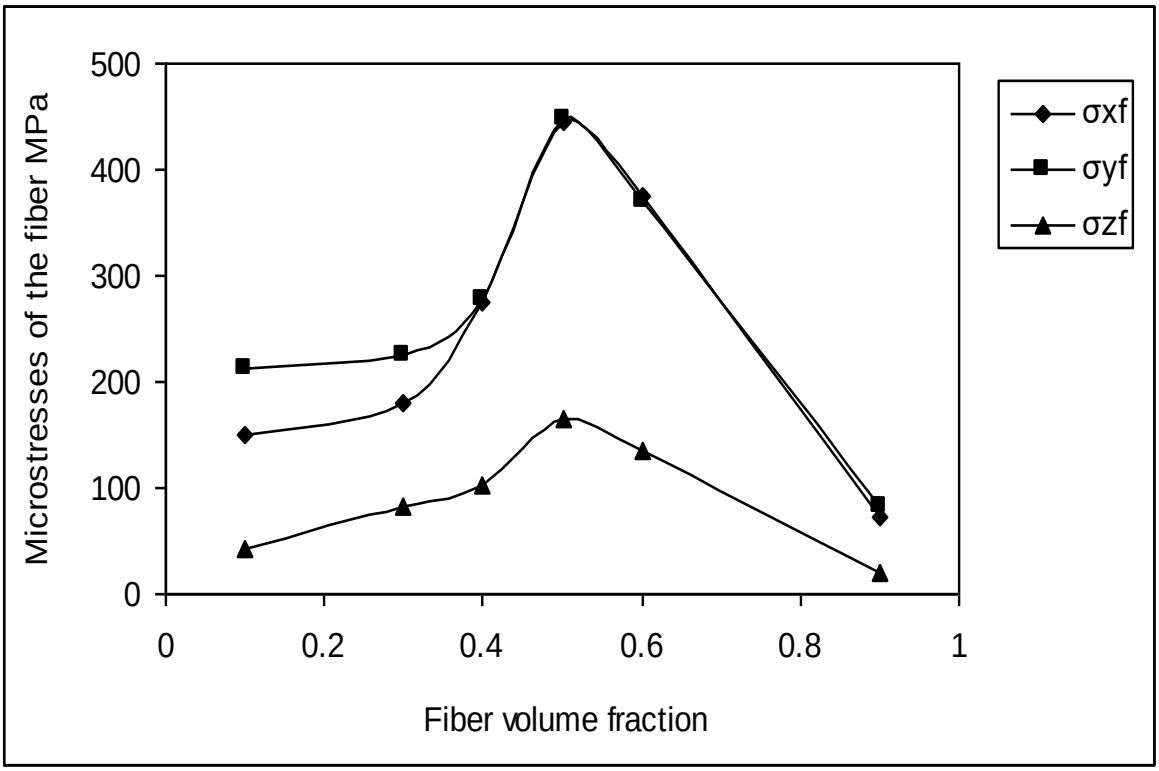

Fig. ٥.٣٧: Effect of fiber volume fraction on the fiber micro stresses MPa at constant fiber diameter for simply supported E-glass/polyester composite beam.

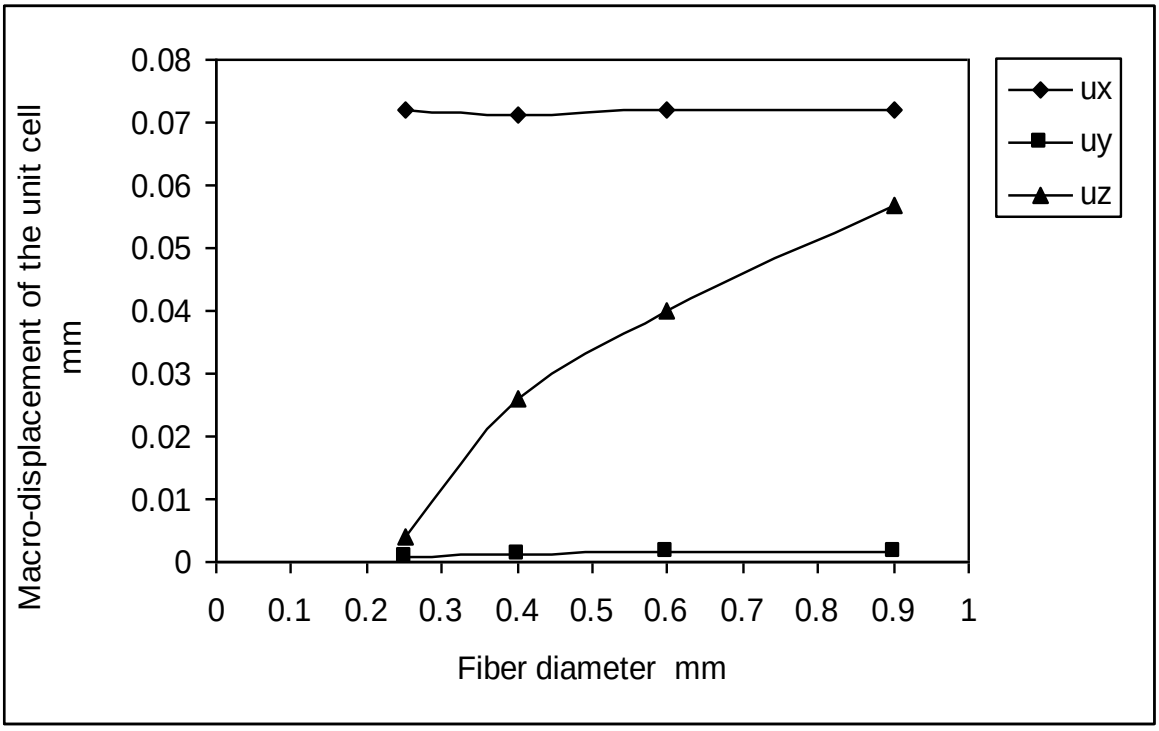

Fig. ٥.٣٨: Effect of fiber diameter on macro-displacement of the unit cell for simply supported E-glass/polyester composite beam at constant fiber volume fraction.

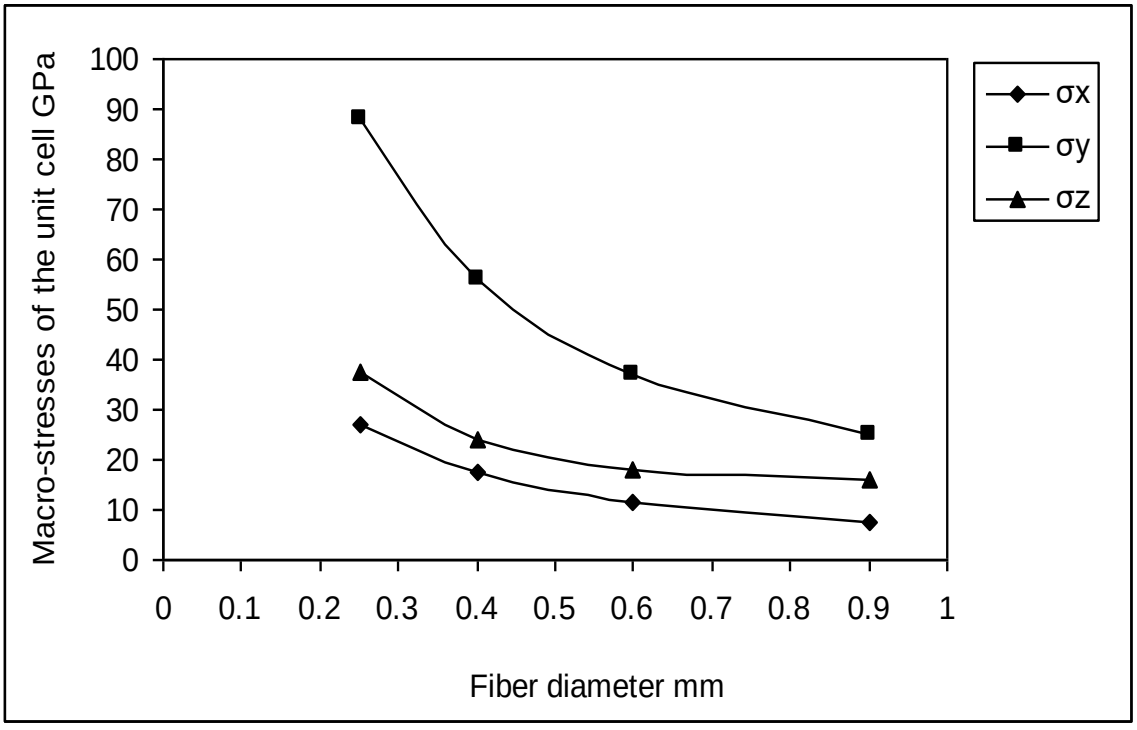

Fig. ٥.٣٩: Effect of fiber diameter on macro-strsses of the unit cell for simply supported E-glass/polyester composite beam at constant fiber volume fraction.

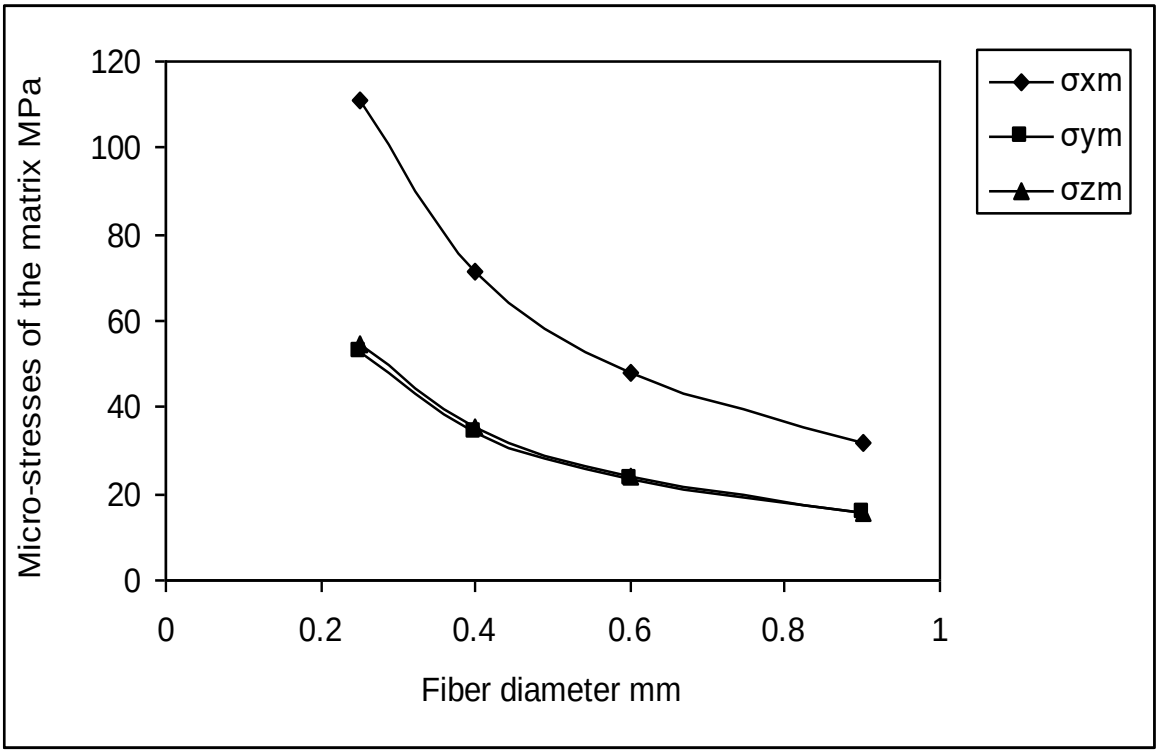

Fig. ٥.٤٠: Effect of fiber diameter on the micro-strsses of the matrix for simply supported E-glass/polyester composite beam at constant fiber volume fraction.

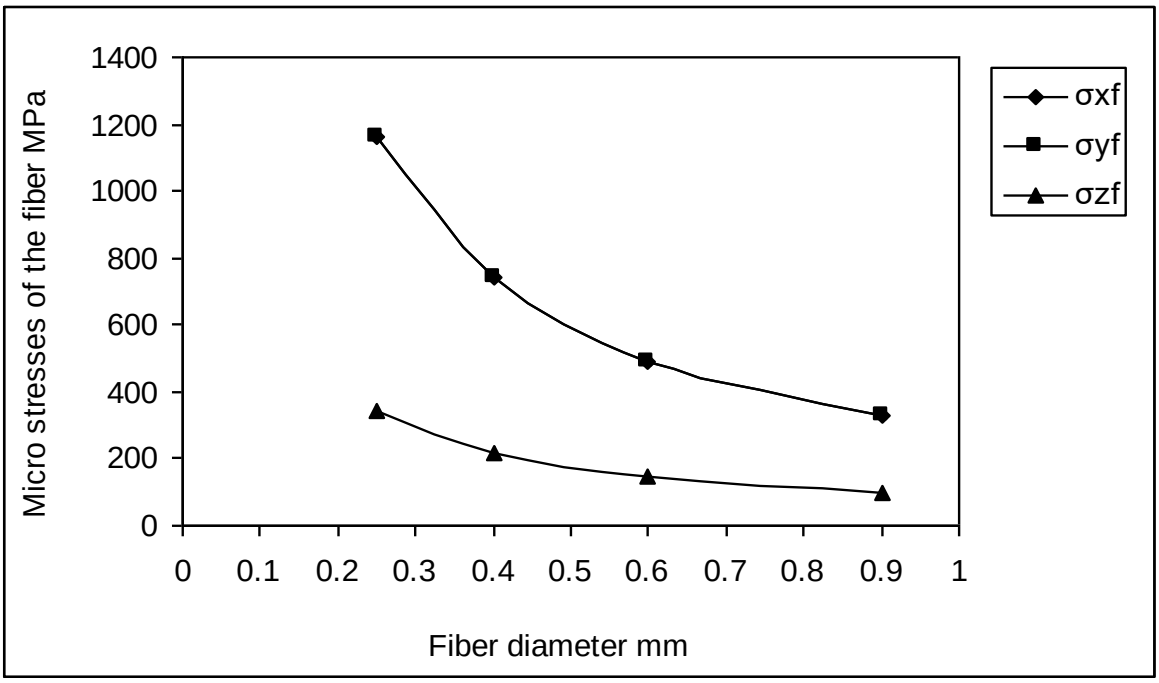

Fig. ٥.٤١: Effect of fiber diameter on the micro-strsses of the fiber for simply supported E-glass/polyester composite beam at constant fiber volume fraction.

References

١. **Robert M. Jones**, ١٩٩٩, "Mechanics Of Composite Materials", Scripta Book Co., Washington, D.C.

٢. **Bhagwan D. Agarwal and Lawrence J. Broutman, ١٩٨٩,** "Analysis And Performance Of Fiber Composites", John Wiley & Sons Inc. Press, New York, U.S.A.

٣. **Geoff Eckold, ١٩٩٥,** "Design And Manufacture Of Composite Structures", First ed., Jaico Publishing House, Bombay, India.

٤. **Ashby M. F. And Jones D. R. H., ١٩٨٨,** "Engineering Material ٢: An Introduction To Microstructure, Processing And Design"**,** Pergamon Press, London, U.K.

٥. **Shuguang Li, ١٩٩٩,** "On The Unit Cell For Micromechanical Analysis Of Fiber-Reinforced Composites", Proc. Roy. Soc. Vol. ٤٥٥, pp. ٨١٥-٨٣٨, London, U.K.

٦. **Hashin Z., ١٩٨٣,** "Analysis Of Composite Material – A survey", ASME., J. Appl. Mech., Vol. ٥٠, pp. ٤٨١-٥٠٥.

٧. **Aboudi J., ١٩٨٩,** "Micromechanical Analysis Of Composites By The Method Of Cells", ASME., J. Appl. Mech., Rev. ٤٢, pp. ١٩٣-٢٢١.

٨. **Barry P. W., ١٩٧٨**, "The Longitudinal Tensile Strength Of Unidirectional Fibrous Composites", J. of Materials Sci., Vol. ١٣, pp. ٢١٧٧-٢١٨٧.

٩. **Malcolm D. J., ١٩٧٨,** "A Microstructure Approach To Numerical Analysis Of Composite", Fiber Sci. & Tech., Vol. ١١, pp. ١٩٩-٢١٦, Applied Science Publishes Ltd., England.

١٠. **Hashin Z., ١٩٧٩,** "Analysis of Properties of Fiber Composite with Anisotropic Constituents", ASME, J. Appl. Mech., Vol. ٤٦, pp.٥٤٣-٥٥٠.

١١. **Zhang W. C. And Evans K. E., ١٩٨٨,** "Numerical Prediction Of The Mechanical Properties Of Anisotropic Composite Materials", Comp. & Struct. Vol. ٢٩, No. ٣, pp. ٤١٣-٤٢٢, Pergamon Press.

١٢. **Shuguang Li, ٢٠٠٠,** " General Unit Cell For Micromechanical Analysis Of Unidirectional Composite", www.elsevier.com/locate/compositesa, composites, Part A٣٢, pp. ٨١٥-٨٢٦.

١٣. **Shuguang Li And Zhenmin Zuo, ٢٠٠٠,** "Unit cell And Micromechanical Finite Element Analysis Of Unidirectional Fiber-Reinforced Composites",

ECCM٩, Composites: From Fundamentals To Exploitation, ٤-٧ June, Brighton, U.K.

١٤. Laws N. And Mclaughlin R., ١٩٧٩, "The Effect Of Fiber Length On The Overall Moduli Of The Composite Material", J. Mech. Phys. Of Solids, Vol. ٢٧, pp. ١-١٨, Pergamon Press Ltd.

١٥. Schultrich B., ١٩٧٨, "The Influence Of Fiber Discontinuities On the Stress-Strain Behavior Of The Composite", Fiber Sci. And Tech., Vol. ١١, pp.١-١٨, Applied Sci. Publishers Ltd. England.

١٦. Ali Akbar Akbarzadeh, ١٩٧٨, "Effect Of Broken Fibers On The Strength Of Unidirectional Composite Materials", Fiber Sci. And Tech., Vol. ١١, pp. ٢١٧-٢٢٨, Applied Sci. Publishers Ltd. England.

١٧. Göran Tolf, ١٩٨٣, "Mechanical Behavior Of A Short-Fiber Composite", Fiber Sci. And Tech., Vol. ١٩, pp. ٩١-١٠٩, Applied Sci. Publishers Ltd. England.

١٨. Lauke B., Schultrich B., And Barthcl R., ١٩٨٥, "Contribution To The Micromechanical Interpretation Of Fracture Work Of Short-Fiber-Reinforced Thermoplastics", Comp. Sci. And Tech., Vol. ٢٣, pp. ٢١-٣٥, Applied Sci. Publishers Ltd. England.

١٩. Agarwal B.D., And Bansal R.K., ١٩٧٩, "Effect Of An Interfacial Layer On The Properties Of Fibrous Composite:A Theoretical Analysis", Fiber Sci. And Tech., Vol. ١٢, pp.١٤٩-١٥٨, Applied Sci. Publishers Ltd. England.

٢٠. Laws V., ١٩٨٠, "Micromechanical Aspects Of The Fiber-Cement Bound", Composites, April, Butterworth & Co. Publishers Ltd.

٢١. **Shirazi-Adl A., ١٩٨٩,** "An Interface Continuous Stress Penalty Formulation For The Finite Element Analysis Of Composite Media", Compo. And Stru., Vol. ٣٣, No. ٤, pp.٩٥١-٩٥٦, Pergamon Press.

٢٢. **Le Petitcorps Y., Pailler R. And Naslain R., ١٩٨٩,** "The Fiber/Matrix Interfacial Shear Strength In The Titanium Alloy Matrix Composites Reinforced By Silicon Carbon Or Boron CVD-Filaments", Composites Sci. And Tech., Vol. ٣٥, pp. ٢٠٧-٢١٤, Elsevier Sci. Publisher Ltd.

٢٣. **Shastry B. P. And Venkateswarw Raw G., ١٩٧٧,** "Effect of Fiber Orientation On Stress Concentration In A Unidirectional Tensile Laminate Of Finite Width With A Central Circular Hole", Fiber Sci. And Tech., Vol. ١٠, pp. ١٥٢-١٥٤, Applied Sci. Publishers Ltd., England.

٢٤. **Paul T. K. And Rao K. M., ١٩٨٩,** "Stress Analysis Around Circular Holes In FRP Laminates Under Transverse Load", Comp. And Stru., Vol. ٣٣**,** No. ٤, pp. ٩٢٩-٩٣٩, Pergamon Press.

٢٥. . **Brett A. Bednaryk, ٢٠٠٠,** "Modeling Woven Polymer Matrix Composites with MAC/GMC", http://www.Google.com, Available on line at http://gltrs.grc.Nasa.gov/GLTRS, NASA/CR, ٢٠٠٠-٢١٠٣٧٠, Ohio Aerospace Institute, U.S.A.

٢٦. **Prem E.J. Babu, S. Savithri, U.T.S. Pillai And B.C. Pai, ٢٠٠٤,** "Application Of Generalized Method Of Cells Principle To Particulate-Reinforced Metal Matrix Composites", http://www.Google.com, Regional Research Laboratory, Kerala, India.

٢٧. **Ö. Soyakasap, ٢٠٠٥,** "Micromechanical Models For Bending Behavior Of Woven Composites", http:// www.google .com. ٤٦th AIAA/ASME/ASCE/AHS/

ASC Stru., Structural Dynamics & Materials Conference ١٨-١٢-٢٠٠٥, Austin, Texas.

٢٨. **V.L. Tagarielli, N.A. Fleck and V.S. Deshpand, ٢٠٠٤,** "Collapse Of Clamped And Simply Supported Composite Sandwich Beam In Three Point Bending", www. Elsevier.com/locate/compositeb, Available online at www.sience direct.com, Univ. of Cambridge, U. K.

٢٩. **McCrum N.G., Buckley C.P. and Bucknall C.B., ١٩٩٧,** "Principles Of Polymer Engineering", ٢nd Ed., Oxford Univ. Press.

٣٠. **Botton W., ١٩٩٨,** "Engineering Materials Technology", ٣rd Ed., McGraw-Hill, New York, U.S.A.

٣١. **Yeh, Hsien-Yang and Richards, W. Lance, ١٩٩٦,** "Yeh-Stratton Criterion for Stress Concentrations on Fiber-Reinforced Composite Materials", on line at http://www.Google.com, NASA Contract No. NCC ٤-١٠٧ November ١٩٩٦, NASA Contractor Report ١٩٨٠٥٤, Dryden Flight Research Center Edwards, California ٩٣٥٢٣-٠٢٧٣, U.S.A.

٣٢. **Yeh, Hsien-Yang and Richards, W. Lance, ١٩٩٧, "Failure Study of Composite Materials by the Yeh-Stratton Criterion",** on line at http://www.Google.com, National Aeronautics and Space Administration, NASA Technical Memorandum ١١٣٠٨٧, Dryden Flight Research Center Edwards, California ٩٣٥٢٣-٠٢٧٣, U.S.A.

٣٣. Sarkissov, Alex., Meijer, Han E. H. and Fischer, Hartmut R., ٢٠٠١, "Influence of the Particle Morphology on the Micro-and Macromechanics of Nano-Reinforced Materials", journal of "Innovative Materials , TNO TPD", on line at http://www.Google .com, Netherlands.

٣٤. Chakraborty, D., and Pradhan, B., ٢٠٠٢, "Fracture Behaviour of FRP Composite Laminates with Two Interacting Embedded Delaminations at the Interface**",** Journal of REINFORCED PLASTICS AND COMPOSITES, Vol. ٢١, No. ٨/٢٠٠٢, http://www.sagepublications.com, Turkey.

٣٥. Karakuzu, R., Aslan, Z. and Yücel, U. K., ٢٠٠٣, "Elasto-Plastic Finite Element Analysis of Fully Clamped Laminated Thermoplastic Composite Plates", Journal of REINFORCED PLASTICS AND COMPOSITES, Vol. ٢٢, No. ٦/٢٠٠٣, http://www.sagepublications.com, Turkey.

٣٦. He, K., Ganesan, R. and Hoa, S. V., ٢٠٠٤, "Interlaminar Stress and Delamination Analysis of Internally-tapered Composite Laminates**",** Journal of "REINFORCED PLASTICS AND COMPOSITES", Vol. ٢٣, No. ٧/٢٠٠٤, http://www.sagepublications.com, Turkey.

٣٧. KÜÇÜK, M., (٢٠٠٤), "An Investigation on Buckling Behavior of Simply Supported Woven Steel Reinforced Thermoplastic Laminated Plates

with Lateral Strip Delamination**",** Journal of REINFORCED PLASTICS AND COMPOSITES, Vol. ٢٣, No. ٢/٢٠٠٤, http://www.sagepublications.com, Turkey.

٣٨. ZOR, M., S_ EN, F. AND TOYGAR, M. E., ٢٠٠٥, "An Investigation of Square Delamination Effects on the Buckling Behavior of Laminated Composite Plates with a Square Hole by using Three-dimensional FEM Analysis", Journal of

REINFORCED PLASTICS AND COMPOSITES, Vol. ٢٤, No. ١١/٢٠٠٥, http://www.sagepublications.com, Turkey.

٣٩. Talookolaei, R.A. J. and Ahmadian, M.T., ٢٠٠٧, "Free Vibration Analysis of a Cross-Ply Laminated Composite Beam on Pasternak Foundation", Journal of Computer Science ٣ (١): ٥١-٥٦, Center of Excellence in Design, Robotics and Automation, School of Mechanical Engineering, Sharif University of Technology, Azadi Ave., Tehran ١١٣٦٥, Iran

٤٠. De wild W.P., ١٩٨٨, "What Are Composite Materials", Proc. ١st Int. On-Computer Aided Design in Composite Material Technology, South Hampton, U.K.

٤١. Dally, J.W. and Riley, W.F., ١٩٨٠ "Experimental Stress Analysis", McGraw-Hill Book Company, New York,

٤٢. Chandrupatla, T.R. and Belegundu, A.D., ١٩٩٧ "Introduction to Finite Element in Engineering", ٢nd Ed., Prentice hall, New Delhi..

٤٣. Al-Ithary, Haneen Z., ٢٠٠٢ "Micromechanics Analysis of Unidirectional Fiber-Reinforced Composite Materials", M. Sc. Thesis, Univ. of Babylon, Hilla, Iraq.,

٤٤. Krishan, K. C. and Mare, A. M., ١٩٩٩ "Mechanical Behavior of Materials", Prentice-Hall, Upper Saddle River, New Jersey, U.S.A.,.

٤٥. Timoshinko, S. P. and J. N. Goodier, ١٩٧٠ "Theory of Elasticity", ٣rd Ed. McGraw-Hill, New York, U.S.A.,.

٤٦. Sing, S., ١٩٨٨ "Theory of Elasticity", Khanna Publisher, New Delhi..

٤٧. Barkanov, E. ٢٠٠١ "Introduction To Finite Element Method", Institute of Materials and Structures, Riga Technical University.

٤٨. Li. S. and Reid, S. R., ١٩٩٢ "On The Symmetry Conditions For Laminated Fiber-Reinforced Composite Structures", Int. J. Solids Structures, vol. ٢٩, No. ٢٣, pp. ٢٨٧٦-٢٨٨٠, Pergamon Press, Great Britain..

٤٩. Roark, R. J. and Young, W. C. ١٩٩٩ "Formulas For Stress and Strain", Int. Student Edition, ٧th Ed., McGraw-Hill, Kugakusha Ltd., Tokyo, Japan. On line athttp://www.google.com.

٥٠. Segerlind, L. J., ٢٠٠٢ "Applied Finite Element Analysis", ٢nd Ed., John Wiley & Sons, New York, U.S.A..

٥١. Rao, S. S., ١٩٨٨ "The Finite Element Method In Engineering ", ٢nd Ed., Pergamon Press, London, U.K..

٥٢. Ross, C. T. F., ١٩٩٠ "Finite Element Methods In Engineering Science", Ellis Horwood Ltd., Chichester, England..

٥٣. Cook, Robert D., ١٩٩٥ "Finite Element Modeling For Stress Analysis", ١st Ed., John Wiley & Sons Inc., New York, U.S.A..

٥٤. Office of Aviation Research, ١٩٩٧ "Fiber Composite Analysis and Design:

Composite Materials and Laminates", www.Google.com, Volume ١, U.S. Department of Transportation (DOT), Federal Aviation Administration (FAA), National Technical Information Service, Springfield, Virginia, U.S.A..

٥٥. Khurmi, R. S., ١٩٨٢"Strength of Materials", ١٢th Ed., S. Chand & company Ltd., New Delhi, India..

٥٦. **J. J. Toma,** ١٩٧٩"Engineering Mathematics Handbook", ٢nd enlarged Ed., McGraw-Hill Book Company, New York, U.S.A..

٥٧. **Waheed, Salwan O.,** ٢٠٠٥"Dynamic Analysis of Fiber-Reinforced Composite Shell Structure under Action of Impulsive Excitation", MSC. Thesis, Univ. of Babylon, Hilla, Iraq.

٥٨. **ANSYS**R**,** ١٩٩٨"Engineering Analysis System Theoretical Manual", http://www.ANSYS.com, Version ٥.٤.

٥٩.**Pratrap, R.,** ٢٠٠٤"Getting Started With Matlab A Quick Introduction For Scientists And Engineers", Version-٦, Oxford University Press, Oxford, U.K.,.

٦٠. **Brian D. Hahn,** ١٩٩٧"Essential Matlab for Scientists and Engineers", Arnold Press, Hodder Headline Group, London, U.K.

٦١. **Robert C. Reuter, Jr,** ١٩٧١"Concise Property Transformation Relations for an- isotropic Lamina", J. of Composite Materials, April, pp. ٢٧٠-٢٧٢, Washington, U.S.A.

٦٢. **Shigley, J. E., and Mischke, C. R.,** ٢٠٠١"Mechanical Engineering Design" McGraw-Hill Higher Education Press, New York,.

٦٣. **Hibbeler, R. C.,** ١٩٩٧"Mechanics of Materials", Prentice Hall Inc., New Jersey.